Escola d'Enginyeria de Telecomunicació i Aeroespacial de Castelldefels
UNIVERSITAT POLITÈCNICA DE CATALUNYA

TREBALL FINAL DE GRAU

TÍTOL DEL TFG: Structural analysis of adhesive performance in aircraft repair patches made with adhesive bonded joints

TITULACIÓ: Bachelor's Degree in Aerospace Systems Engineering

AUTOR: Sergi Elias Lahuerta

DIRECTORS: Jose Ignacio Rojas Gregorio, Siddharth Pitta

DATA: 4th May 2023

Títol: Anàlisi structural del comportament de l'adhesiu en làmines de reparació d'aeronaus fabricades amb unions adhesives
Autor: Sergi Elias Lahuerta
Director: Jose Ignacio Rojas Gregorio, Siddharth Pitta
Data: 4 de maig del 2023

Resum

Els components d'una aeronau com el bastidor, el fuselatge, les ales, els estabilitzadors, etc. són les anomenades estructures de l'aeronau. Normalment es fabriquen amb una combinació de materials, com ara aliatges d'alumini i de titani, compostos i altres materials avançats. L'ús d'alumini a les aeronaus permet estructures més lleugeres i resistents que requereixen menys combustible per volar, el que resulta en un millor rendiment i abast i una reducció dels costos operatius. Els aliatges d'alumini utilitzats a les aeronaus tenen unes relacions de resistència a pes elevades i una bona resistència a la fatiga, cosa que els fa ideals per a estructures i elements de fixació.

Després de la construcció, les estructures se sotmeten a proves i inspeccions rigoroses per verificar la seva resistència i durabilitat, incloses proves estàtiques i de fatiga que simulen l'estrès que experimentarà l'estructura en vol. L'enfocament d'aquesta tesi se centra en les proves estàtiques d'una junta adherida utilitzada en la construcció d'avions.

Les juntes unides són un tipus de fixació mecànica que s'utilitza en la construcció d'avions on dos o més components s'uneixen per materials adhesius, sovint un tipus de resina epoxi. Aquestes unions ajuden a distribuir l'estrès uniformement per tota l'estructura. No obstant això, d'acord amb els resultats obtinguts, la tensió sobre una unió no és uniforme. Les proves estàtiques es realitzen mitjançant el programari Abaqus CAE, que es basa en l'anàlisi d'elements finits (FEA). A FEA, es crea un model digital de l'estructura i s'apliquen diverses càrregues per veure com respon. La informació de les proves estàtiques s'utilitza per avaluar el rendiment de l'estructura i identificar àrees potencials de debilitat o fallada.

Com ja s'ha esmentat, en aquest treball, es realitzaran diverses simulacions de la junta de solapament simple per conèixer com respon l'adhesiu quan s'aplica una força de tracció a les plaques unides, així com el seu homòleg amb reblons, com si es tractés d'una màquina d'assaig universal, i com actua l'adhesiu en el cas de començar a desenganxar-se. A més, també se sotmetrà a aquestes proves estàtiques un exemplar que s'assembla a un pegat real, ja que està format per plaques sobre plaques. Els resultats obtinguts ens indiquen que la tensió de la unió no és constant, ni amb adhesiu ni reblons, i que l'apilament de plaques sobre plaques ajuda a disminuir la càrrega a la zona a reparar.

Title: Structural analysis of adhesive performance in aircraft repair patches made with adhesive bonded joints
Author: Sergi Elias Lahuerta
Director: Jose Ignacio Rojas Gregorio, Siddharth Pitta
Date: 4th May 2023

Overview

The components of an aircraft such as the frame, fuselage, wings, stabilizers, etc. are the so-called aircraft structures. They are usually made from a combination of materials including aluminum alloys, titanium, composites, and other advanced materials. The use of aluminum in aircraft allows for lighter, stronger structures that require less fuel to fly, resulting in improved performance and range and reduced operating costs. Aluminum alloys used in aircraft have high strength-to-weight ratios and good fatigue resistance, making them ideal for structures and fasteners.

After construction, the structures undergo rigorous testing and inspection to verify their strength and durability, including static and fatigue tests that simulate the stress the structure will experience in flight. The focus of this thesis is on the static testing of a bonded joint used in aircraft construction.

Bonded joints are a type of joining technique used in aircraft construction where two or more components are joined together by adhesive materials, often a type of epoxy resin. These joints help distribute stress evenly throughout the structure. However, in accordance with the results obtained in this project, the stress over a joint is not uniform. The static tests are performed using the software Abaqus CAE, which is based on Finite Element Analysis (FEA). In FEA, a digital model of the structure is created, and various loads are applied to see how it responds. In this research, the information from the static tests is used to evaluate the performance of the structure and identify potential areas of weakness or failure.

As said, in this work, different simulations will be carried out for the single lap joint to find out how the adhesive responds when a tensile force is applied to the joined plates, as well as its homologue with rivets, as if it was tested in a universal testing machine, and how the adhesive acts in the case of peeling. In addition, a specimen that resembles a real patch, as it is made up of plates on plates, will also be subjected to these static tests. The results obtained indicate that the stress of the bond is not constant, neither along adhesive nor with rivets, and that the stacking of plates on plates helps to reduce the load in the area to be repaired.

Contents

INTRODUCTION

Aircraft structures refer to the design and assembly of the frame, fuselage, wings, stabilizers, and other components of an aircraft. These structures are usually made of a combination of materials such as aluminum alloys, titanium, composites, and other advanced materials. The choice of materials and construction methods depends on the specific requirements of the aircraft, including its weight, strength, and mission requirements. The structures are then built and joined using a combination of manual and automated processes, such as drilling, riveting, bonding, and fastening.

The use of aluminum in aircraft allows for lighter, stronger structures that require less fuel to fly. This results in improved performance and range of the aircraft, as well as reduced operating costs. Aluminum alloys used in aircraft, such as AA2024-T3 and AA7075-T6 discused in this thesis, typically have high strength-to-weight ratios and good fatigue resistance, meaning that they can withstand repeated loading over time without failure. Not only are they used for structures, but also for fasteners, such as rivets and bolts.

After the structures have been built, they undergo a series of rigorous tests and inspections to verify their strength and durability. This includes static and fatigue tests, where the structure is subjected to repeated loads over time to simulate the stress it will experience in flight. This thesis is focused on static test of the specimen chosen that will act as a bonded joint on an aircraft repair patch.

Bonded joints are a type of joining technique used in aircraft construction to join two or more components together by applying adhesive materials. The adhesive, often a type of epoxy resin, forms a strong, permanent bond between the components and helps distribute stress evenly throughout the joint.

There are several types of bonded joints used in aircraft construction, including fillet joints, scarf joints, and lap joints. Fillet joints are commonly used to join the skins of an aircraft's fuselage or wing to the underlying structure. Scarf joints are used to join two pieces of material at an angle, while lap joints are used to join two pieces of material end-to-end. In the experiment, we will study the single lap joint, with the help of Ph.D. Siddharth Pitta, who provided the dimensions for the lap joint. Therefore, some choices and argumentations will recall to his doctoral work and research [11] [12]. Additionally, a specimen of an intended realistic repair path was also studied in this bachelor’s degree thesis.

The mentioned static tests are performed with software Abaqus CAE created and developed by Dassault Systémes with is based on Finite Element Analysis (FEA). Static tests in FEA are numerical simulations used to evaluate the behavior of a structure under a static, or unchanging, load. In FEA, a digital model of the structure is created, and various loads are applied to the model to see how it responds. Static tests in FEA are used to determine the strength and stability of a structure, as well as the distribution of stresses and strains within the structure. This information is used to evaluate the performance of the structure and identify potential areas of weakness or failure.

All the points mentioned above will be explained in this document and divided into six chapters. In the first chapter, the theory related to aircraft structures and adhesive bonding is presented. The second chapter presents the materials used in the construction of the specimens, as well as the presentation of the static test method. The third chapter explains the finite element method and how it is viewed by the user (that would be the engineer). The fourth and fifth chapters show the results obtained for the single lap joint and the realistic patch. Finally, comments on the work and the results obtained will be included in the conclusions section.

CHAPTER 1. FUNDAMENTALS

1.1 Structural parts of aircraft

The structural components of an aircraft are made of a wide variety of materials, such as wood in the case of early aircraft, steel, and aluminum today, although composites such as carbon or glass fiber reinforced epoxies (CFRE and GFRE) are also beginning to be used to achieve new characteristics that cannot be achieved with conventional materials.

The structure of the vehicle, its skin and other components are joined with rivets, screws, and other types of joints, as well as welding and adhesives. This project focuses on the explanation and performance of adhesive joints.

In the following paragraphs, the structural parts of an airplane are mentioned and explained [1] [9]. Cristian Ribas already explained the structural parts in his master's thesis [18], but it is important to get the idea of the structures to understand the joints to form this structure.

- Fuselage: The fuselage is the body of the aircraft. In it, there is the necessary space to carry cargo, passengers, accessories, and other objects depending on the intended use of the vehicle. Also, part of the fuselage serves to support the wings of the aircraft as well as the empennage, from a structural point of view. There are three different techniques to build the fuselage structure or skeleton depending on how the forces will be transmitted to the structure (truss, monocoque, semi-monocoque) [18].

1. Truss-Type: In this construction method, longerons are welded in place to form a well braced framework. Horizontal and vertical bars are added to the longerons as well as additional diagonal struts so that the final structure is capable of resisting both tensile and compressive stresses. To the truss structure, it can be wrapped with, for example, aluminum plates or fabric (formerly) to finish the fuselage construction [18].

2. Monocoque: This type of construction is based on the fuselage skin being attached to formers/rings so that the skin is the main carrier of all stress forces. The resistance provided by the skin to stresses in the proximal zones of the vertical elements such as the formers/rings and the bulkhead is very good. However, monocoque construction is not highly tolerant to surface deformation. For example, a soda can is able to withstand stresses at the ends of the can, but it will easily collapse if a small force is applied to the side [18].

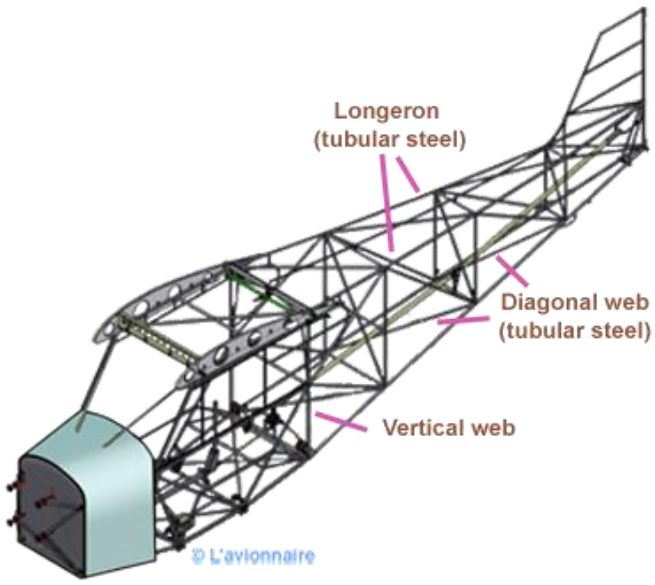

Fig. 1.1 Truss-type structure of the fuselage [25].

3. Semimonocoque: A modification of the monocoque construction was developed to improve the strength-to-weight ratio. Semimonocoque structure is also equipped with vertical elements such as the rings and the bulkhead, but it is also equipped with longitudinal elements such as the stringers which have the function of resisting loads that cause the fuselage to flex. To join the vertical elements, the stringer is used, which together with the spars, also support the compression and traction loads so that the fuselage does not flex [18].

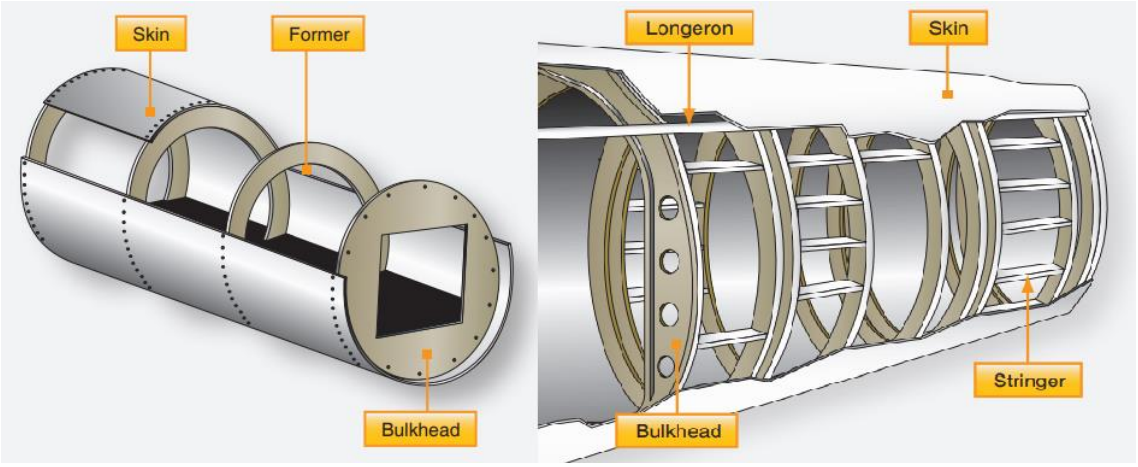

Fig. 1.2 On the left: monocoque. On the right: semimonocoque [1].

- Wings: Are the parts of the aircraft that have the function of providing lift to the aircraft, and their shape can change throughout the flight to give the lift force according to the movements and performances desired by the pilot.

The wings are attached to the fuselage and, like the fuselage, must have a good structure to withstand stress. In addition, their design is not the same in all aircraft, since it depends on the size of the vehicle, its weight, and the desired rate of climb, among other factors.

Generally, the wings have a design reminiscent of a cantilever, that is, they are only attached on one side, so that no external bracing is needed. On the other hand, there are other types of wings that, in addition to having the above-mentioned attachment, are also attached with cables and/or support rods that are usually made of steel. They are called semi-cantilever wings.

Fig. 1.3 Comparison of semi-cantilever wing and a cantilever wing [20].

When it comes to build wings, aluminum is commonly used as well as wood covered with fabric. However, building technology has evolved over the years, so that modern aircraft wings tend to be made from lighter and stronger materials such as CFRE, other composites, or combination of materials to achieve a great strength-to-weight ratio.

- Empennage: Also known as tail section, is the rear part of an airplane. Most empennage consist of horizontal stabilizer and a vertical stabilizer joined in the tail cone in order to stabilize the flight dynamics of pitch and yaw. These stabilizers are built almost the same as a regular wing since they are capable of generating lift or downforce.

- Flight control surfaces: A fixed-wing aircraft can be controlled in the lateral, longitudinal and vertical axes with the assistance of control surfaces. These are the ailerons, elevators, and rudder(s), as well as other secondary or auxiliary surfaces such as flaps, spoilers, and slats.

1.2 Joining methods

To achieve a structure, the elements that form it must be joined together. The different methods of joining that are most used in aeronautics are explained below [3] [11] [18]:

- Adhesive bonding: this type of joining consists in bonding two materials with the use of adhesive technology. Aircraft structure designers use adhesive to join fiberglass-reinforced plastic components and sandwich structures in various combinations of wood, paper, plastic, and metal and,

consequently, allows different materials to be joined together, such as ceramic to metal, plastic to metal, metal to metal, etc.

- Welding: two components made of metal or thermoplastic are joined by melting them in the joining spot. Once the heat is removed, the material is continuous across the joint. Advanced welding techniques such as lasers or electron beams are interesting for some works. However, welding is not widely used in structures as it can significantly change the material properties due to the joint spot turning out to be an alloy because of the melting of the two metals involved.

- Soldering and brazing: these are similar processes to welding. The components to be joined are not melted, but a softer material is such as brass or tin to make it run between them and act like and adhesive. It is cheaper than welding and can only be used under relatively low-stress and relatively low-temperature environments.

- Bolted and riveted: bolts and rivets are a type of fasteners that hold two or more thing together. The bolt has an unthreaded part of its length, where the components to be joined will be housed, while in the threaded part, there will be a nut that will hold the assembly. On the other hand, a rivet has no threaded part and the primary purpose of it is to join plates permanently, therefore a disassembly implies destroying the riveted joint.

- Hybrid joining combines adhesive bonding and a fastener such as rivets or any other threaded device. Its use is due to produce joints with properties additional to those obtained from a single technique.

In this research, we will focus on the use of adhesive bonding because of its efficiency, good strength-to-weight ratio, and improved fatigue life.

1.3 Adhesive bonded joints

A structure is said to be bonded when two elements or assemblies are joined with adhesives. Therefore, the structural strength of the assembly relies on the chemical bond of the adhesive and not on conventional fasteners such as screws, rivets, bolts, and other fasteners [4]. As mentioned before, adhesive bonding is widely used in construction for secondary structures. In recent years, the use of adhesives in aircraft construction and repair has increased as new advanced composite materials become more prevalent in aircraft engineering. For example, in order to join two metal plates, rivets or soldering would generally be chosen for joining before adhesive technology expansion.

1.4 Adhesion theories

There are several theories of adhesion between two surfaces to be joined, called substrates or adherents, that need to be considered in order to understand

adhesive bonding and what happens between the adhesive and adherend at the microscopic level. Although all theories apply in this field, mechanical theory, and adsorption (wetting) theory are more relevant in the field of aeronautical engineering [4].

1.4.1 Mechanical theory

According to mechanical theory, the surface of any material is not smooth, but rough. It contains a pores, cavities, peaks, and valleys. Therefore, the adhesive penetrates these surface irregularities and displaces the air found in them. This theory is consistent with the fact that a good level of roughness guarantees that the adhesive is well joined to the adherent [14].

1.4.2 Adsorption theory (wetting)

This theory states that adhesion is the result of the molecular contact of the two parts, so it is meant to develop interfacial forces between the adhesive and the substrates. Maximum wettability between the glue and the surface to be bonded is required. In other words, close contact between adhesive and adherent is crucial to assure maximum adhesion strength [4].

In terms of surface preparation, wetting is the technique of maintaining continuous contact between the adhesive and the adherent. **Fig. 1.5** shows the comparison of complete and incomplete wetting process. We will be getting a good wetting when the adhesive flows well into the cavities and pores of the surface and the highest bond strength will be achieved. Otherwise, if the adhesive has no adequate contact and thus there are interfacial defects, the bond strength will be weakened [14].

1.4.3 Electrostatic theory

According to this theory, adhesion is possible due to electrostatics effects between adhesive and substrate. Theoretically, because the adhesive and the adherent have different electronic bands, an electron transfer occurs to equalize Fermi levels*. This phenomenon could induce the formation of a double electrical layer at the interface and the resulting electrostatic forces can contribute to the adhesive strength. Also, this theory gains support due to the fact of observing electrical discharges when peeling an adhesive from a substrate [2] [14].

1.4.4 Diffusion theory

The diffusion theory assumes that the adhesion strength of polymers is due to mutual diffusion (interdiffusion) of chains of macromolecules across the interface and the adhesion strength of polymers to themselves (autohesion) and this process creates an interphase. Therefore, this theory is principally applicable

when both the adhesive and the substrate are polymers with long-chain molecules that are capable of movement and mutually soluble; such mechanism is supported by Voyutskii [21]. When diffusion event is presented, joint strength depends on many factors such as temperature, contact time, molecular weight of polymers involved, etc. [2].

Fig. 1.4 On the left, diffusion or interdiffusion. On the right, mechanical interlocking [19].

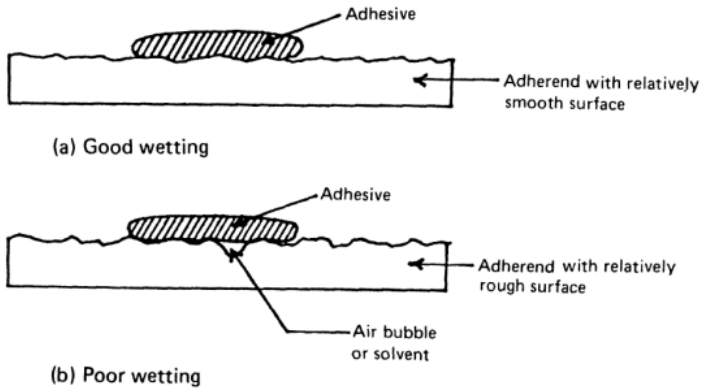

Fig. 1.5 Examples of good and poor wetting by an adhesive spreading across a surface [14].

1.5 Adhesive failures

To understand failure, two concepts related to the holding forces between the substrate and the adhesive must be considered: 1) the adhesion or bond strength of the adhesive to the substrate, and 2) the cohesion or internal strength of the adhesive.

In joints, there are loads that will stress the structure and the joint, and they may collapse and break. Depending on how the loads are transmitted and/or the quality of the adhesive or substrate, one will break sooner than the other. The **Fig. 1.6** shows the different types of adhesive bond failure [11] [13].

- Adhesive failure: When separation occurs at the substrate-adhesive interphase, because, e.g., the adhesive was not correctly applied, or the bonding surface was not correctly prepared. It may be observed that the adhesive remains on only one of the two adhesives. This type of failure is not desirable in any case.

- Cohesive failure: Adhesive fails, that is, the adhesive breaks due to the high stresses to which it is subjected and remains on both substrates. Desirable.

- Mixed or intermediate failure occurs when there is an adhesive failure and a cohesive failure at the same time.

- Substrate failure: The substrate or adhesive is broken. In this case, the interphase connection between the adhesive and the substrate is stronger than the substrate itself.

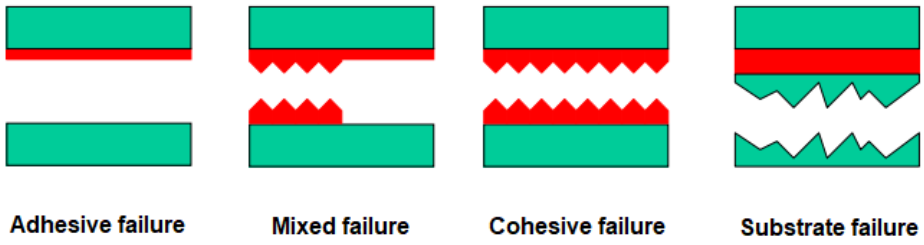

Fig. 1.6 Adhesive failures [8].

Most common failures are adhesive failure and substrate failure. As a rule, the joints are calculated so that, if failure occurs, it occurs in the adherend. Fortunately, almost all failures start at the edges of the joint and can therefore be detected in time.

By working with the specimens and having their respective failure tests performed, the type of failure of the specimen can be evaluated visually based on the state of the adhesive and the substrate.

1.6 Types of adhesives

The selection of suitable adhesives is based on static strength requirements, temperature range in which the adhesive will operate and curing.

Depending on how the user needs to apply the adhesive, adhesives for aircraft structures can be presented in the form of tape, paste or foam [4] [11].

1.6.1 Film adhesives

Tape adhesives are thin and glue-impregnated films that are deposited on the substrate and have a peelable sheet to uncover the tape.

The advantages of their use are that they do not require pre-mixing and their application is very easy. Also, the glue spread along the sheet is perfectly homogeneous, thus achieving a constant cohesion. However, it is usually the most expensive presentation of adhesives, in addition to requiring refrigeration (18º C) for storage.

The toughness of the glue depends on the hardening agent used. Its thermal service range is good so that the greater the toughness the lower the maximum operating temperature.

1.6.2 Paste adhesives

Paste adhesives should be applied with a putty knife or other spreading equipment. They are available in one or two components and cure at room temperature or with heat. The components of two-component paste adhesives are epoxy resin in liquid form and the hardener component.

The advantage is that cooling is not necessary. The negative side of these is that they must be mixed and, therefore, errors in the proportions can occur, although there are dispensers and mixers that deal with this problem, and there is also the difficulty of establishing a glue line with constant thickness and cohesion.

1.6.3 Foam adhesives

Although they are foam type, they are available in paste or tape formats. Foam adhesives are based on epoxy resin, which in turn contains a foaming agent whose function is to increase the volume of the adhesive during curing. The expansion of the foam adhesive during curing increases between 1.3 and 5 times (density between 192 to 720 kg/m³). In tape, it has a thickness of 0.35 to 0.508 mm. They are widely used in sandwich structure repairs or to fill voids and corners. The choice between film and paste depends on the size of the honeycomb core cells under repair.

1.7 Aircraft repair patches and reinforcements

During the lifespan of an airplane, it must confront with many loading scenarios causing initiation and propagation of cracks in the aircraft structure. The main objective of a repair of the skin of aircraft is to retorn to the original strength in the damaged area.

Cracked structures are usually repaired using what is called “Crack Patching”. In this technique a repair patch is attached to the damaged or weakened structure either using mechanical fasteners or adhesive bonding. Repair patches can be made from metallic or non-metallic materials. The metallic patches are usually made of aluminum, steel, or titanium. In the case of non-metallic patches, two main materials are used: boron/epoxy and graphite/epoxy. Also, laminated metallic materials are used which combine the advantages of using both metallic and composite structures. They are formed of thin aluminum alloy sheets that hold within layers of composites. The selection of the type of repair patch depends on many factors including patching efficiency, operating temperature, residual stress, cost, inspections, and weight.

The simple setup of an adhesive bonded patch is usually composed by repair patch layers bonded to the cracked parent structure in a way that the fibres of the patch are perpendicular the structural damage and parallel to the applied stress as shown in **Fig. 1.7**. The bonding of the repair patch to the parent structure is usually done using either epoxies or modified acrylics as an adhesive [15].

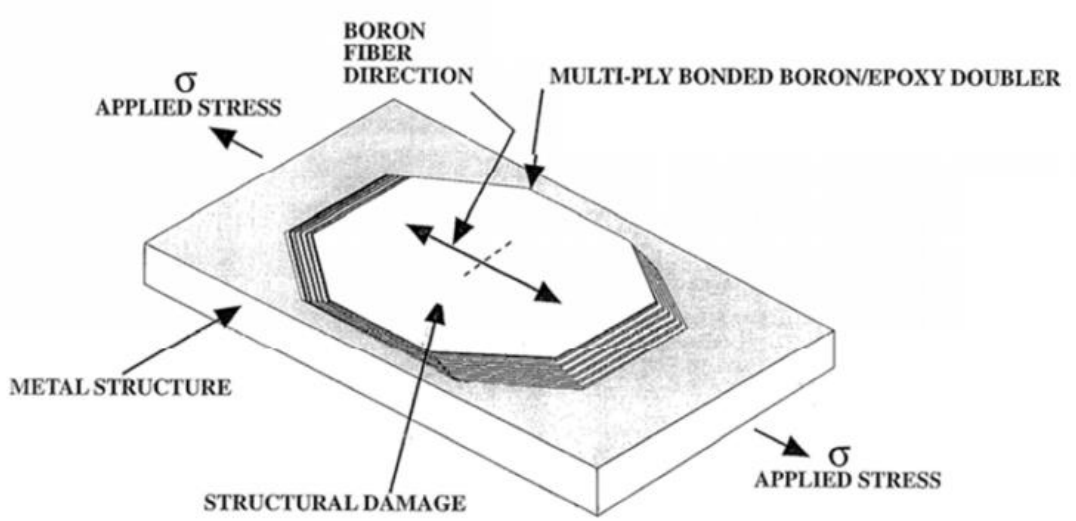

Fig. 1.7 Typical bonded composite patch repair [16].

1.8 Surface preparation

To get a well bonded joint, surface preparation is required. Before applying the adhesive on the plates, the surfaces of metal or composite substrates needs to be abraded with sandpaper with a grit size of 80 and then of grit size of 40, to remove the oxidation layer for metal surfaces. Note that it is crucial to create the abrasion at a direction of 45º to improve the shear strength of adhesive bond. After abrasion, the surfaces are cleaned with acetone to remove impurities and grease, which can negatively affect the quality of the bond. Finally, a thin finite layer of Araldite 2031 is applied between the surfaces to be bonded and then get them closer to each other until obtaining physical contact. Each time adhesive is applied, the bond is cured at 40ºC for 16 hours [11].

1.9 Stress distribution over a joint

Fig. 1.8 shows, in a generic way, the degree of shear stress acting along the adhesive in a bonded joint subjected to tensile forces. The shear stress is maximum in the edge zone and minimum in the central zone. The ends of the bonded joint are the main focus of inspection [4].

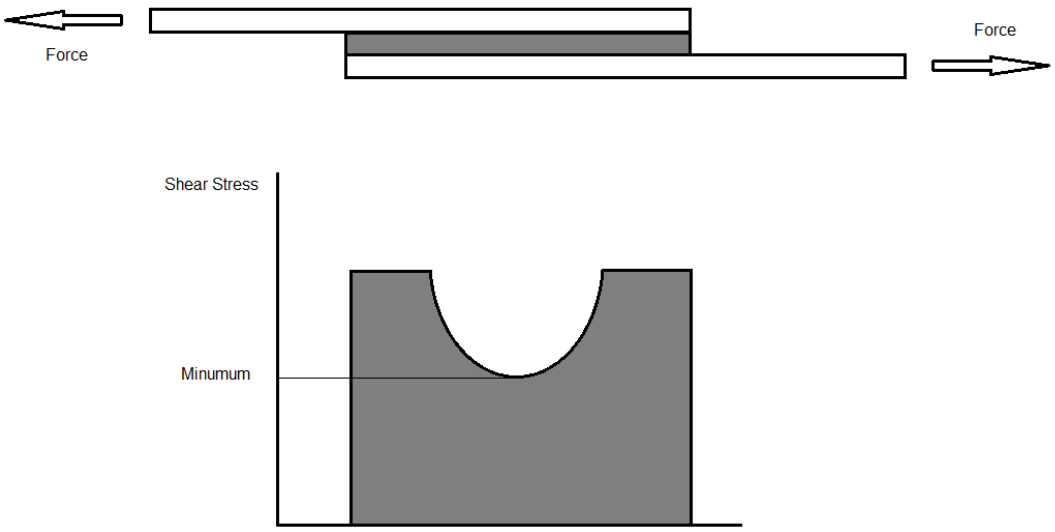

Fig. 1.8 Shear stress of a bonded joint.

CHAPTER 2. MATERIALS AND METHOD

2.1 Aluminum alloys in aeronautics

As explained in previous points, adhesives are useful for joining metal-metal, composite-composite, composite-metal, ceramic-metal, ceramic-metal, etc. components. In the experimental part of this thesis, metallic components, specifically an aluminum alloy, are used to study the performance of the adhesive, so it is interesting to mention and explain the main aluminum alloys that exist and their application in aeronautics.

The aluminum alloys used by the aeronautical industry are the result of combining aluminum (Al) with other metals, such as copper (Cu), manganese (Mn), zinc (Zn), and magnesium (Mg). These alloys are essential in aircraft construction, since they are characterized by their low density (around 2.7 g/cm^3) and high mechanical strength. The most used in this industry are the 2xxx series and the 7xxx series, and, more recently, also the 6xxx and 8xxx series.

2.1.1 2xxx series

Copper is the main alloying agent in this series of aluminum alloys, although magnesium can also be added as a secondary material in some cases. This type of alloy requires heat treatment by copper precipitation to obtain the optimum properties that will give very high mechanical strength, then, such treatment increases the yield strength, as well as an associated elongation loss. They have a yield strength of about 300 to 450 MPa [6].

Component	wt%	Component	wt%
Al	90.7 ~ 94.7	Si	Max 0.5
Cu	3.8 ~ 4.9	Zn	Max 0.25
Mn	0.3 ~ 0.9	Ti	Max 0.15
Mg	1.2 ~ 1.8	Cr	Max 0.1
Fe	Max 0.5		

Table 2.1 Aluminum Alloy 2024-T3 chemical composition in wt% [10].

2.1.2 7xxx series

This group of alloys contains zinc as the main alloying element, although copper and magnesium are also found in smaller quantities. It admits heat treatment and tensile strength up to 620 MPa and yield strength of 590 MPa. Engineers usually choose this type of alloy when parts with mechanical strength between 450 and 650 MPa are required. Also, 7xxx series alloys are used in airframe structures, mobile equipment, and other highly stressed parts [6].

Component	wt%	Component	wt%
Al	90.7 ~ 94.7	Si	Max 0.4
Cu	1.2 ~ 2	Zn	5.1 ~ 6.1
Mn	Max 0.3	Ti	Max 0.2
Mg	2.1 ~ 2.9	Cr	0.18 ~ 0.28
Fe	Max 0.5		

Table 2.2 Aluminum Alloy 7075-T6 chemical composition in wt% [17].

Description	Values for 2024-T3	Values for 7075-T6
Elastic Modulus (E)	72 GPa	72 GPa
Elastic Limit (Yield Strength)	345 MPa	500 MPa
Ultimate Tensile Strength	485 MPa	570 MPa
Elongation at break	18%	11%
Poisson's ratio	0.33	0.33

Table 2.3 Aluminum Alloys 2024-T3 and 7075-T6 mechanical properties [5] [10].

Table 2.3 shows that the elastic modulus for both aluminum alloys is the same. However, AA7075-T6 is able to hold more stress before failure happens.

2.1.3 Comparison of AA 2024-T3 vs. AA 7075-T6 in tensile tests

Fig. 2.1 and **Fig. 2.2** show the stress-strain curves of AA 2024-T3 and AA 7075-T6, respectively. In both figures, the upper row of strain values on the abscissa applies to both the complete true curve and the complete nominal curve. The lower row of strain values applies to the expanded portion of the curves; this expanded portion is essentially identical for both the true and nominal curves [7][18]. *Extra information to understand the difference between true and nominal stress-strain curves are found in A.1.*

For next figure (**Fig. 2.1**). Test specimen thickness, 12.7 mm. Gage length: 44.45 mm. Nominal tensile strength, 464 MPa. True tensile strength, 546 MPa. Nominal yield strength (0.2% offset), 314 MPa. Elongation (in 50.8 mm), 20.0%. Reduction of area, 27%. True strain at maximum load, 16.3%. A log-log plot of the stress-strain curve would yield a slope (n) of 0.21 in the area of uniform plastic deformation [7].

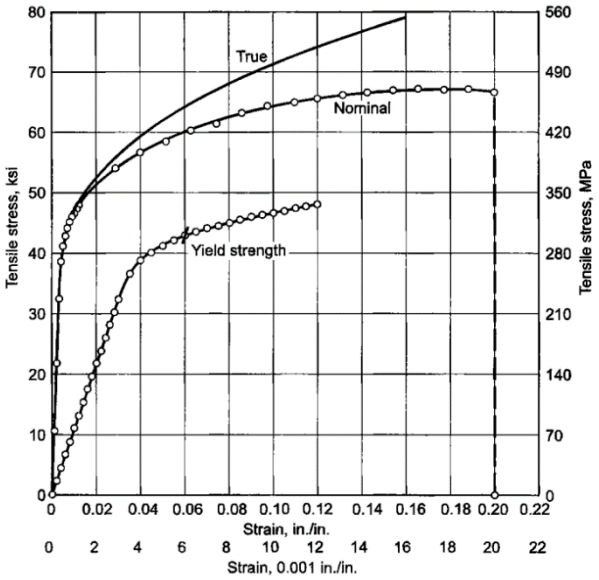

Fig. 2.1 Aluminum Alloy 2024-T3 Stress-Strain curve [7].

For next figure (**Fig. 2.2**). Test direction: transverse. Nominal thickness: 15.9 mm. Gage length: 203.2 mm. Nominal tensile strength, 600 MPa. True tensile strength, 658 MPa. Nominal yield strength (0.2% offset), 531 MPa. Elongation (in 50.8 mm), 10.0%. Reduction of area, 17%. True strain at maximum load, 9.5%. A log-log plot of the stress-strain curve would yield a slope of (n) of 0.10 in the area of uniform plastic deformation [7].

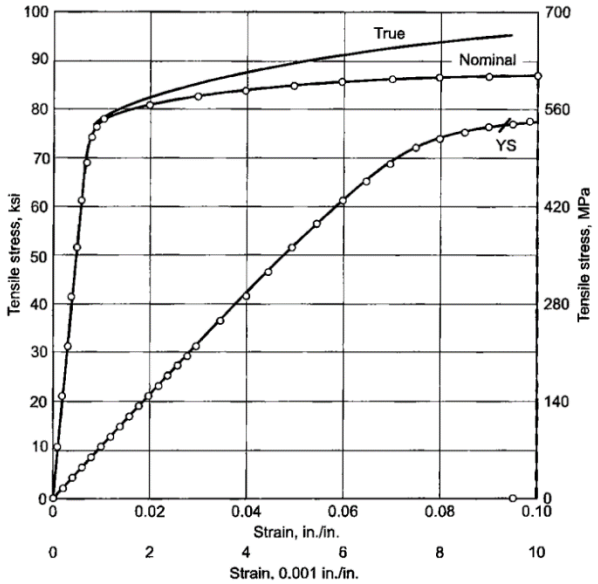

Fig. 2.2 Aluminum Alloy 7075-T6 Strain-Stress curve [7].

2.2 Adhesive

Araldite 2031, a commercial adhesive produced by Huntsman Advanced Materials, GmbH in Switzerland, is used for adhesive bonded and hybrid joints. The two-part thixotropic adhesive called Araldite 2031 is made up of resin and hardener. Because it can join materials that are similar and dissimilar while having strong chemical resistance and low shrinkage, this toughened adhesive was chosen for this thesis experiment. When the surfaces to which the adhesive is bound are thoroughly abraded and are allowed to cure for 16 hours at 40ºC, the glue performs at its optimum [11]. The mechanical properties of the adhesive are shown in the following table:

Description	Value
Elastic Modulus (E)	1.057 GPa
Ultimate Tensile Strength	21.38 MPa
Elongation at break	6.39%
Poisson's ratio	0.4

Table 2.4 Araldite 2031 mechanical properties [11].

2.3 Software

To perform the numerical part in this thesis, Abaqus is the software chosen to do this task. Abaqus CAE is a software that is used for finite element analysis (FEA) and simulation. It is part of a suite of simulation software products from Dassault Systèmes called the SIMULIA brand. Abaqus CAE can be used to model and analyse a wide range of engineering applications, including structural mechanics, heat transfer, fluid dynamics, and electromagnetics. It is a powerful tool for engineers and scientists who need to understand the behaviour of complex systems and materials.

In our case, it will only be used for static tests, initiating elastic and then plastic behaviour until the specimen finally breaks. Therefore, a heat transfer study or the application of fluid mechanics will not be necessary for this thesis.

2.4 Finite Element Method

As mentioned in the software definition, the software achieves the results requested by the FEA. The finite element method (FEM) is a numerical technique for solving partial differential equations (PDEs) that describe physical systems. It is called FEM because it involves dividing the system into a finite number of small elements, or regions, each of which can be treated as a separate unit. Therefore, those elements are so-called "finite elements" and, when connected to the nodes, the assembly is called a finite element model or mesh when working in the software, which will turn out to be the material to be analysed. These finite

elements are then used to approximate the behaviour of the original, more complex problem.

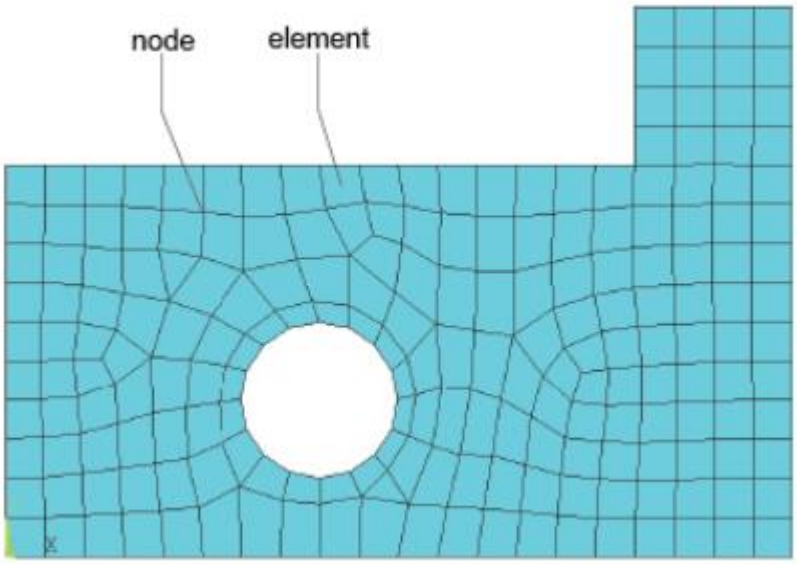

Fig. 2.3 Geometry of an object meshed [22].

The basic idea behind the FEM is to approximate the solution to a PDE over a given region by representing it as a linear combination of simple functions, such as polynomials or trigonometric functions. This allows the solution to be expressed in terms of a small number of unknown coefficients, which can then be determined by solving a system of algebraic equations.

Overall, the FEM is a powerful tool for solving complex engineering problems. It allows engineers and scientists to accurately model and analyse a wide range of physical systems, including structures, fluids, and electromagnetics.

How does it work?

Let's assume we have a continuous physical construction with a particular geometric shape, an actual physical object to work with. Then, we discretize the structure into recognizable individual components, as shown in **Fig 2.3**, whose stiffness and movements can be represented. Each node is able to translate to other location and rotate, thus they can move over 6 Degrees of Freedom, 3 translations and 3 rotations.

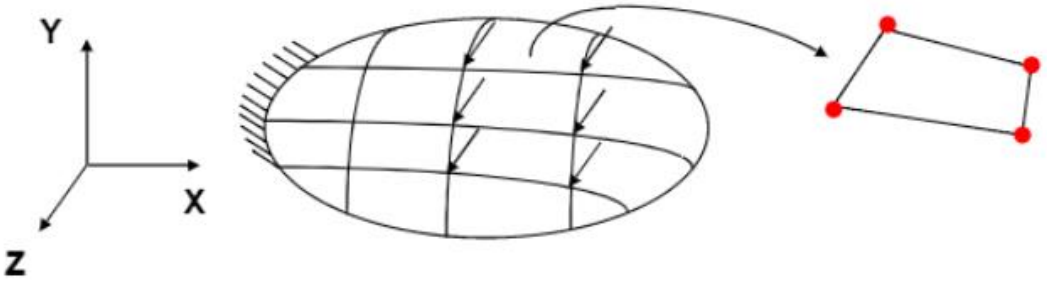

Fig. 2.4 A finite element with its 4 nodes in red [24].

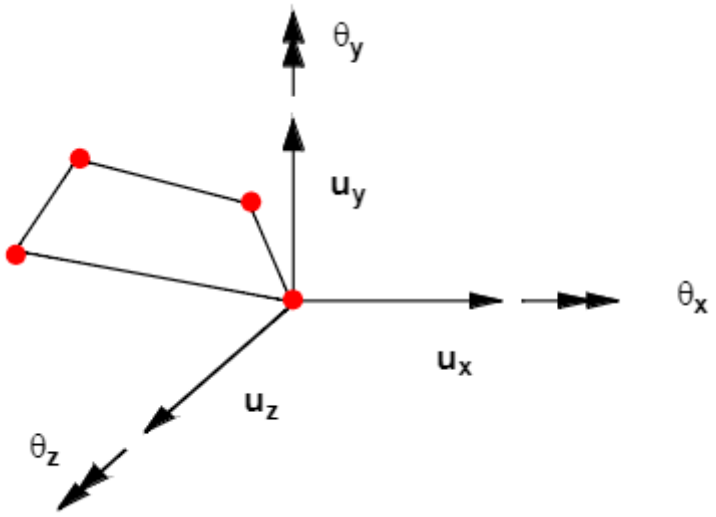

Fig. 2.5 Axis of translation and rotation of the node [24].

The displacement vector of a node can be represented as a vector of 6 elements:

$$\overrightarrow{U_n} = (U_x\,, U_y\,, U_z\,, \theta_1\,, \theta_2\,, \theta_3) \tag{2.1}$$

All structural engineering analyses must satisfy the following three general conditions, which can be used to generate a system of equations in which the displacements are unknown:

1. Forces and moments must be in equilibrium:

$$\Sigma\, \vec{F} = 0\; and\; \Sigma\, \vec{M} = 0 \tag{2.2}$$

2. Strain-displacement relations (also called compatibility of deformations). Ensures that the displacement field in a deformed continuous structure is free of voids and discontinuities.

3. Stress-strain relations (also called constitutive relations) for a linear material, the generalized Hooke's law states:

$$\vec{\sigma} = (\sigma_x\,, \sigma_y\,, \sigma_z\,, \tau_{xy}\,, \tau_{yz}\,, \tau_{xz}) \tag{2.3}$$

$$\vec{\varepsilon} = (\varepsilon_x\,, \varepsilon_y\,, \varepsilon_z\,, \gamma_{xy}\,, \gamma_{yz}\,, \gamma_{xz}) \tag{2.4}$$

$$\{E\} = matrix\ 6x6\ of\ elastic\ constants \quad \textbf{(2.5)}$$

In the context of FEA, matrices are used to represent the stiffness of the elements in the finite element model. For instance, a $\{k^e\}$ matrix can be defined, which contains stiffness values for each node. We can use Hooke's law of stiffness to relate this matrix with a nodal force and vector $\vec{u}$:

$$\vec{f} = \{k^e\} \cdot \vec{u} \quad \textbf{(2.6)}$$

Where $\vec{f}$ is the nodal forces vector, which contains forces and moments applied to the nodes of the element, $\{k^e\}$ is the element stiffness matrix, and vector $\vec{u}$, which contains displacements and rotations of the nodes of the element. If the structure has been meshed into 1000 elements, we will have 1000 $\{k^e\}$ matrices.

All $\{k^e\}$ matrices are merged into one single global stiffness matrix $\{K\}$, in a way that considers single nodes shared by 2 or more elements, which is used to relate the forces acting on the structure and the displacements resulting from these forces in the following manner:

$$\vec{F} = \{K\} \cdot \vec{U} \quad \textbf{(2.7)}$$

Where $\vec{F}$ is the force acting on the structure, matrix $\{K\}$ is the global stiffness matrix and $\vec{U}$ is the displacement after applying $\vec{F}$.

It is important to carefully consider the boundary conditions and the stiffness matrices when performing FEA, as they can have a significant impact on the accuracy and convergence of the solution. Boundary conditions are then applied to prevent rigid body motions, and the system of linear equations is solved for the unknown $\vec{U}$.

Another crucial magnitude in structural analysis is the Von Misses stress, which is a physical quantity proportional to the distortion energy. In structural engineering, it is used in the context of failure theories as an indicator of good design for ductile materials. The Von Mises stress can be easily calculated from the principal stresses of the stress tensor at a point in a deformable solid by the expression:

$$\sigma_{VM} = \sqrt{\sigma_{xx}^2 + \sigma_{yy}^2 + \sigma_{zz}^2 - \left(\sigma_{xx} \cdot \sigma_{yy} + \sigma_{yy} \cdot \sigma_{zz} + \sigma_{xx} \cdot \sigma_{zz}\right) + 3 \cdot (\tau_{xy}^2 + \tau_{yz}^2 + \tau_{xz}^2)}$$

(2.8)

CHAPTER 3. FINITE ELEMENT ANALYSIS

In this chapter, we will show and explain the three stages of FEA (pre-processing, processing, and post-processing), and relate it to the data, materials and simulation that has been performed in the software for a single lap joint, thus the rivet equivalence single lap and the realistic repair path has not the preparation explained, but FEA process is exactly equal.

This is a schematic-summary of the three phases of FEA mentioned above (blue is the pre-processing phase; green, processing phase; and orange, post-processing phase) and contains the steps of each phase in order to have a preliminary before reading the chapter:

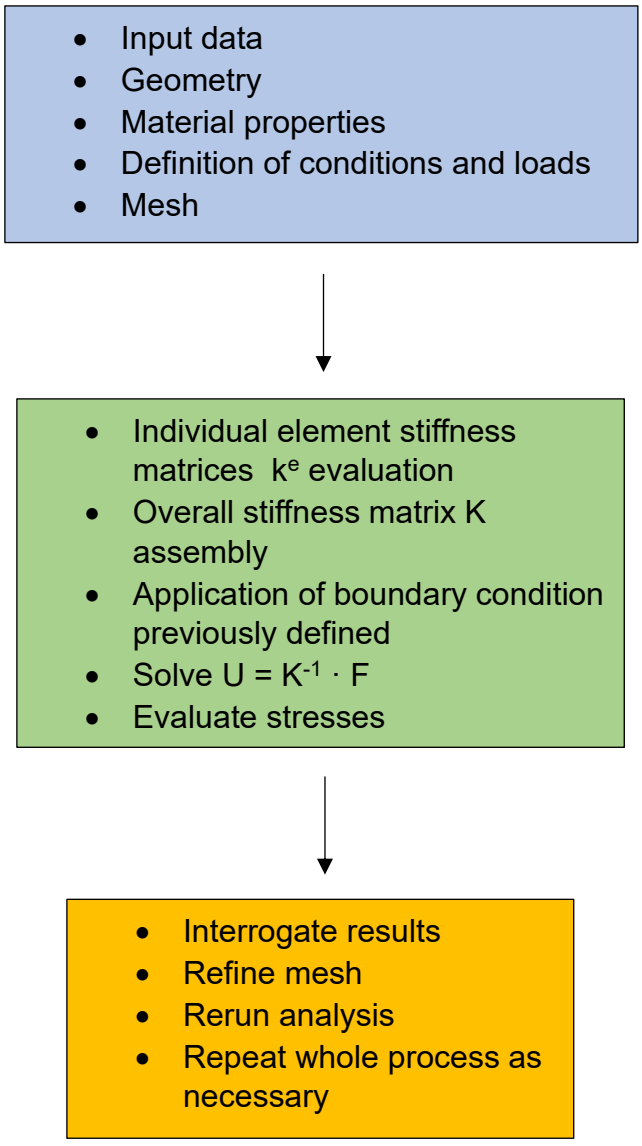

3.1 Pre-processing phase

The pre-processing, also called model preparation, is often the most work-intensive step of the FEA. At this stage, several aspects take place, which basically define the preparation prior to the simulation:

- The geometry of the problem is defined (the real object is simply designed on the computer as if it were a CAD software) and a mesh of this object is obtained based on finite elements.

- The boundary conditions are set, that is, the restricted behavior (velocity and rotation) of the nodes, and application of the forces at the points of interest.

- Definition of the materials to be worked with. For instance, different materials will have different results in a static test, temperature transmission, etc.

3.1.1 Model design and data inputs

As seen in **Fig. 3.1**, the specimen is a bar formed by two substrates or adherents (AA 2024-T3 plates) and a thin layer of Araldite 2031 adhesive between to join them. Both plates have a length of 226 mm, 25.4 mm width, and a thickness of 3 mm. The adhesive is also treated in Abaqus CAE as a thin plate with thickness of 0.25 mm and a length of 101.6 mm, while width is the same as the substrates with value 25.4 mm. It is worth to mention that the three components are joined so that the adhesive is fully covered by the alloy plates.

With the information that has been presented in the previous sections, i.e., characteristics and mechanical properties of the materials used, as well as the dimensions of the layout and boundary conditions, now we explain how the data have been entered into the program to be able to perform the simulations. Although this explanation is not an Abaqus tutorial, we will show step by step what is necessary to achieve the simulations.

To begin with, it is required to create a new project or document to create the file. The first thing to do would be to create the specimen part. As you already know, the specimen you are going to work with has an adhesive part and two substrate parts. In this step, you work with Abaqus CAE as if it were a Computer Aided Design (CAD) program, such as SolidWorks, therefore, you draw the sketch of both parts of the specimen by entering the dimensions and later making an extrusion of 3 millimeters for the substrate and 0.25 millimeters for the adhesive, the latter must be treated as a solid as well. This step is shown in **Fig. 3.2**.

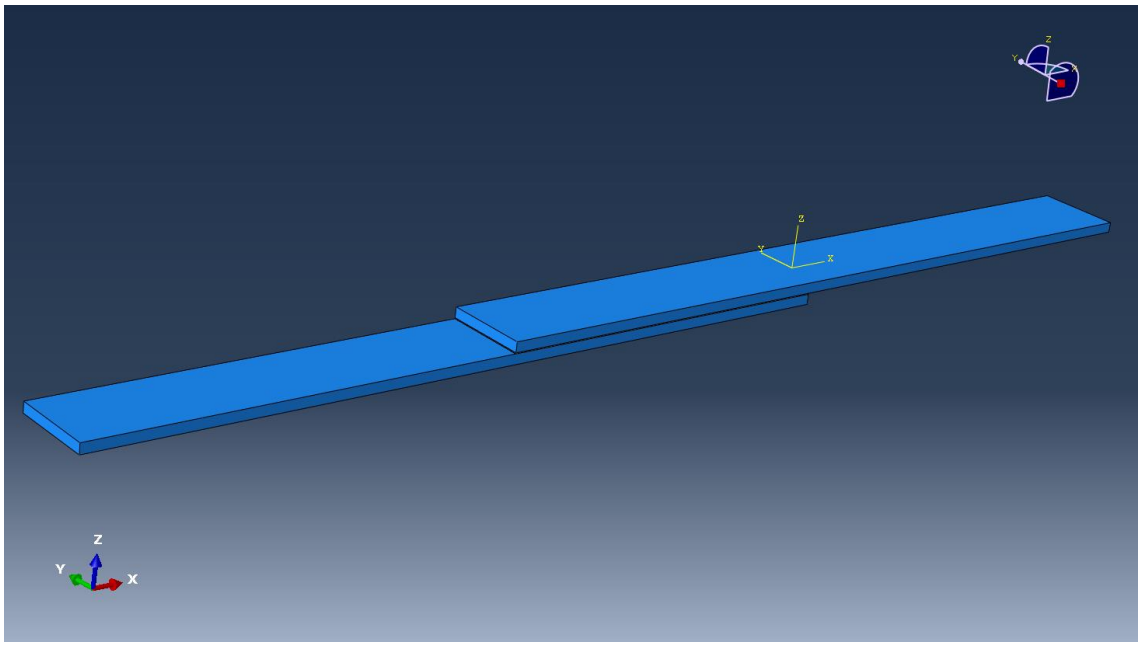

Fig. 3.1 Screenshot of the specimen designed in Abaqus CAE.

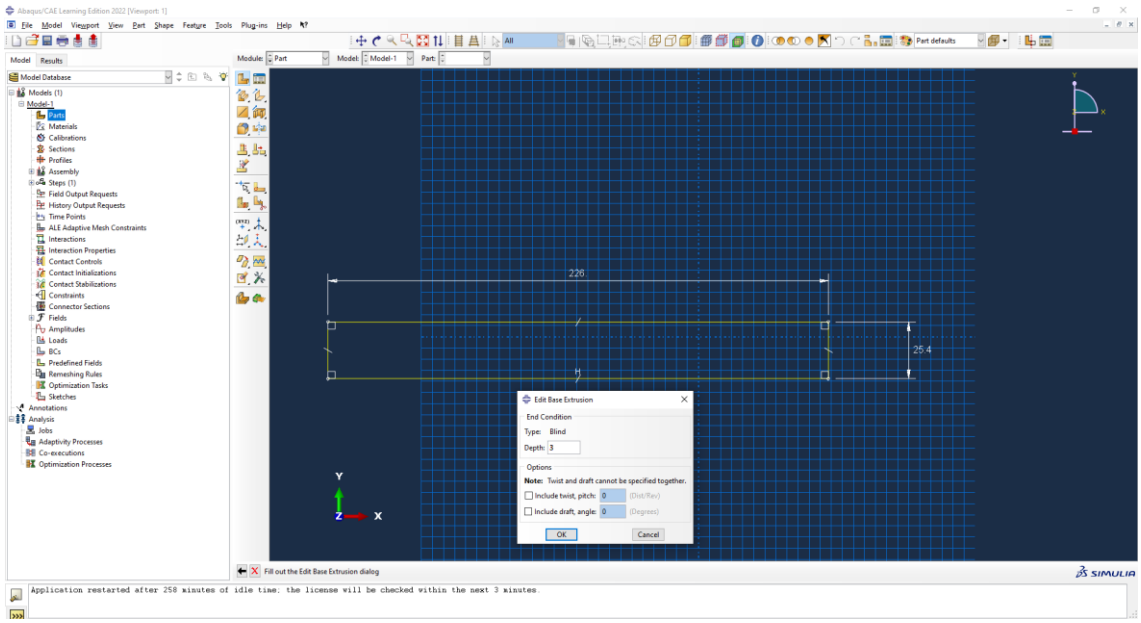

Fig. 3.2 Sketch for one substrate with the extrusion option displayed. Afterwards, the adhesive sketch must be created as well.

3.1.2 Material properties

Now it is time to present the materials and their respective mechanical properties so that the software can make the necessary calculations correctly. In this case, as discussed in previous sections, the two materials used are Araldite 2031 adhesive and aluminum alloy 2024-T3. For this step, Young's modulus and Poisson's ratio are required, at least for linear elastic behavior. Now, data such

as material density or ultimate tensile strength, the latter for plastic or nonlinear analysis, are not required. As seen in **Fig. 3.3**, the Young's modulus introduced is 72000 MPa and Poisson's ratio is 0.33.

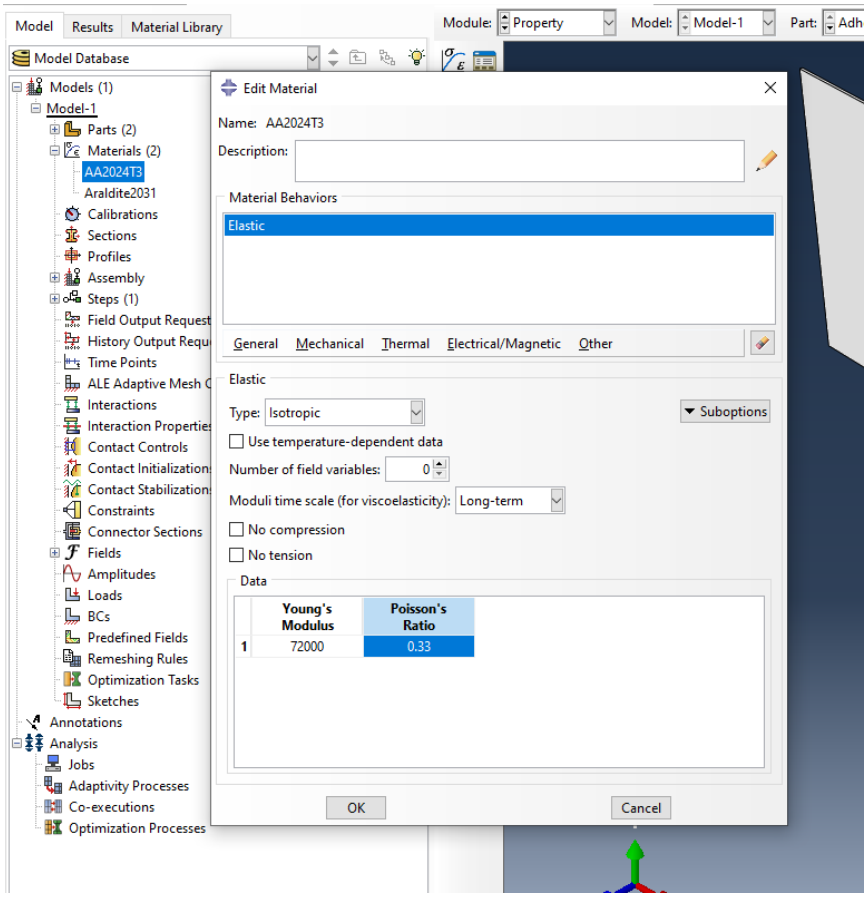

Fig. 3.3 Material properties.

Consider that Abaqus does not require physical units. This software does not ask you for units, but consistency between the entered values. In the last step, the sketch does not have units, but the dimensions are established as they were millimeters. This means that the Young's modulus is in MPa if the force applied is Newtons.

3.1.3 Sections

The so-called sections are the third module that we must create. The purpose of the sections is to define the materials that the parts of the specimen are made of. The materials established in the previous step will be assigned to the section and then the section will be assigned to specific regions of a part. Thanks to this, we can manage to obtain a part, such as a plate, that is made of different materials; one part of the plate could be made of steel and another of wood, for example. In the case of this thesis, the substrate is made of only aluminum alloy and the

adhesive is only adhesive as well, so when selecting the regions, the whole part must be selected.

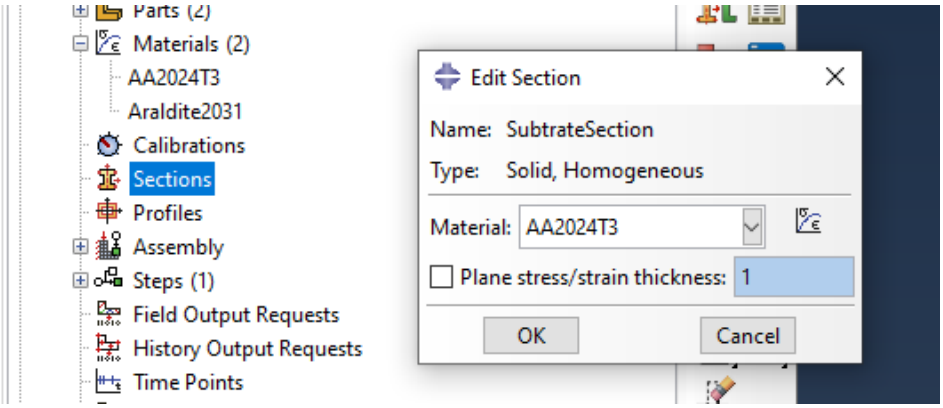

Fig. 3.4 The material for this section is the aluminum alloy.

Now we have the parts of the object and the physical characteristics and mechanical properties associated with them. But they are not yet joined together, and for this the parts must be assembled. The "assembly" module will allow us to assemble all the parts created as desired and define the set of constraints. The actual assembly is composed by three parts, but only two are created. It is just as simple as selecting the substrate part again and a copy will be displayed in the working area.

Now, all the parts are well positioned in such a way that the object to be evaluated is the one we want, as shown in **Fig.** 3.1. However, we still must define the position constraints between them. In this case, there is an adhesive that must be "attached" to the bonding surfaces. To do this, the "tie" constraint must be set to the surfaces in contact between the adhesive and the aluminum alloy. **Fig.** 3.5 shows that a main surface and a secondary surface must be chosen to define this position constraint. This step must be performed two times, one for each face of the adhesive.

3.1.4 Steps

Let's move on to the next module. A basic concept in Abaqus is the division of the problem history into *steps* (please, do not confuse these steps with the steps that one must follow to prepare a specimen, that is, each of the above-mentioned modules). A step is any convenient phase of the history, for instance a thermal transient, a creep hold, a dynamic transient, etc. In its simplest form, a step can be just a static analysis in ABAQUS/Standard of a load change from one magnitude to another. In this thesis, for the sake of simplicity, each of the steps is left with the default values imported. There is an initial step, which is the one that has no load applied to the specimen, and the following step called "LoadStep1" that is related to the loads which will be stablished in the "Load" module.

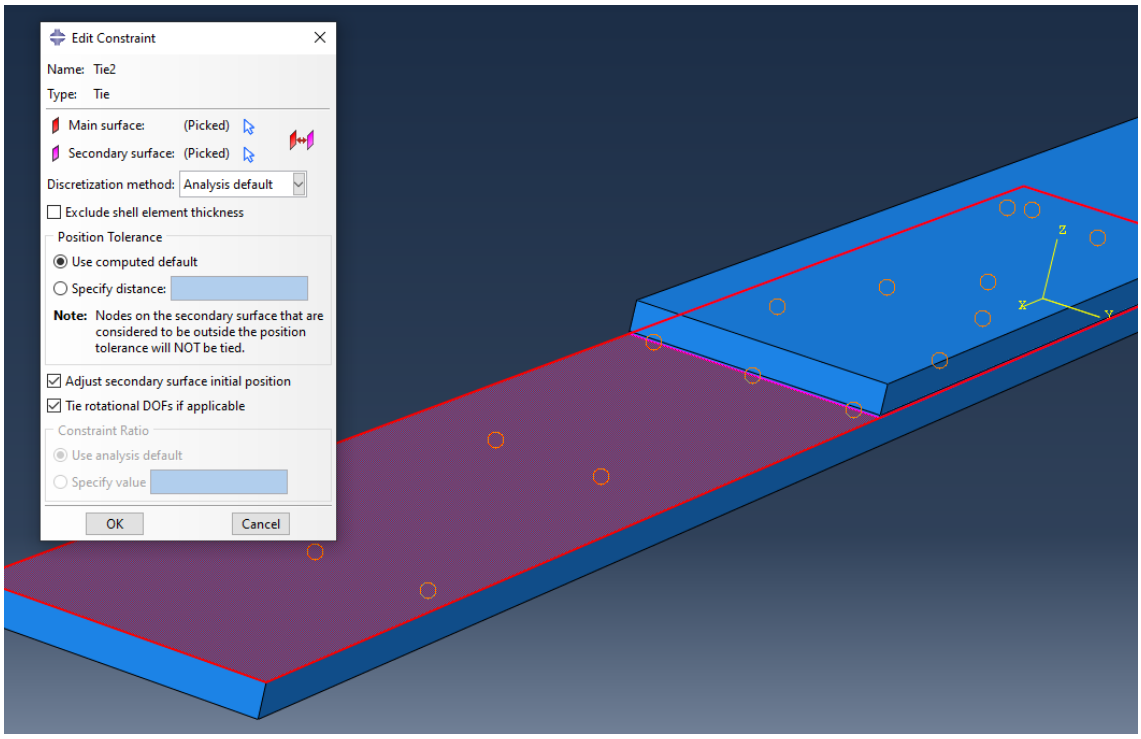

Fig. 3.5 Main surface in red, which refers to the adherent and secondary surface in purple, which is the adhesive (only one line can be seen).

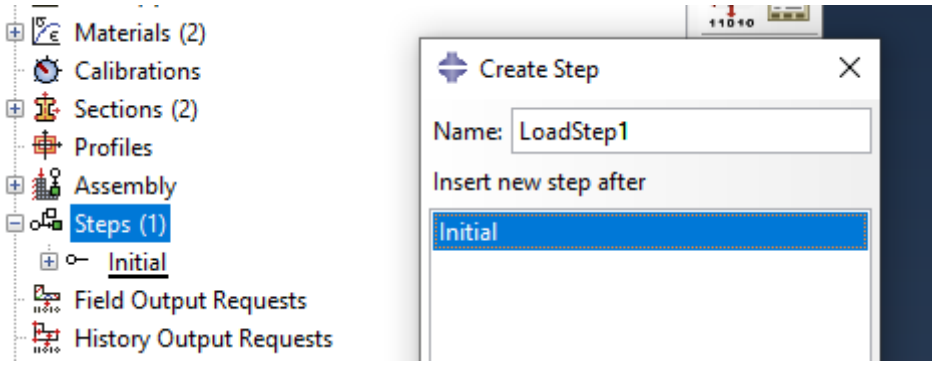

Fig. 3.6 Creation of the step called “LoadStep1”.

Note that the number of steps may vary according to the results we want to obtain. For example, the first load to be tested is 4000 N, but if after this test, we want to make another test with a load of 8000 N, a new step should be added.

3.1.5 Loads and boundary conditions

The next module to be filled in is the load itself and must be treated as a boundary condition as well. Many types of loads are available when choosing one, such as moment, pressure, surface traction, pipe pressure, gravity, bolt load and Coriolis force. For now, the pressure option is the way to go. Pressure, also called stress

or tension, in structural analysis, is a load distributed in a given area and the units would be MPa.

As we already know from physics, pressure is the force per unit area exerted by a gas, a liquid or a solid on a surface in a direction perpendicular to it. By convention, pressure is considered positive if the direction of the force vector points towards the surface resulting in compression. In this thesis, we need to pull (that is, to make a traction or tensile test to) the part, so we introduce negative pressure values to flip the vector outwards.

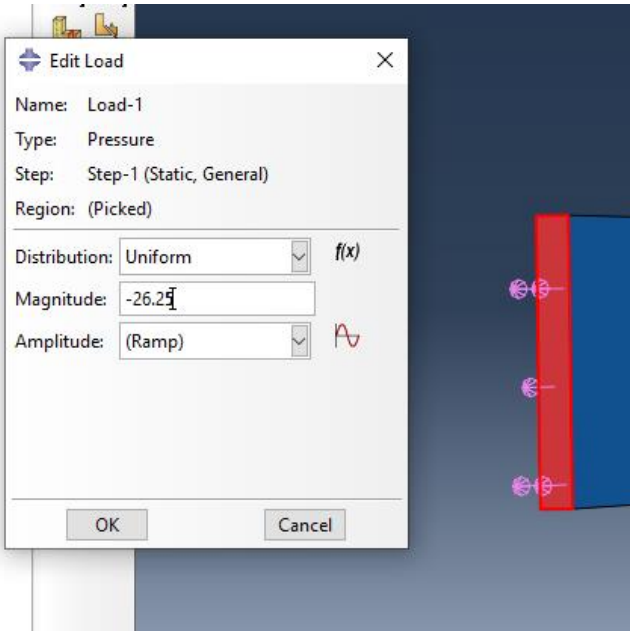

Fig. 3.7 Stress applied to extreme side of the specimen with a magnitude of 26.25 MPa and a minus sign.

The next step is to define the boundary conditions. What we want to communicate to Abaqus is that one end of the sample is fixed, it will not move, as if it were nailed to the floor or ceiling of a room. In the case of a laboratory, performing a tensile test on a UTM, it would be one of the two clamps that has no displacement, as the other would be in charge of stretching.

This option is based on the fact that the chosen surface cannot move. From a finite element analysis point of view, it is that the nodes that make up the immobile surface have 0 degrees of freedom, then the displacement vector has its 6 components equal to zero, following the form of vector number **(2.1)** in section **2.4**.

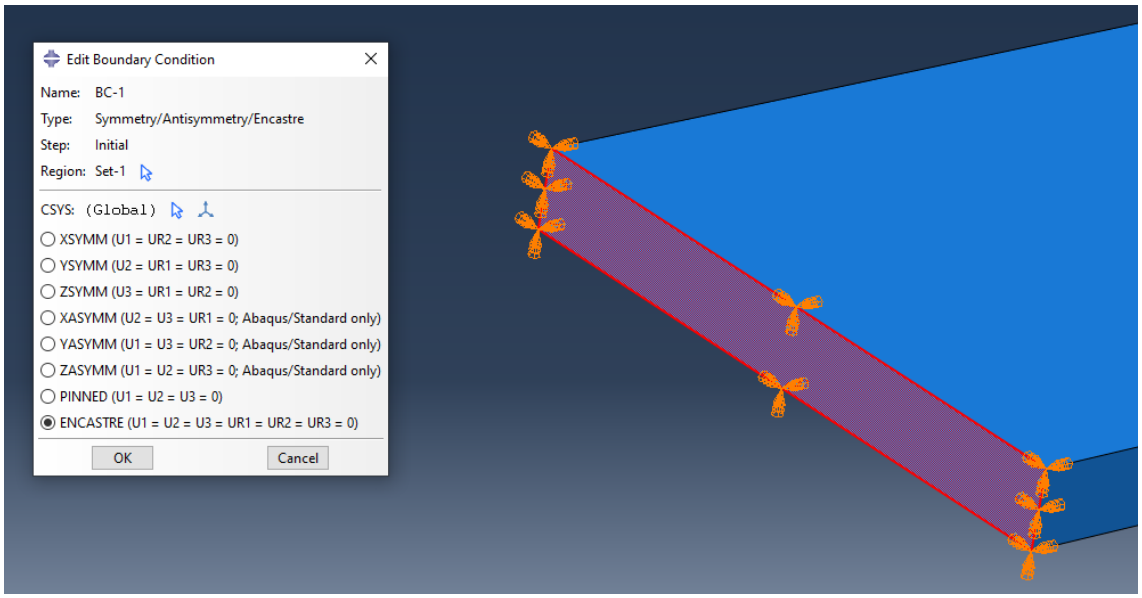

Fig. 3.8 Encastré applied in the other extreme side of the exemplar in which the displacement vector is 0, so the nodes that coincide with the selected surface will not be displaced nor rotated during simulations.

3.1.7 Mesh

As explained in section 2.4, any object or material to be subjected to FEA must be meshed. With the "mesh" option in the drop-down menu of the "part" module, we can mesh that part. Therefore, we have to mesh each of the parts that make up the specimen.

To do this, it is first necessary to determine the size of the mesh elements. The "seed" option in the toolbar at the top of the program window will be used to determine their size. However, Abaqus CAE Student Edition is limited to 1000 nodes, but it is still enough to get good results, so you should choose an approximate size of the elements so that the assembly does not exceed 1000 nodes. In **Fig.** 3.9, we can see how the overall size chosen is 7 (adimensional) for the substrate and 5 for the adhesive, resulting in a total of 912 nodes and 356 elements.

Finally, the option “mesh” will allow us to see our specimen meshed and ready to prepare the job.

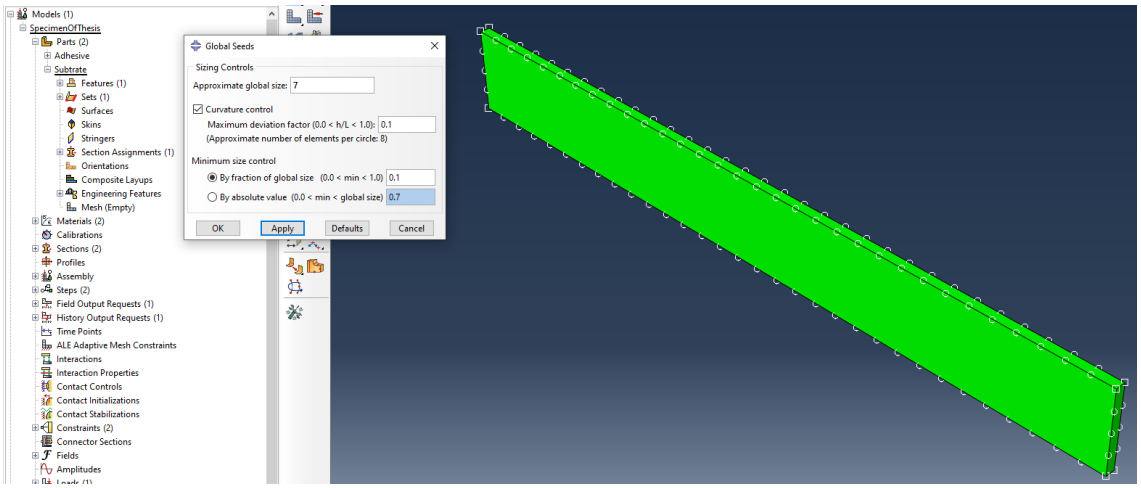

Fig. 3.9 In the pop-up window, approximate global size is 7. Next to it, the substrate being divided into elements.

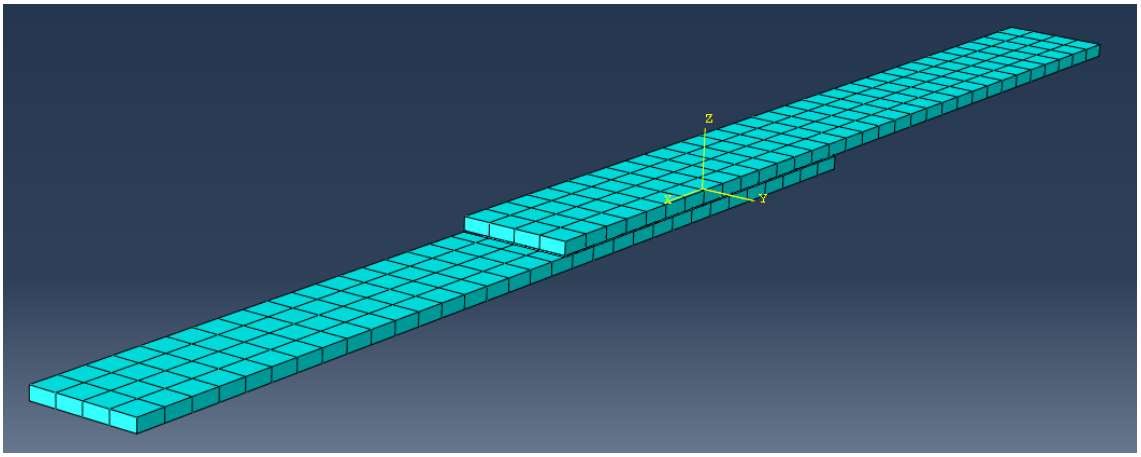

Fig. 3.10 Mesh. 912 nodes and 356 linear hexahedral elements of type C3D8R.

3.2 Solving phase with solver

In this stage, execution and calculations occur. However, it is the least work-intensive stage of FEA. The main goal of this second stage is to compute the displacement of the nodes, which can be obtained thanks to the forces, geometry, and material properties set before. After that, data, such as stresses and reaction forces, can be obtained from these displacements as well. As said, FEA gets the vector displacement from the force value entered from the user, hence the formula **(2.7)** is altered so that:

$$\vec{U} = \{K\}^{-1} \cdot \vec{F} \qquad \textbf{(3.1)}$$

Recall that global stiffness matrix $\{K\}$ needs to be assembled with the individual matrices of elements of $\{k^e\}$, explained in section **2.4**. Depending on the

complexity of the structure, many equations must be solved (let's say 1000, 10000 or 100000), but $\{K\}$ matrix will probably be banded (that is, the matrix tends to be diagonal, with more "distant" values will be equal to 0) and computational algorithms will take advantage of this fact [22].

Afterwards, the boundary conditions are applied, equation **(3.1)** is solved for the structure, and finally stresses and plots can be obtained.

With the boundary conditions, loads and physics of the problem presented, it only took about 10 seconds to get the job completed (technical specs of the computer used: Intel Core i7-4770K, Nvidia GeForce GTX 1660 Super, 12 GB RAM). The analysis to get displacements, stresses, plots, and visual deformations of the specimen is called "Job-1" as seen in **Fig. 3.11**, and it can count as the final step or final module as the ones exposed in section **3.1**.

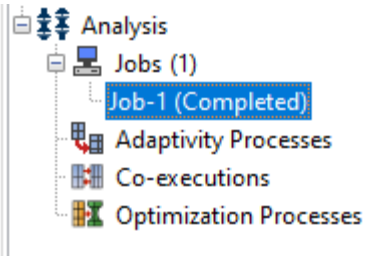

Fig. 3.11 The work is completed and ready to show results.

3.3 Post-processing phase

The results of the solution are given in the form of stress plots (maximum principal, minimum principal, maximum shear, von Mises, etc.), deformed geometry or distorted shape and listings of nodal displacements (u_x, u_y, u_z). Picture files can be created to obtain hard copies, or individual programs written to read the results file and carry out further data processing, if required.

Moreover, the user must check if results are coherent and make sense, but also may validate with a real experiment. In this stage too, the engineer can redefine the mesh and start the solver again to get finer results.

CHAPTER 4. STUDY OF A SINGLE LAP JOINT

The main objective of this chapter is to show the results of the static test simulations as well as their explanation and argumentation for a single lap joint. In addition, this chapter will be divided into four parts: asymmetric effects, Von misses' stresses depending on percentage of debonding, stresses redistribution changing adhesive to rivets (which is a more typical joining technique than adhesive bonding in aircraft) and redesigning of joint with rivets. Here is a reminder of the dimensions for the parts of the lap joint:

Part	Length	Width	Thickness
AA Plate (x2)	226	25.4	3
Araldite Adhesive	101.6	25.4	0.25

Table 4.1 Dimensions of the specimen parts, all units in mm.

4.1 Asymmetric effects

In this thesis, we have opted for the single lap type of junction. Some research already done on the single lap joint [4][23] states that, when forces are applied, the joint will behave asymmetrically, i.e., the shape will no longer have axial symmetry due to the modification of its main shape. The reason of this fact is due to the bending moment generated because of the misalignment of the tensile forces of both sides of the lap joint, causing this out-of-plane deformations [23].

Fig. 4.1 and **Fig. 4.2** show the specimen before and after applying force, respectively. On one hand, the first figure displays the specimen from the XZ plane, and the symmetric plane XY (only can be seen as a dotted line) that splits the sample into two halves. On the other hand, the second figure shows our specimen after applying force. In it, we can see the asymmetric deformation, and how the aluminum plates are bent as a "S" shape.

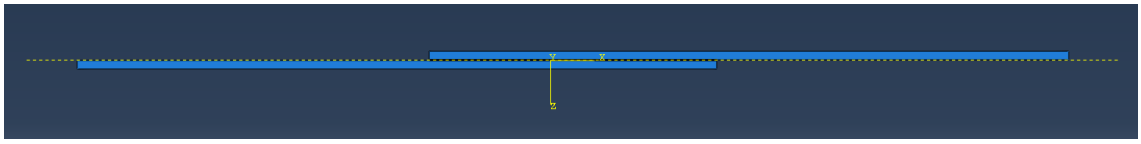

Fig. 4.1 Specimen before forces are applied; dotted line is symmetric plane.

Fig. 4.2 Specimen after forces are applied.

4.2 Distribution of debonding stresses

In this section, Von Misses stresses for debonded evolution joints are presented. The main objective of this part is to show the stress distribution of the adhesive with 0% of debonding (that is, the full area of adhesive is functional), and how the stress is redistributed in a way that the adhesive starts coming off the aluminum plates with the length reduced 10%, 20%, 30% and 40% of its total. Additionally, the forces applied have values of 2000, 4000, and 8000 Newtons.

Next three figures, (**Fig. 4.3**, **Fig. 4.4**, and **Fig. 4.5**) show the results obtained for 2000, 4000, and 8000 Newtons. The length of the adhesive at the beginning is 101.6 mm; then, it is shortened 10% (5% on both sides) and becomes 91.44 mm long; when shortened 20%, 30%, and 40%, its length becomes 81.28, 71.12, and 60.96 mm, respectively. Moreover, the remaining adhesive is placed at a centered position, as adhesive would start peeling off from both edges at the same time because of the large stresses concentrated in the edges.

The test specimen has been loaded under tensile forces in the linear elastic region, which is expected to give linear stress-strain results. And so it is. The shape of the graphs is the same, only their values increase by a factor two from **Fig. 4.3** to **Fig. 4.4**, and from this to **Fig. 4.5**. Thus, for example, at the beginning of the adhesive layer (0% in the abscissa axes), for 2000 N, 4000 N and 8000 N, the maximum values are 28.77 MPa, 57.54 MPa and 115.08 MPa, respectively. This proportional behavior is fulfilled for all debonding percentages.

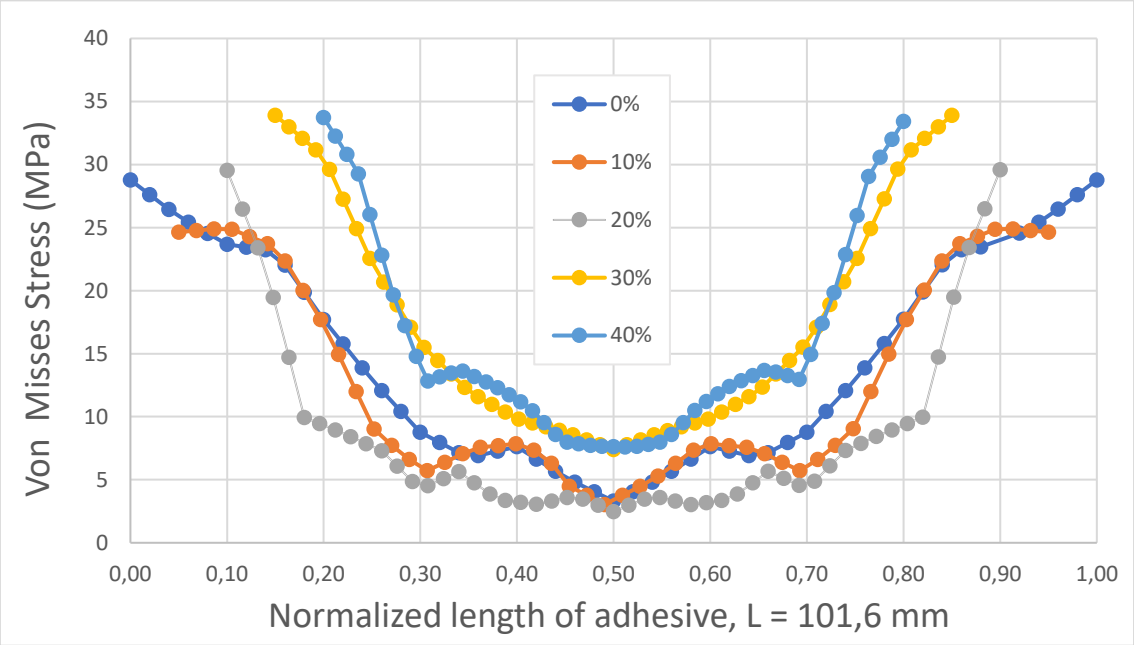

Fig. 4.3 Von Misses stresses for 2000 N.

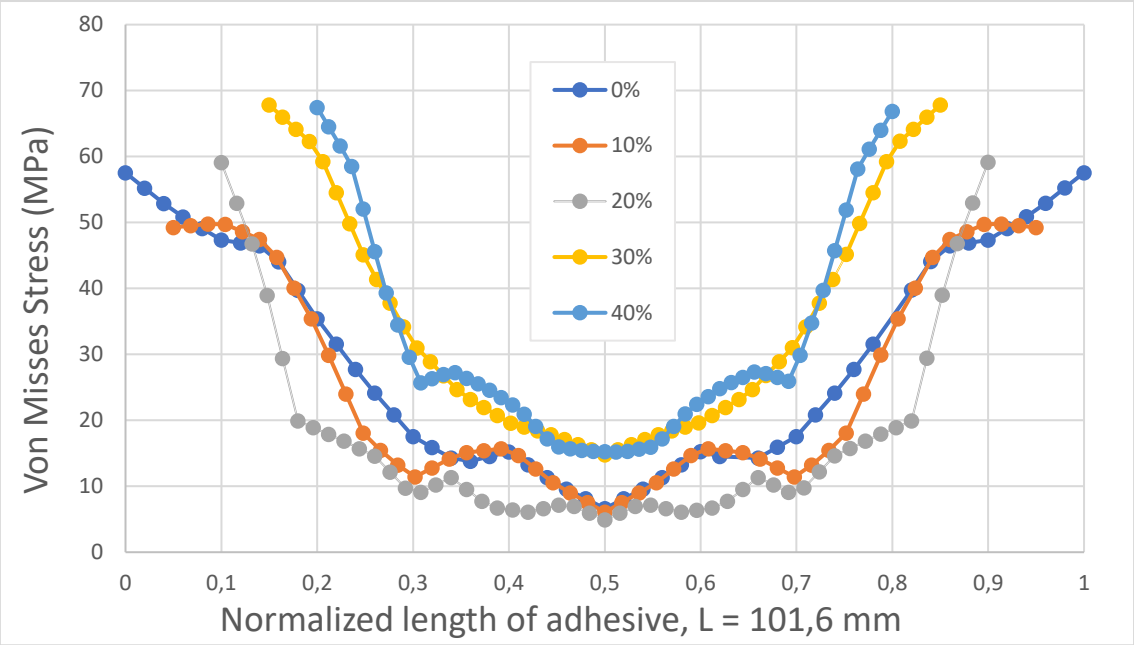

Fig. 4.4 Von Misses stresses for 4000 N.

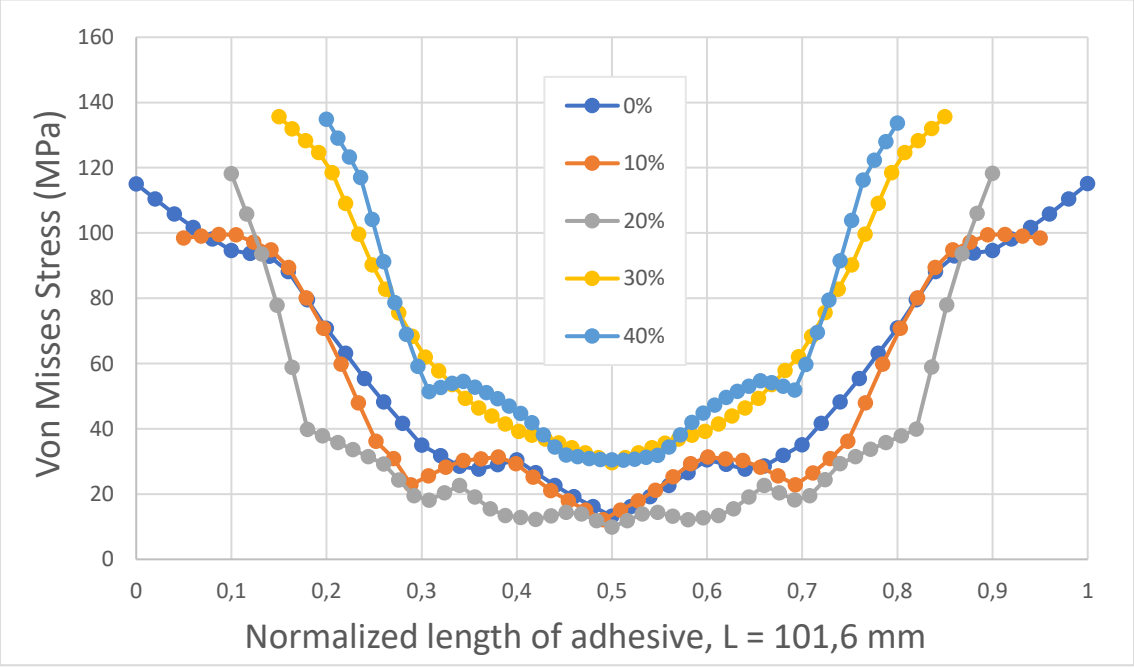

Fig. 4.5 Von Misses stresses for 8000 N.

When it comes to the stress distribution in the adhesive layer, the highest stresses are concentrated in the edges (beginning and end) of the adhesive layer, and the stress is lower as we get closer to the center, where stresses reach their mininum. Additionally, as the length of the adhesive layer becomes shorter due to debonding, the stress values tend to increase, i.e., as the adhesive layer gets shorter, the joint becomes less safe due to higher stress concentrations.

4.3 Stresses over aluminum plates

Although we want to study the performance of the adhesive bond, it is also important to comment on how the aluminum plates behaved. It was expected that the parts where the adhesive is no longer adhered are not stressed. From a structural point of view, these parts are not working.

Fig. 4.7 shows the stress over the aluminum plates of our specimen with a tensile force of 8000 N. The results for other tested loads, such as 2000 and 4000 N, are not shown because results are proportional, and hence the shape of the plots is qualitatively the same. In the figure, five graphs are displayed, which refer to the five states of the aluminum suggested before. Three clearly differenced sections can be seen.

Starting from the right-hand side, the aluminum undergoes a constant stress of about 105 MPa for all five configurations. To move on, the left part shows that for peeled adhesives, the aluminum suffers very little stress compared to 0%, it is reduced with the evolution of breakage, i.e., such part of the aluminum ceases to have contact with the adhesive and is not stressed and thus it is not stretched as well; in other words, with each reduction of effective adhesive length, this part of the aluminum finds it more difficult to achieve significant stress (that is, to be loaded). From a numerical point of view, for L_{plate} = 0 mm, it is seen that with the fully functional adhesive there is a stress of about 73 MPa; for the plate with 10% of the adhesive peeled, the stress is 17 MPa; and for the other samples with peeled adhesive, the stresses are in the order of 1 MPa. To begin with, the results for the sample with 0% of peeled adhesive do not follow a straight line, there are scattered values instead, and it is difficult to identify any clear pattern in the stress values or any empirical expression that could fit these scattered values. For the other samples, the stress vs adhesive length shows similar trends: it increases near the edges and is quite constant in the central sections. The sample with 30% of adhesive peeled is an exception, as it shows stress values higher than in the other cases. We have not found an explanation to the distinct behavior of the results for the samples with 0% and 30% of adhesive peeled. The stress values in the central sections are: for 10%, 60 MPa; for 20%, 54 MPa; for 30%, 77 MPa and two peaks at l = 0.12 and l = 0.5 with values 90 MPa both; for 40%, 60 MPa.

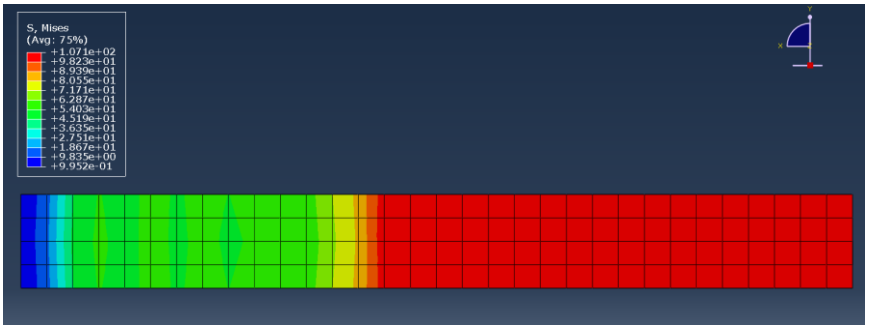

Fig. 4.6 Visual example of stress distribution from user's view (8000N@20%).

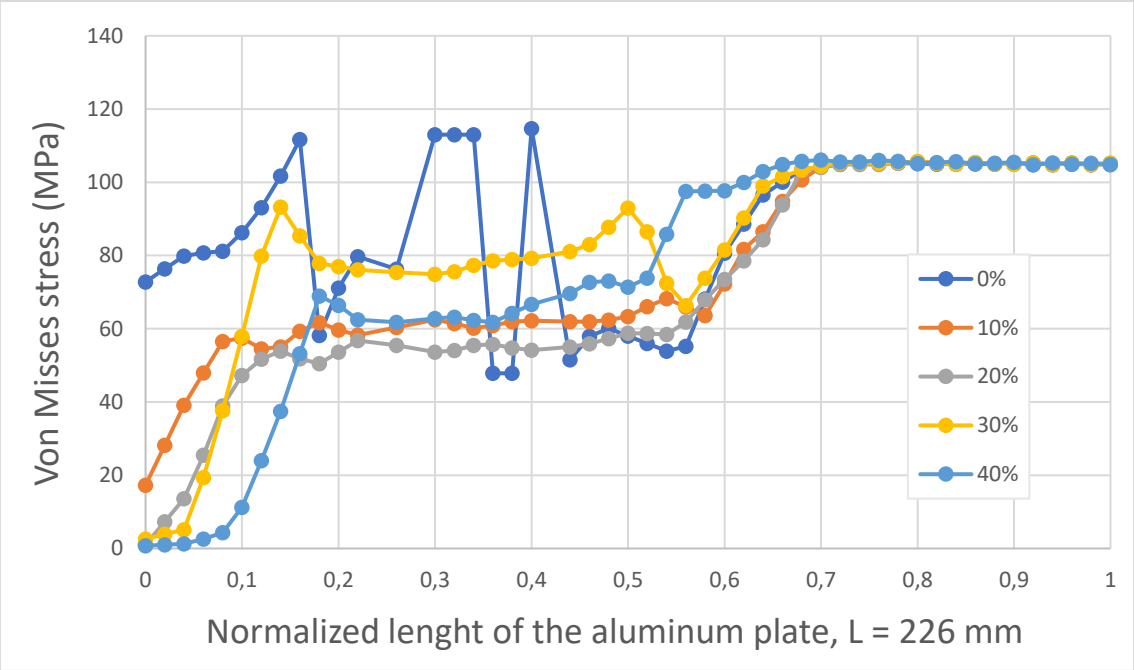

Fig. 4.7 Stresses along the aluminum plates.

4.4 Stress-elongation relation

In this section, the stress response vs. elongation is shown. In this thesis, only the linear regime of the stress-elongation curve has been considered.

We already know that the applied force is 8000 N, results in approximately 105 MPa, which is the force limit of the simulation, and, therefore, is the highest value for the stress in **Fig** 4.8 and it is accomplished for the five models under static tests.

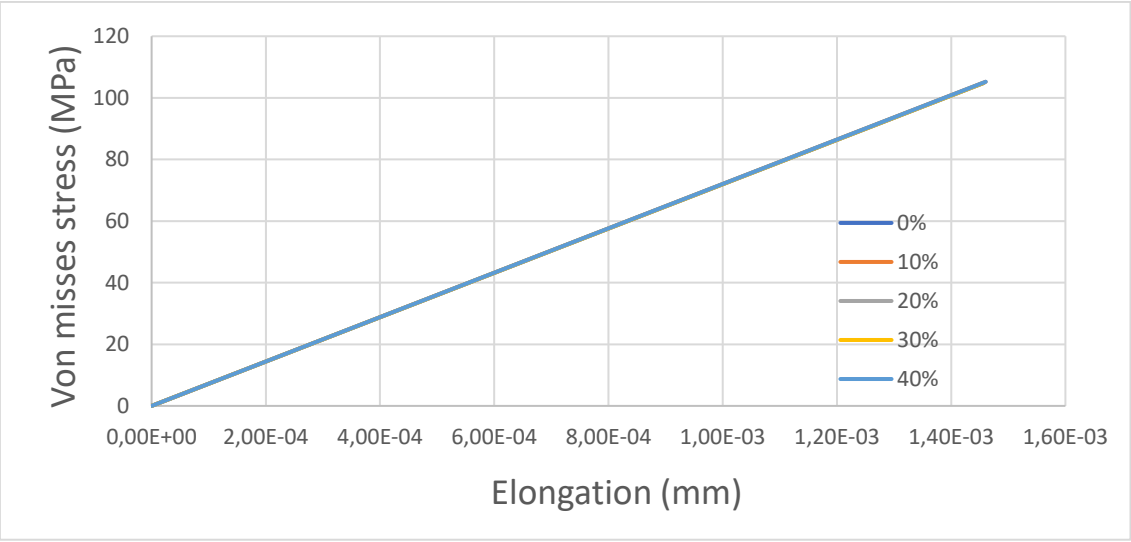

Fig 4.8 Stress-elongation relation of the test specimen.

The elongation values obtained are very similar for the different adhesive configurations. Since the differences are very small, the five plots are superimposed. The following **Table 4.2** shows the values for each simulation to see the numbers in detail.

% peel	0%	10%	20%	30%	40%
Elongation (10^{-3} mm)	1.45728	1.46029	1.45687	1.45658	1.46054

Table 4.2 Elongation of the specimen at 8000 N.

The elongations obtained do not follow any logical order and it is difficult to draw a solid conclusion, since, for example, the elongation for the 10% configuration is longer than for the 20% configuration. Furthermore, the elongation for 20% is longer than that for 30%. However, the 0% with respect to 10% is shorter than the latter. The normal behavior would be for the elongation to become longer, shorter, or remain constant.

At this point, we can only argue what could have been the errors introduced for the result not to be good or not to be as expected. One reason could be the modification of the meshes; to create the different lengths of the adhesive, its sketch is modified and consequently, its mesh and nodes, and their quantity is not proportional to the sizes introduced. Another reason may be that, seeing that the results are very similar, we can assume that the elongation is the same for all, so it remains constant for all configurations, but that the calculation has introduced error and makes this supposed constancy vary a little.

$$Diff\% = \frac{1.46054 - 1.45658}{1.45658} \cdot 100\% = 0.27\% \qquad \textbf{(4.1)}$$

Formula **(4.1)** shows the largest variation comparing the highest value with smallest value from **Table 4.2**.

4.5 Rivets equivalence

The use of rivets in aviation is much more common than adhesive to make joints. Although this thesis is focused on adhesive joints, it is interesting to observe the stress distribution if the single lap joints were joined with rivets instead of adhesive. To carry out the transformation and achieve equivalence, the stress of the adhesive would have to be distributed to certain points, which would be the rivets.

The riveted specimens used in this work are designed in accordance with Federal Aviation Administration (FAA) regulations of aircraft maintenance [1]. In these regulations, the design of aircraft riveted joints is based on rivet diameter D. The standards set by the FAA suggest a minimum rivet pitch (distance between rivets)

of 3D, but an average of 4D to 6D between rivets. A minimum rivet-edge distance of 2.5D should be maintained between edges of the joint and rivets.

Therefore, for our specimen joint change, with rivets of diameter of 4.8 mm, the distances elected for the study are 5.3D for the rivet pitch and 2.65D for the rivet-edge distance. This way, the study and the layout of the sample are accomplishing FAA safety regulations. Additionally, as the adhesive is 101.6 mm, 4 rivets would fit perfectly in the joint zone, that is, as shown in the **Fig.** 4.9, a spacing of 25.4 mm between rivets is the obtained distance between rivets (5.3 times 4.8 mm) and 12.7 mm as rivet-edge length (2.65 times 4.8 mm) and the material is AA 2024-T3, same as the plates. Moreover, the four holes that house the rivets would be drilled with a diameter of 5 mm in order for the rivets to fit properly [11]. Dimensions of the aluminium alloy plate are kept (226 mm long x 25.4 mm wide x 3 mm thick).

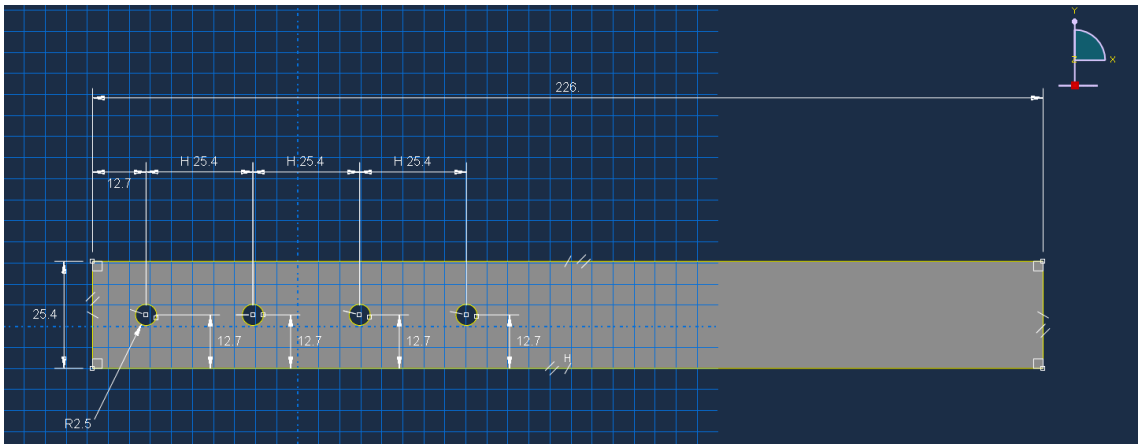

Fig. 4.9 Aluminum alloy plate sketch.

4.5.1 Results for the simulation of the static test

The static test was carried out in the same way as for the adhesive bonded specimens. The same boundary conditions were defined and with the dimensions already established above. Since this is linear static test, it does not matter whether the rivets are made of AA 2024-T3 or AA 7075-T6, as they have the same Young's modulus (72 GPa) discussed in section 2.1.2. However, only one test was performed for a single force of 8000 N, as opposed to the three tests with load 2000, 4000 and 8000 N done before, since the results will only differ in terms of linear proportion, so the shape of the graphs are the same. **Fig.** 4.10 shows the results obtained for the single lap joint with rivets:

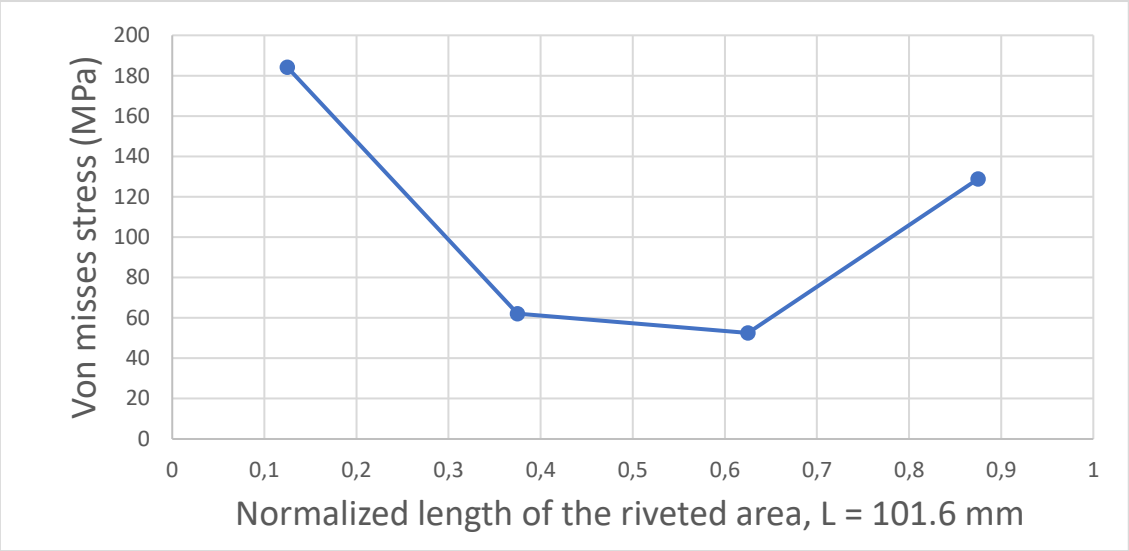

Fig 4.10 Stresses on the rivets.

The results obtained for the stress distribution of the riveted samples is reminiscent of the stress distribution of the adhesive bonding or any type of bond (that is, higher stress values on both edges, and minimum in the middle of the sample), except that in this case the stress is not distributed over a surface but on determined points, these being the rivets. As seen in **Fig.** 4.10, rivets have approximate stress values of 184 MPa, 62 MPa, 53 MPa and 129 MPa, from left to right. The load is distributed in a way that first rivet withstands 43.1 %; second, 14.5%; third, 12.4%, and last one, 30.2%.

Not only are the rivets subjected to shear forces, but also the aluminum plate around the rivet in the riveted area is stressed by the direct contact of the fastener. As seen in **Fig.** 4.11, the plate stress is distributed in such a way as if the riveted hole was a "stress source", unlike the adhesive bond which was intended to be constant as shown in **Fig.** 4.6 and **Fig.** 4.7.

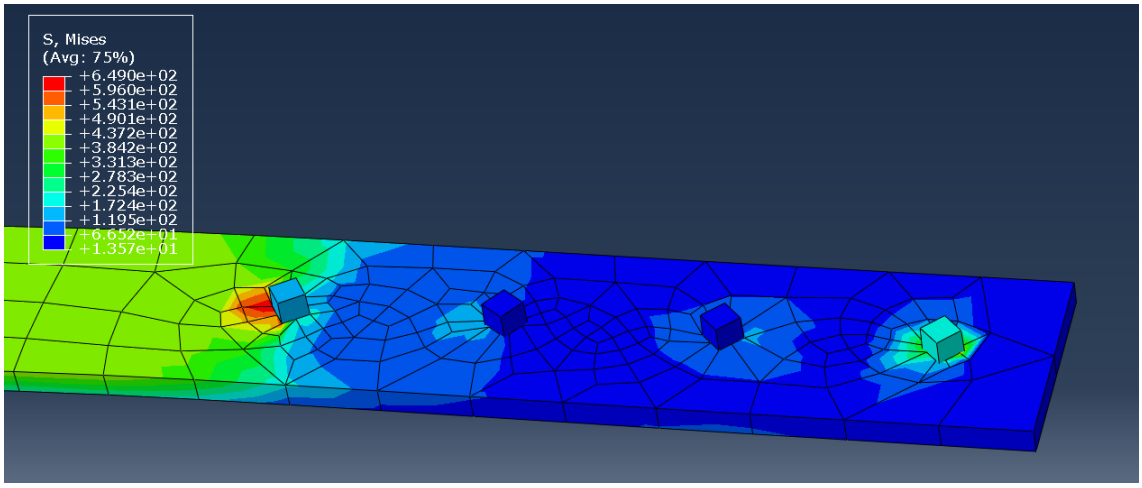

Fig. 4.11 Colored-based stresses over one plate and rivets.

4.5.2 Mesh selection. Poor mesh vs. good mesh

Obviously, since this is a FEM-based exercise, the mesh for the riveted specimen must be defined. Depending on the number of elements and nodes and how they are distributed, the results will be more or less close to reality. Unfortunately, Abaqus Learning Edition is limited to 1000 nodes, which makes it really difficult to get to an accurate result or not getting errors while submitting the job.

The mesh for the specimen used in this simulation is composed by 968 nodes with 400 elements (396 linear hexahedral elements of type CSS8 and 4 linear hexahedral elements of type C3D8R). The rivet has a mesh size of 100 and the mesh size chosen for the plate is 11. Consequently, the mesh that we got with these parameters is the one shown in **Fig. 4.12**, which is dissimilar from the ones that can help obtaining improved results (actually, an example of the meshes that an engineer would prefer is shown in **Fig. 4.13**). The rivets become four cubes or dices as the design of them is overly simplistic as well to fit in the Abaqus Learning Edition.

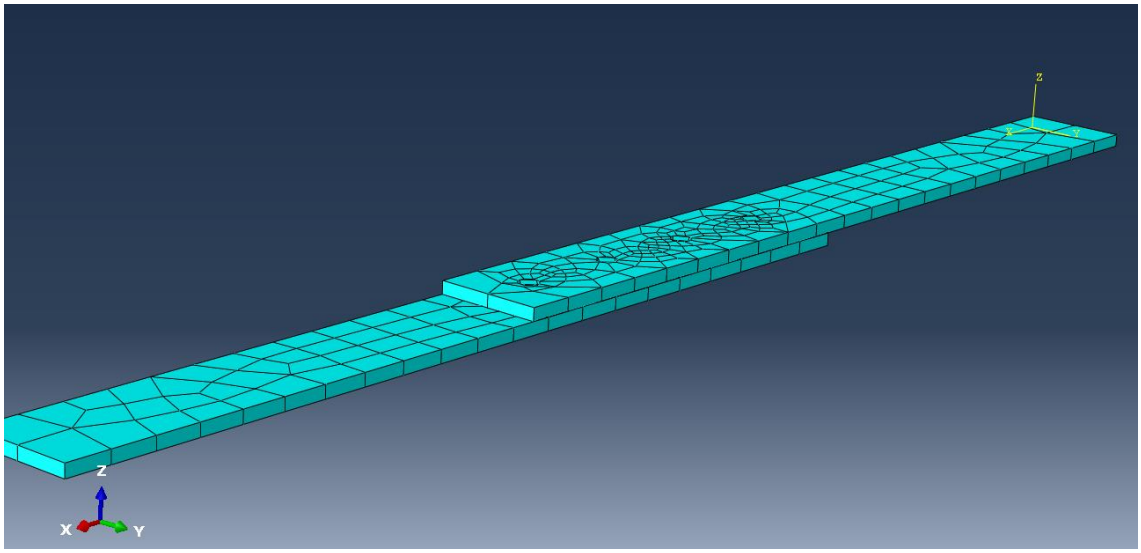

Fig. 4.12 Riveted specimen meshed.

Fig. 4.13 displays an example of how a good mesh for the riveted specimen. It is composed by 15454 quadratic tetrahedral elements of type C3D10 that sum up a total of 28106 nodes, which clearly surpasses the limit imposed by Abaqus Learning Edition and we cannot do these simulations. However, the results would be more accurate to reality and computing time would be longer.

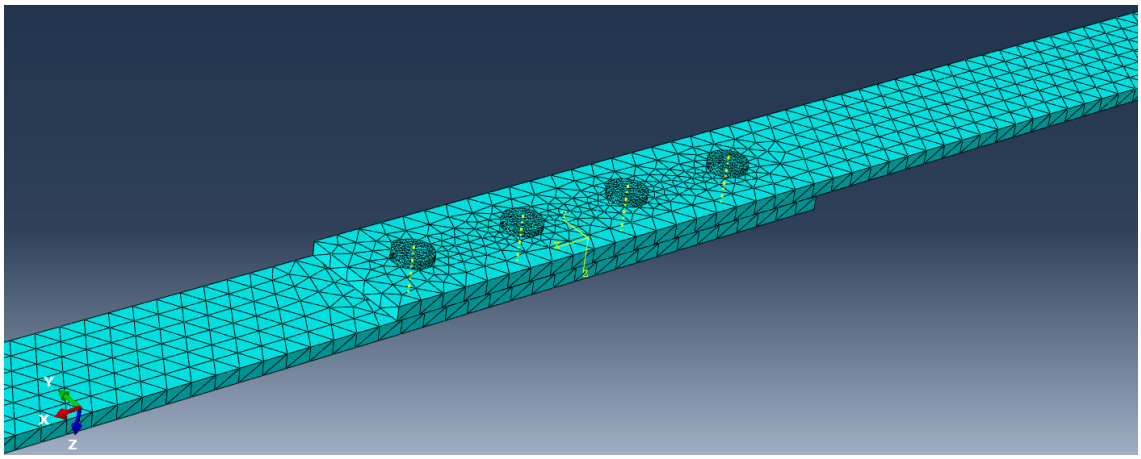

Fig. 4.13 Riveted specimen properly meshed.

CHAPTER 5. STUDY OF A REALISTIC REPAIR PATCH

The main objective of this chapter is to show the results of the static test simulations as well as their explanation and argumentation for a realistic repair patch, which is usually formed by two or three doublers one on top of each other joined to the fuselage (see **Fig.** 1.7). Three simulations were carried out in this chapter, obtaining three results for one doubler, for two doublers, and three doublers on top of the substrate plate (that would correspond to the fuselage of the aircraft), in order to compare them and maybe perceive differences on shear stresses. The adhesive #1 joins the doubler number #1 with the plate, adhesive #2 joins doubler #1 with doubler #2, and adhesive #3 joins doubler #2 with doubler #3. This is not actually a joint since it is not about joining two different plates.

Part	Length	Width	Thickness
AA Plate	300	25.4	3
Doubler #1	200		
Doubler #2	150		
Doubler #3	100		
Adhesive #1	200		0.25
Adhesive #2	150		
Adhesive #3	100		

Table 5.1 Dimensions of the specimen parts, all units in mm.

Fig. 5.1 First model.

Fig. 5.2 Second model.

Fig. 5.3 Third model.

5.1 Asymmetric effects

Fig. 5.4 and **Fig. 5.5** show the specimen before and after applying force, respectively. On one hand, first figure displays specimen from XZ plane, and the symmetric plane XY (only can be seen as a dotted line) that cuts sample into two halves. On the other hand, second figure shows our specimen after applying force. In it, we can see the asymmetric deformation, and how the aluminum plates are bent as a "U" (i.e., the so-called out-of-plane deformation). All three configurations with one, two or three doublers have asymmetric effects, but only third configuration is shown.

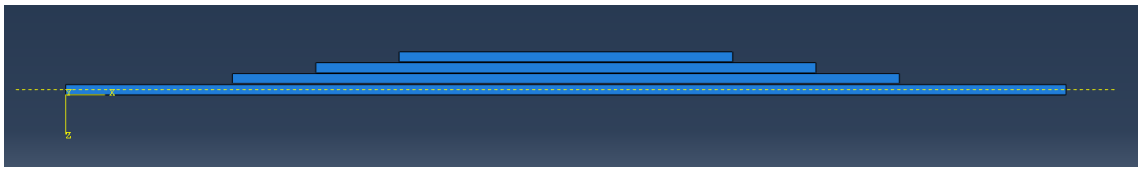

Fig. 5.4 Specimen before forces are applied; dotted line is symmetric plane.

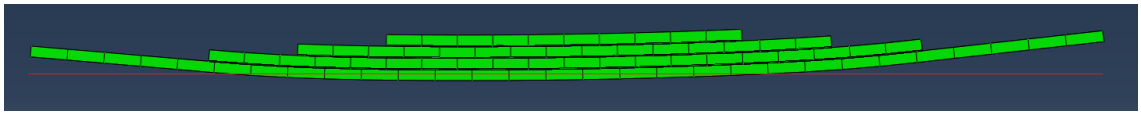

Fig. 5.5 Specimen after forces are applied.

5.2 Stresses over plate

In this section, we will see how the stresses are distributed in the substrate plate of the three simulated models, and comment on the graphs and results obtained. A tensile force of 8000 N has been used for the calculation of the results shown in **Fig. 5.6**.

At first glance, the results for simulation #1 is different from the results for simulations #2 and #3. The sections of the substrate plate in simulation #1 would be subjected to a constant 105 MPa stress, while in the other simulations there would be a decrease in stress in the doublers area, because the doublers carry load, and thus the load carried by the substrate decreases. However, in those sections where the main plate is not covered by doublers, the Von misses stress is 105 MPa for all three models.

In the case of the second model, the stress decreases to a constant value of 88 MPa from l = 0.3 to l = 0.7, and for the third model the minimum stress zone, which is about 73 MPa, is between *l = 0.4* and *l = 0.6* (seems that the more doublers there are, the more the load is distributed among them and, therefore, the less load the main board receives, since it is distributed among the doubler). This characteristic is interesting when deciding how many doublers the repair patch should have, since the center of the patch is where the structural damage

to be repaired is located and, therefore, receive a smaller or decreased load so that the crack does not become larger. Thus, the engineer or maintenance technician must make a trade-off between using more material (more expensive) and protecting more or using less material (cheaper) and being less safe.

In the right part of the plots, the stress is no longer constant or changes abruptly. This is due to the boundary conditions of the Abaqus program which may not be appropriate, yet it does not affect the results or the overall conclusion.

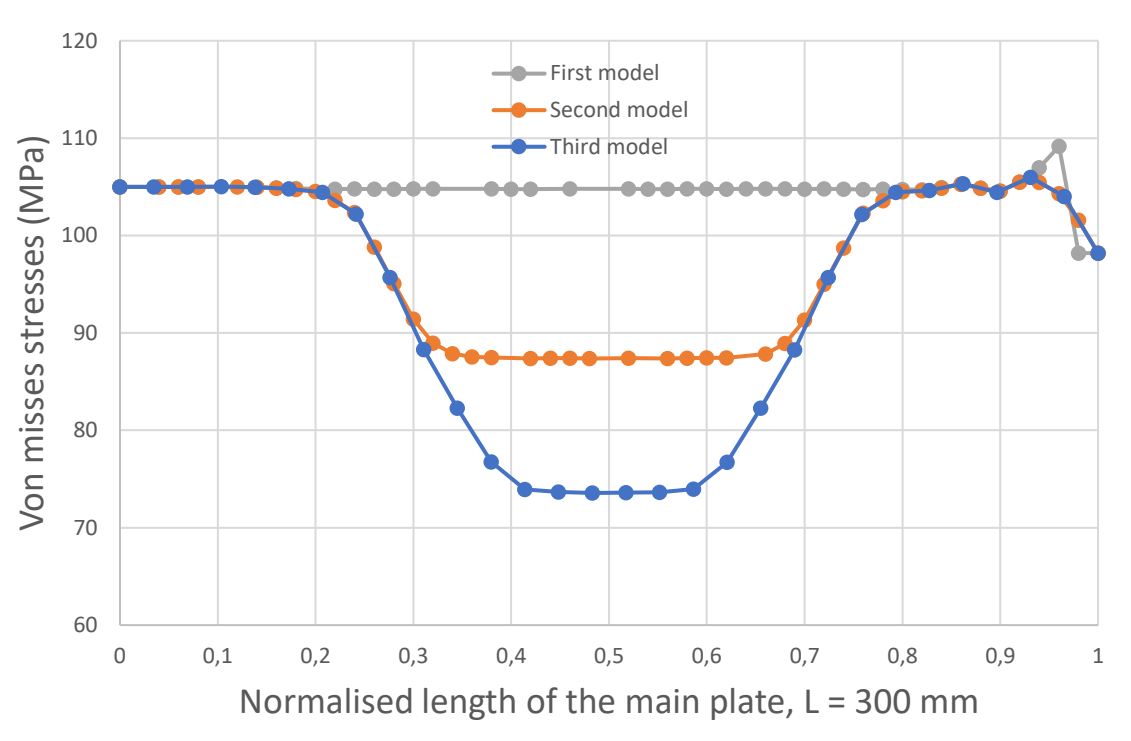

Fig. 5.6 Stress distribution over the substrate plate in the simulations.

5.3 Stresses over adhesives

In this section, we will see how the stresses are distributed in the adhesive layers of the three simulated models, and comment on the graphs and results obtained. A tensile force of 8000 N has been used for the calculation of the results. The legends of the graphs show “Adhesive #1”, “Adhesive #2” and “Adhesive #3”, referring to the 3 adhesive layers used and presented in **Table 5.1**, **Fig. 5.1**, **Fig. 5.2** and **Fig. 5.3**.

As expected from the previous results, the stress is not distributed uniformly. The adhesive close to the edges is more stressed than that in the middle zone. In **Fig. 5.7**, highest values are located at $l = 0$ and $l = 1$, where they reach 0.835 MPa and 0.81 MPa. In the mid-zone (from $l = 0.35$ to $l = 0.65$), a constant stress 0.77 MPa is observed. Although the Von Misses stresses distribution looks like the classical joint distribution with a second order polynomial shape, the maximum value and minimum value are not that different:

$$Diff\% = \frac{0.835\ MPa - 0.770\ MPa}{0.835\ MPa} \cdot 100\% = 7.78\% \quad \textbf{(5.1)}$$

This means that in a practical case there would not be much difference in the stress in the edges of the adhesive layer compared to the middle zone, so the load transfer is quite homogeneous, even though a maximum and a minimum exist. Additionally, this could be related to the result obtained for the first simulation (see **Fig. 5.6**), which shows that the main plate suffers a constant stress, meaning that the almost-constant response of the adhesive is a consequence of the fact that the plate, the adhesive and the doubler behave as a solid bar where there is a constant stress in each cross-sectional plane.

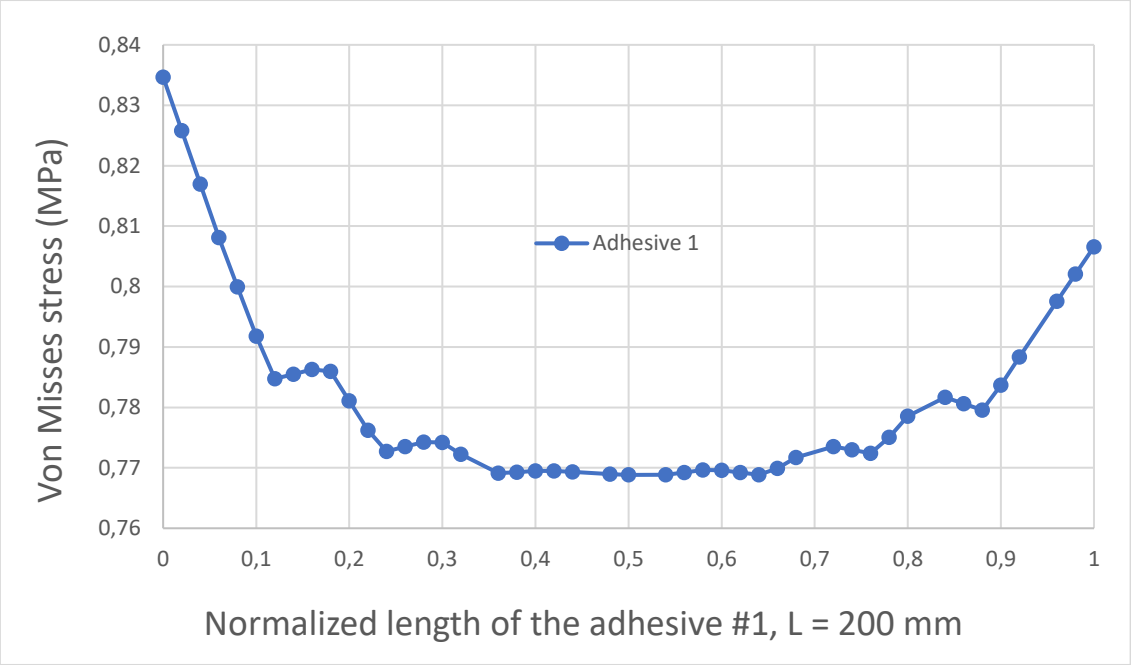

Fig. 5.7 Stresses distribution for adhesive #1.

Fig. 5.8 shows the results for the simulation of the second model. Adhesive #2 has a typical shear stress distribution response, although the smaller values are fairly equal and remain constant at approximately 0.5 MPa. On the other hand, adhesive #1 also has a classical stress distribution between *l = 0.2* and *l = 0.8*, but the stresses decrease considerably when approaching the edges.

On the other hand, stresses distributions of adhesive layers in model #3 shown in **Fig. 5.9**, adhesives #1 and #2, behave the same as in model 2, however, adhesive #3 is constant with values around 0.07 MPa. The plots of adhesives #1 and #2 wave a little without losing the explained shape.

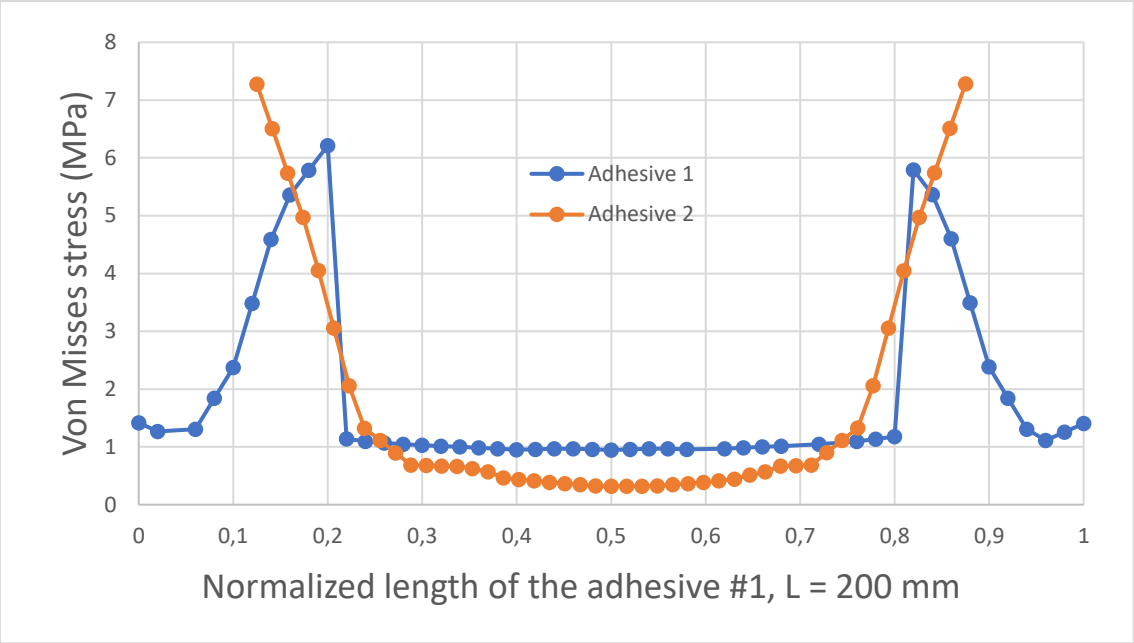

Fig. 5.8 Stresses distribution for adhesives #1 and #2.

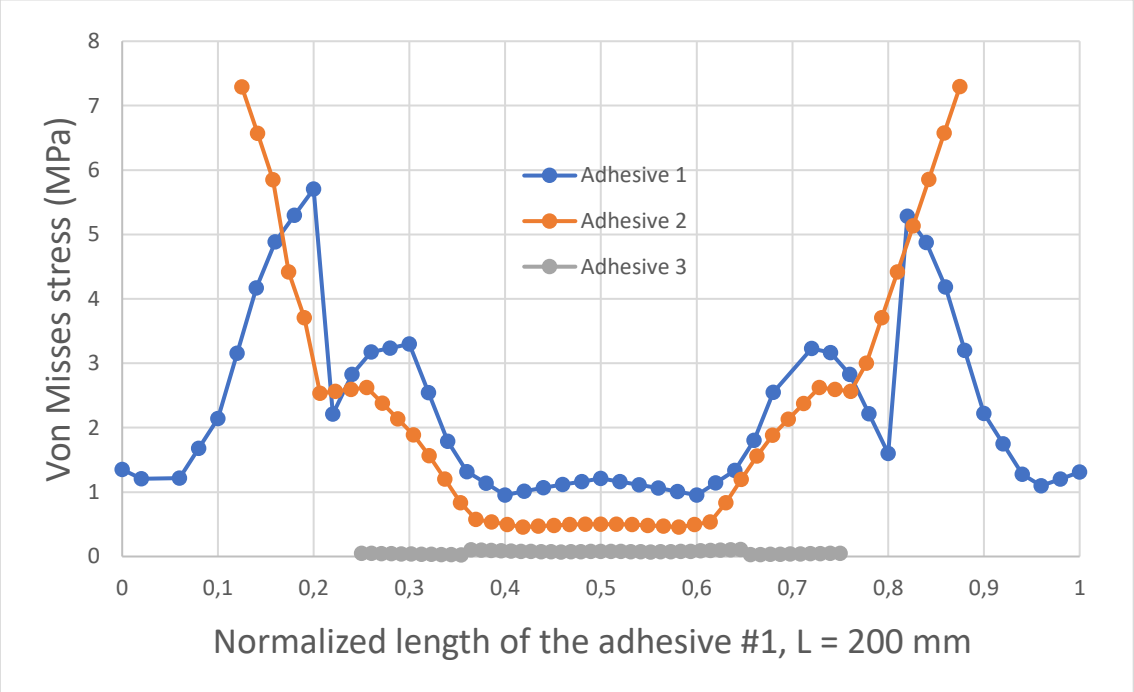

Fig. 5.9 Stresses distribution for adhesives #1, #2 and #3.

5.4 Stresses over the doublers

In this section, **Fig. 5.10**, **Fig. 5.11** and **Fig. 5.12** show the stress distributions along the doublers.

In the first model, there is only one doubler, and it seems to have a constant stress along it of around 0.16 MPa, a lot smaller than the 105 MPa in **Fig. 5.6**. This very small numerical result reinforces the conclusion, explained in the previous section **5.3** which was about the adhesive, that with a single patch, the main aluminum plate carries the entire load. Also, between *l = 0* and *l = 0.1*, the graph shows an unexpected sudden peak maybe for the reasons explained in other sections, such as low mesh quality and/or boundary conditions, since the specimen is symmetric across *l = 0.5*.

For the second model, the response of the doublers changes drastically from the previous one. It seems that in this configuration, doubler #1 suffers a lot more, as the distribution used to be 0.16 MPa and increases up to 35 MPa, which is the maximum, and it is constant in the central sections of the doubler, while in the edges the stress is not so high. Central sections of the doubler, while in the edges the stress is not so high.

Last model is simulated as well. Doubler #1 has even more stress on it with 42 MPa. The stress distribution in doubler #3 has the same shape as the stress distribution for doubler #2 in model #2. The Von Misses stress in the mid doubler is behaving as a more-or-less sine function with fluctuating values (maximums and minimums). These fluctuating values are located at abscissa values such that coincide with the edge zone of the doublers #3 (that is, the two minimums coincide with edges of doubler #3).

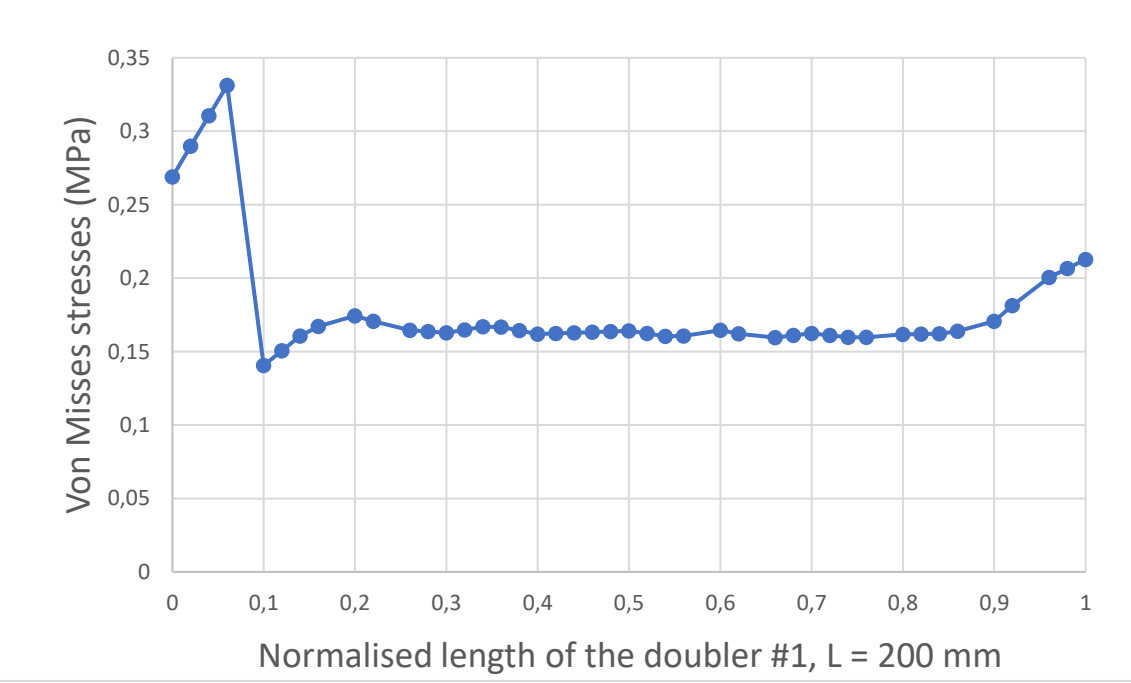

Fig. 5.10 Stresses over the doubler in first model.

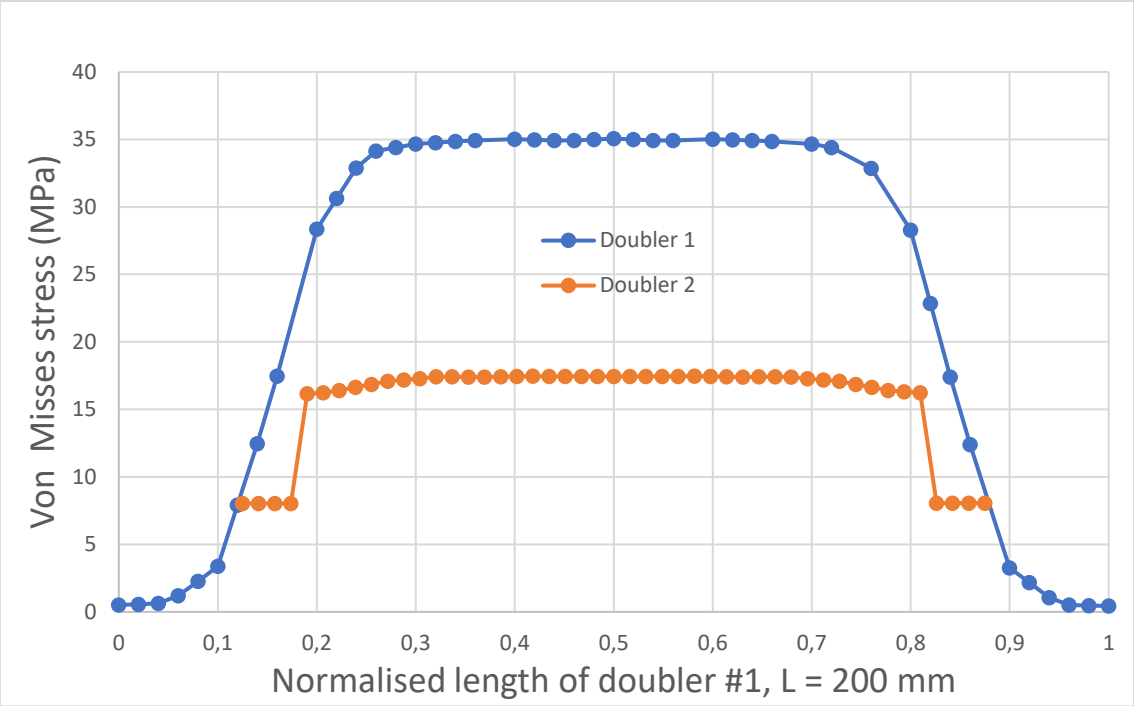

Fig. 5.11 Stresses over the doublers in second model.

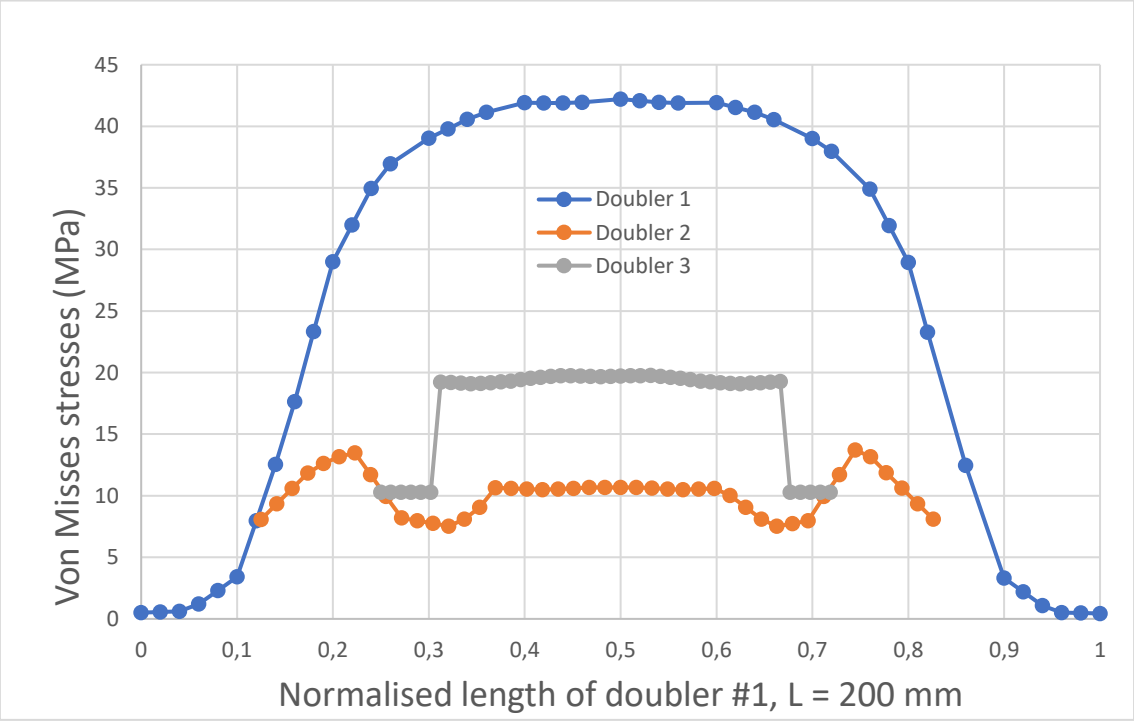

Fig. 5.12 Stresses over the doublers in third model.

In conclusion, we can see that using a single doubler is useless for reparation since almost 100% of the load is carried by the main plate and only serves to bend it (asymmetrical effects). However, the load distribution changes drastically for the plate, the doublers, and the adhesive, in the case of the other models. Several factors can contribute to the different load distribution behavior observed in all three simulations:

1. Load sharing: With two and three patches, the load applied to the aluminum plate is distributed between them, resulting in a lower load on each individual patch. This can reduce the concentration of stress on the plate and promote a more uniform load distribution across the entire joint.

2. Increased effective bonded area: With two and three patches, the effective bonded area between the plate and the patches is increased, resulting in a larger area available for load transfer. This can reduce the stress concentration at the edges of the patch and promote a more even distribution of stress throughout the joint.

3. Improved joint stiffness: The presence of more than one patch may increase the overall stiffness of the joint, which can result in a more evenly distributed load across the entire joint. This can minimize localized stress concentrations and reduce the risk of failure in the adhesive joint.

Apart from the reasons or factors explained above, an interesting result is the additional bending stresses, which increase with the number of doublers and may also help to increase the overall stress on the doublers. These stresses are the ones which only act normal or perpendicular to the surface and Abaqus refers them as S33 that is solidary to Z-axis. The overall deduction for this is that the stress concentration in the repaired area is highest for the lower number of patches or doublers, but the additional bending stresses are smaller. *Numerical results for S33 are found in section **C.4**.*

5.5 Stress-elongation relation

In this section, the stress response vs. elongation is shown. In this work, only the linear regime of the stress-elongation curve has been considered, same for the single lap joint.

We obtain an obviously linear result in the stress-elongation curve since the plastic regime is not treated. As with the previous stress-elongation relationship, the lines overlap because of the small variation between numerical results. Thus, the resulting elongation values are shown in the following **Table 5.2** for clarity.

Model	First	Second	Third
Elongation (10^{-3} mm)	1.45824	1.45823	1.45823

Table 5.2 Elongation of the specimen at 8000 N.

These results seem more coherent than the results that we obtained for the single lap joint (such results were obtained the same procedure as the ones shown in **Table 5.2**, so here is a clue that indicates values form **Table 4.2** are possibly wrong and far from reality). First model has more elongation than two others. This leads to the conclusion that the number of doublers may be related to the elongation of the main plate. The fewer doublers there are, the more it will elongate. Additionally, elongation for third model may have been rounded from, for example, from 1.46E-3 mm and this would reinforce the conclusion. However, even if this is true, the values are only 0.0001E-3 mm apart. This difference is too small to assume at first glance that there really is a relationship with the doublers and simply that the elongation also remains constant regardless the external plates.

But finally, we will advocate or opt for the first hypothesis, since by common sense after cross-checking with reality, it is the one that makes more sense with what we argued.

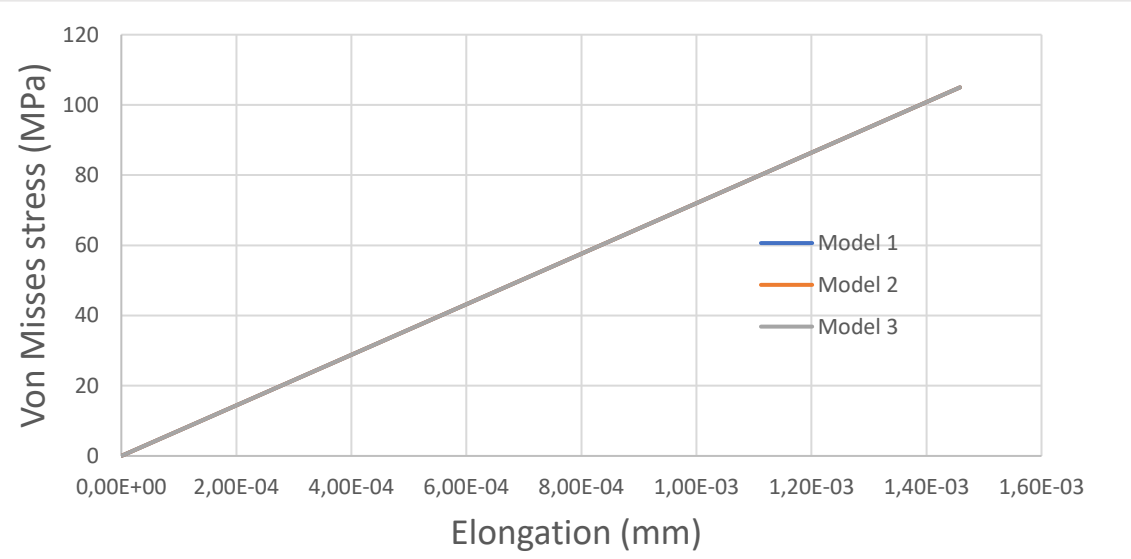

Fig 5.13 Stress-elongation relations for the three models.

CONCLUSIONS

Numerical simulations to predict the behavior of a single lap junction and realistic aircraft repair patches have been performed in an acceptable manner with Abaqus Learning Edition software. One of the main objectives was to obtain the stress distribution in the linear elastic regime of mentioned structures for static loads of 2000, 4000 and 8000 N.

The single lap joint is the simplest type of joint and has an asymmetric response, i.e., it has a tendency to bend out of the plane of symmetry. For static structures, it is not recommended to use this type of joint, nor it is widely used in the field of aeronautics. For example, it would only serve to join thin plates. In terms of adhesive bonding, the load is distributed as expected: higher stress at the edges and minimum stress in the central part of the joint. Additionally, in the substrate, the stress is constant along the joint and smaller than in the part where there is no adhesive. Therefore, if the substrate is of very poor quality, it is very likely to break before the bond itself (the type of failure would be substrate failure).

Comparing the results between the five tested adhesive debonding lengths, a tendency is seen that when the adhesive layer is shorter, it receives more load (since the bond area is smaller and therefore the same amount of force is distributed in a smaller area) and both its minimum and maximum stresses increase. The maximum overall stress can be expected to occur when the adhesive has a very small length close to zero, thus the load would be concentrated in a given point as if the joint had only one rivet.

However, adhesive bonded joints can be more difficult and time-consuming to create than other types of joining techniques such as fastening, and the curing process for the adhesive can be slow and require special equipment. Adhesive bonded joints also require special handling and preparation of the surfaces to be joined, and the bond strength can be affected by temperature and humidity. These are some of the reasons why still, so far, the traditional riveted joints are more widely used than adhesive bonding. That is the reason for the existence of a simulation for a rivets equivalence for the single lap joint.

In the study of the equivalence of the rivets, it has been observed that, in the same way as in the adhesive bonded joints, the external rivets carry a higher percentage of load than the internal ones, indicating that, in normal conditions, the external rivets are going to break before the internal ones. Therefore, in a rivet-based repair patch, it would not be enough to join it with a single line of rivets following its silhouette, but it would be necessary to use more rows and columns of rivets as proposed by Cristian Ribas in his master's thesis [18].

On the other hand, in the study of the realistic patch, it is also observed that there is an asymmetric response as the previous sample. However, this asymmetry would not be perceptible in the reality since in the simulation a flat fuselage has been assumed, when in real life, we know that the fuselage of a conventional commercial aircraft is curved.

The stress distribution in the plate is a crucial factor in determining the number of doublers needed in a patch repair. As the number of doublers increased, the stress concentration over the main plate in the joint zone or repaired area decreased. It is important to remind, and it is that the engineer must balance the use of more material (and greater cost) leading to higher safety or less material (and lower cost) but lower safety. In model number one, the adhesive joint has an expected stress distribution like the single lap joint, but with small variation between maximum and minimum stress, almost constant stress distribution. Second and third model behave similarly, with atypical response for adhesive #1, and adhesive #3 is not stressed at all compared to others. Also, inner doublers tend to suffer from more stress, which is a trade-off between having more doublers and more safety on the fuselage cracked and, at same time, those doublers being more stressed due to the load transmission. Load sharing is the main factor or reason for the stress distribution over the doublers, that is, they are able to transfer the load to each other. In addition to this, the stress concentration in the repaired area is highest for the lower number of patches or doublers as mentioned, but the additional bending stresses are smaller.

When it comes to the actual FEA, the jobs and simulations have been carried out with no further struggle. However, 1000 nodes limitation is too low and frustrating for professional work, considering that a current job could be composed of around 30000 nodes, and that is only if studying a simple riveted single lap joint.

FEA software allows engineers to perform complex simulations that would be difficult or impossible to perform experimentally. Node limitations in FEA can have a negative impact on the accuracy of the simulation results. The accuracy of the simulation depends on the distribution of nodes and the accuracy of their placement, and this issue may appear in some of the results obtained in the study.

REFERENCES

[1] FAA-H-808-31A, “Aircraft Structures”, Chapter 1 in *Aviation Maintenance Technician Handbook – Airframe Volume 1*, United States Department of Transportation, FAA, Airman Testing Standards Branch, Oklahoma City, OK (2018)

[2] Marcel Dekker, Inc., “Theories and Mechanisms of Adhesion”, Chapter 3 in *Handbook of Adhesive Technology – Second Edition, Revised and Explained*, Pizzi, A., Mittal, K.L., Eds., Marcel Dekker, Inc., Cimarron Road, Monticello, NY, USA (2003)

[3] Cutler, J., “Processes”, Chapter 7 in *Understanding Aircraft Structures*, Liber, J., Ed., Blackwell Publishing Inc., Main Street, Malden, MA, USA (2005)

[4] Esteban Oñate, A., *Materiales y elementos aeronáuticos. Técnico de Mantenimiento Aeronáutico. Módulo 6 EASA 66*, Paraninfo, Ed., Madrid, España (2016)

[5] Esmaeili, F., Zehsaz, M., Chakherlou, T.N., Barzegar, S., “Fatigue life estimation of double lap simple bolted and hybrid (bolted/bonded) joints using several multiaxial fatigue criteria”, Chapter 67 in *Materials and design*, Elseiver, Ed., pp. 583-595, Tabriz, Iran (2014)

[6] Davis, J.R., “Aluminum and aluminum alloys”, *Alloying: Understanding the basics*, ASM International, Ed., USA (2001)

[7] The materials information society, *Atlas of Stress-Strain Curves 2nd Edition*, ASM International, Ed., Materials Park, Novelty, OH (2002)

[8] Departamento Técnico de Loctite España, *Tecnología de la Adhesión. Curso de Adhsivos* presented by Mario Madrid

[9] LNVM, Society Group of Institutions, Singh, S., *Airframe and Aircraft Components*, Graphic Syndicate, Ed., Naraina, New Delhi, India (2007)

[10] Monsalve, A., Valencia, N., Páez, M., Sepúlveda, Y., “Evaluación a fatiga rotatoria de aluminio 2024-T3”, *Anales de Mecánica de la Fractura*, Vol. 20, pp 450-455 (2003)

[11] Pitta, S., Rojas, J.I., Crespo, D., *Comparison of the response of different configurations of aircraft repair patches under static and dynamic loading*, EETAC-UPC, Castelldefels, Spain (2019)

[12] Pitta S, Carles VDLM, Roure F, Crespo D, Rojas JI. “On the static strength of aluminium and carbon fibre aircraft lap joint repairs”, *Compos. Struct*., 201(1), pp 276-290 (2018)

[13] Quini, J.G., Marinucci, G., “Polyurethane Structural Adhesives Applied in Automotive Composite Joints”, *Materials Research*, 15(3), pp 434-439 (2012)

[14] Al-kawaz, A., “Theories of Adhesion”, *Paints and Adhesives*, University of Babylon, Babylon, Irak

[15] Gharib, H., *A Review on Structural Health Monitoring of Adhesive Bond in Aircraft Repair Patches*, RearchGate (2015)

https://www.researchgate.net/publication/282121093

[16] Ruzek, R., “Wing repair using an adhesively bonded boron composite patch – design and verification”, *International Journal of Structural Integrity*, 6(2), pp 259-278 (2015)

[17] The Aluminum Association, *International Alloy Designation and Chemical Composition Limits for Wrought Aluminum and Wrought Aluminum alloys*, The Aluminum Association, Inc., 1400 Crystal Drive, Suite 430, Arlington, VA (2018)

[18] Ribas, C., Pitta, S., Rojas, J.I., *Comparison of the response of different rivet layout patterns in aircraft repair patches*, EETAC-UPC, Castelldefels, Spain (2021)

[19] Clearfield, H. M., McNamara, D. K., Davis, G. D. *Adherent surface preparation for structural adhesive bonding*, Lee, L. H., Ed., Plenum Press, New York (1991)

[20] CFI Notebook, “Aircraft Components & Structure”, *Aerodynamics and Performance*

https://www.cfinotebook.net/notebook/aerodynamics-and-performance/aircraft-components-and-structure

[21] Voyutskii, S., *Autohesion and Adhesion of High Polymers*, Wiley-Interscience, New York (1963)

[22] The Open University, “Introduction to finite element analysis”, *Science Maths Technology*, United Kingdom (2015)

https://www.open.edu/openlearn/science-maths-technology/introduction-finite-element-analysis/

[23] Nozaka, K., K. Shield, C., F. Hajjar, J., “Design of a test specimen to assess the effective bond length of carbon fiber reinforced polymer strips bonded to fatigued steel bridge girders”, *Journal of Composites of Construction*, 9(4), pp 304-312 (2005)

[24] Christensen, D., “Introduction to finite element analysis for university courses and research”, *MSC Software* (2011)

[25] Vioux, D., L'avionnaire, *Light Aircraft* (2010) Last access: 4th February 2023.

https://www.lavionnaire.fr/AngLightaircraft.php

APPENDICES

APPENDIX A. COMPLEMENTARY INFORMATION

A.1 True and nominal stresses and strains

It is common during uniaxial (tensile or compressive) testing to equate the stress to the force divided by the original sectional area and the strain to the change in length (along the loading direction) divided by the original length. In fact, these are “engineering” or “nominal” values. The true stress acting on the material is the force divided by the current sectional area. After a finite (plastic) strain, under tensile loading, this area is less than the original area, as a result of the lateral contraction needed to conserve volume, so that the true stress is greater than the nominal stress. Conversely, under compressive loading, the true stress is less than the nominal stress.

Consider a sample of initial length L_0, with an initial sectional area A_0. For an applied force F and a current sectional area, A, conserving volume, the true stress can be written:

$$\sigma_T = \frac{F}{A} = \frac{FL}{A_0 L_0} = \frac{F}{A_0}(1 + \varepsilon_N) = \sigma_N(1 + \varepsilon_N) \qquad \textbf{(A.1)}$$

where σ_N is the nominal stress and ε_N is the nominal strain. Similarly, the true strain can be written:

$$\varepsilon_T = \int_{L_0}^{L} \frac{dL}{L} = ln\left(\frac{L}{L_0}\right) = ln(1 + \varepsilon_N) \qquad \textbf{(A.2)}$$

The true strain is therefore less than the nominal strain under tensile loading but has a larger magnitude in compression. While nominal stress and strain values are sometimes plotted for uniaxial loading, it is essential to use true stress and true strain values throughout when treating more general and complex loading situations. Unless otherwise stated, the stresses and strains referred following are true (von Mises) values.

A.2 Advantages and drawbacks of bonding and riveting

During the course of this thesis, thanks to the search for information and the results obtained, we can obtain some advantages and disadvantages of both glued and riveted joints. Maybe, some advantages of one type of joining method are the drawback of the other. The following are some of them but are the most important to know.

The advantages of bonded joints are:

- Ability to join similar and different materials (metal to metal, composite to metal, composite to composite, etc).
- Stress distribution uniform within the area of the adhesive.
- Lack of perforation reduces stress on determined points.
- Decreased joint weight.

The drawbacks of bonded joints are:

- Waiting so long from preparing until fully functional, in other words, curing time long, and during this curing, the adhesive may deal with humidity and unfavourable environment.
- Disassembly of the joint means the destruction of it.
- Temperature limitations.
- Toxicity and hazardous material.

The advantages of riveted joints are:

- Cheap.
- Ability to join similar and different materials (metal to metal, composite to metal, composite to composite, etc).
- Simple disassembly and reassembly for reparation.
- Easy to create joint with tools and not so experienced technician.

The drawbacks of riveted joints are:

- Unintended loosening from vibrations.
- Technician may introduce defects while creating joint, such as tilted drilling, wrong size of the fastener and not enough rivets.
- Stress concentred only in the rivet.
- Since the most used material of rivets is metal, corrosion may appear.

APPENDIX B. RESULTS FOR SINGLE LAP JOINT

B.1 Load of 2000N

B.1.1 Adhesive 0% peeled

Normalised length from L = 101,6 mm	Stress (MPa)
0,00	28,7704
0,02	27,6092
0,04	26,448
0,06	25,4272
0,08	24,5433
0,10	23,6615
0,12	23,445
0,14	23,2285
0,16	22,0321
0,18	19,8715
0,20	17,7118
0,22	15,7858
0,24	13,8598
0,26	12,0696
0,28	10,4138
0,30	8,76017
0,32	7,94651
0,34	7,13287
0,36	6,90611
0,38	7,26141
0,40	7,61454
0,42	6,63712
0,44	5,65969
0,46	4,79775
0,48	4,0507
0,50	3,30498
0,52	4,05051
0,54	4,79603
0,56	5,65828
0,58	6,63702
0,60	7,61561
0,62	7,26532
0,64	6,91504
0,66	7,14599
0,68	7,95882
0,70	8,77166
0,72	10,421

0,74	12,071
0,76	13,8603
0,78	15,7898
0,80	17,7192
0,82	19,8844
0,84	22,05
0,86	23,2429
0,88	23,4572
0,92	24,5523
0,94	25,4347
0,96	26,455
0,98	27,6144
1,00	28,7738

B.1.2 Adhesive 10% peeled

Normalised length from L = 91,44 mm	Stress (MPa)
0,00	24,6253
0,02	24,7595
0,04	24,8937
0,06	24,868
0,08	24,2915
0,10	23,715
0,12	22,356
0,14	20,0253
0,16	17,6945
0,18	14,9452
0,20	11,988
0,22	9,03074
0,24	7,72245
0,26	6,61733
0,28	5,71202
0,30	6,38904
0,32	7,06606
0,34	7,56376
0,36	7,70426
0,38	7,84476
0,40	7,33479
0,42	6,30595
0,46	4,48579
0,48	3,76214
0,50	3,03878
0,52	3,76319
0,54	4,48759
0,56	5,27963
0,58	6,3084
0,60	7,33716
0,62	7,84596
0,64	7,70415
0,66	7,56233
0,68	7,06414
0,70	6,38738
0,72	5,71063
0,74	6,61868
0,76	7,72621
0,78	9,03778
0,80	11,9951
0,82	14,9525
0,84	17,7012
0,86	20,0307

0,88	22,3603
0,90	23,7183
0,92	24,2944
0,94	24,8705
0,96	24,8956
0,98	24,7615
1,00	24,6274

B.1.3 Adhesive 20% peeled

Normalised length from L = 81,28 mm	Stress (MPa)
0,00	29,5489
0,02	26,4653
0,04	23,3817
0,06	19,4605
0,08	14,7028
0,10	9,94749
0,12	9,44771
0,14	8,94793
0,16	8,41683
0,18	7,85445
0,20	7,29192
0,22	6,07791
0,24	4,86389
0,26	4,53688
0,28	5,09598
0,30	5,65479
0,32	4,7645
0,34	3,8742
0,36	3,35282
0,38	3,2002
0,40	3,0476
0,42	3,31699
0,44	3,58639
0,46	3,47015
0,48	2,96829
0,50	2,46642
0,52	2,9694
0,54	3,47243
0,56	3,58594
0,58	3,30974
0,60	3,03354
0,62	3,19067
0,64	3,34789
0,66	3,87339
0,68	4,76753
0,70	5,66168
0,72	5,10573
0,74	4,54934
0,76	4,87966
0,78	6,09785
0,80	7,31604
0,82	7,87096
0,84	8,42563

0,86	8,95496
0,88	9,45889
0,90	9,96282
0,92	14,725
0,94	19,4895
0,96	23,413
0,98	26,4938
1,00	29,5747

B.1.4 Adhesive 30% peeled

Normalised length from L = 71,12 mm	Stress (MPa)
0,00	33,9017
0,02	32,9863
0,04	32,0708
0,06	31,1554
0,08	29,6131
0,10	27,2613
0,12	24,9095
0,14	22,5577
0,16	20,6821
0,18	18,8839
0,20	17,0856
0,22	15,502
0,24	14,4436
0,26	13,3851
0,28	12,3267
0,30	11,5887
0,32	10,9769
0,34	10,3652
0,36	9,79902
0,38	9,50188
0,40	9,20474
0,42	8,9076
0,44	8,55831
0,46	8,17017
0,48	7,78203
0,50	7,39456
0,52	7,78223
0,54	8,1699
0,56	8,55757
0,58	8,90675
0,60	9,2047
0,62	9,50265
0,64	9,8006
0,66	10,3686
0,68	10,9817
0,70	11,5949
0,72	12,3348
0,74	13,3942
0,76	14,4537
0,78	15,5131
0,80	17,0981
0,82	18,8949
0,84	20,6918

0,86	22,5666
0,88	24,9202
0,90	27,2737
0,92	29,6273
0,94	31,1644
0,96	32,0786
0,98	32,9928
1,00	33,907

B.1.5 Adhesive 40% peeled

Normalised length from L = 60,96 mm	Stress (MPa)
0,00	33,7142
0,02	32,2646
0,04	30,815
0,06	29,2552
0,08	26,0289
0,10	22,8027
0,12	19,6708
0,14	17,2281
0,16	14,7854
0,18	12,8364
0,20	13,1555
0,22	13,4745
0,24	13,6168
0,26	13,1911
0,28	12,7653
0,30	12,2991
0,32	11,7362
0,34	11,1734
0,36	10,4763
0,38	9,53431
0,40	8,59235
0,42	7,98528
0,44	7,85475
0,46	7,72422
0,48	7,64305
0,50	7,61728
0,52	7,59151
0,54	7,66083
0,56	7,81455
0,58	7,96827
0,60	8,58969
0,62	9,5384
0,64	10,4871
0,66	11,2091
0,68	11,8072
0,70	12,4053
0,72	12,8654
0,74	13,2677
0,76	13,6701
0,78	13,542
0,80	13,2499
0,82	12,9577
0,84	14,9279

0,86	17,3878
0,88	19,8477
0,90	22,8636
0,92	25,955
0,94	29,0464
0,96	30,5699
0,98	31,9931
1,00	33,4164

B.2 Load of 4000 N

B.2.1 Adhesive 0% peeled

Normalised length from L = 101,6 mm	Stress (MPa)
0	57,5409
0,02	55,2182
0,04	52,8955
0,06	50,854
0,08	49,0864
0,1	47,3229
0,12	46,89
0,14	46,4571
0,16	44,0637
0,18	39,7425
0,2	35,423
0,22	31,5711
0,24	27,7191
0,26	24,1389
0,28	20,8272
0,3	17,5202
0,32	15,8929
0,34	14,2656
0,36	13,8123
0,38	14,5229
0,4	15,2289
0,42	13,2741
0,44	11,3192
0,46	9,59538
0,48	8,10128
0,5	6,61007
0,52	8,10113
0,54	9,59218
0,56	11,3167
0,58	13,2742
0,6	15,2312
0,62	14,5306
0,66	14,2921
0,68	15,9178
0,7	17,5434
0,72	20,8423
0,74	24,1422
0,76	27,7208
0,78	31,5797
0,82	39,7689

0,84	44,1002
0,86	46,4858
0,88	46,9145
0,9	47,3432
0,92	49,1046
0,94	50,8695
0,96	52,9099
0,98	55,2288
1	57,5476

B.2.2 Adhesive 10% peeled

Normalised length from L = 91,44 mm	Stress (MPa)
0	49,2507
0,02	49,5191
0,04	49,7875
0,06	49,7357
0,08	48,5827
0,1	47,4298
0,12	44,7117
0,14	40,0501
0,16	35,3885
0,18	29,8898
0,2	23,9752
0,22	18,0607
0,24	15,4446
0,26	13,2344
0,28	11,4242
0,3	12,7782
0,32	14,1323
0,34	15,1275
0,36	15,4085
0,38	15,6895
0,4	14,6694
0,42	12,6117
0,44	10,5541
0,46	8,97147
0,48	7,52417
0,5	6,07769
0,52	7,52649
0,54	8,97529
0,56	10,5594
0,58	12,6169
0,6	14,6744
0,62	15,6919
0,64	15,4083
0,66	15,1246
0,68	14,1282
0,7	12,7747
0,72	11,4212
0,74	13,2374
0,76	15,4525
0,78	18,0758
0,8	23,9905
0,82	29,9053
0,84	35,4025

0,86	40,0616
0,88	44,7207
0,9	47,4365
0,92	48,5888
0,94	49,7411
0,96	49,7912
0,98	49,523
1	49,2549

B.2.3 Adhesive 20% peeled

Normalised length from L = 81,28 mm	Stress (MPa)
0	59,0979
0,02	52,9305
0,04	46,7631
0,06	38,9203
0,08	29,4049
0,1	19,8949
0,12	18,8954
0,14	17,8958
0,16	16,8336
0,18	15,7089
0,2	14,5837
0,22	12,1557
0,24	9,72765
0,26	9,07384
0,28	10,192
0,3	11,3095
0,32	9,52891
0,34	7,74833
0,36	6,70563
0,38	6,40038
0,4	6,09522
0,42	6,63401
0,44	7,1728
0,46	6,94026
0,48	5,93654
0,5	4,93281
0,52	5,93883
0,54	6,94489
0,56	7,17186
0,58	6,61946
0,6	6,06707
0,62	6,38136
0,64	6,69578
0,66	7,74682
0,68	9,53512
0,7	11,3234
0,72	10,2114
0,74	9,09864
0,76	9,75937
0,78	12,1958
0,8	14,6321
0,82	15,7419
0,84	16,8513

0,86	17,9099
0,88	18,9178
0,9	19,9257
0,92	29,4502
0,94	38,979
0,96	46,8261
0,98	52,9877
1	59,1493

B.2.4 Adhesive 30% peeled

Normalised length from L = 71,12 mm	Stress (MPa)
0	67,8034
0,02	65,9724
0,04	64,1414
0,06	62,3104
0,08	59,2252
0,1	54,5219
0,12	49,8186
0,14	45,1153
0,16	41,3641
0,18	37,7675
0,2	34,1709
0,22	31,0038
0,24	28,8869
0,26	26,7701
0,28	24,6532
0,3	23,1773
0,32	21,9538
0,34	20,7302
0,36	19,598
0,38	19,0037
0,4	18,4094
0,42	17,8151
0,44	17,1166
0,46	16,3403
0,48	15,564
0,5	14,7892
0,52	15,5645
0,54	16,3399
0,56	17,1152
0,58	17,8135
0,6	18,4095
0,62	19,0054
0,64	19,6012
0,66	20,7373
0,68	21,9636
0,7	23,1898
0,72	24,6697
0,74	26,7886
0,76	28,9075
0,78	31,0264
0,8	34,1965
0,82	37,7902
0,84	41,3839

0,86	45,1336
0,88	49,8407
0,9	54,5478
0,92	59,2549
0,94	62,3288
0,96	64,1572
0,98	65,9856
1	67,8139

B.2.5 Adhesive 40% peeled

Normalised length from L = 60,96 mm	Stress (MPa)
0	67,4285
0,02	64,529
0,04	61,6296
0,06	58,5092
0,08	52,0569
0,1	45,6046
0,12	39,3411
0,14	34,4558
0,16	29,5705
0,18	25,6729
0,2	26,311
0,22	26,949
0,24	27,2336
0,26	26,3821
0,28	25,5306
0,3	24,598
0,32	23,4724
0,34	22,3467
0,36	20,9524
0,38	19,0685
0,4	17,1846
0,42	15,9705
0,44	15,7095
0,46	15,4484
0,48	15,2861
0,5	15,2346
0,52	15,183
0,54	15,3217
0,56	15,6291
0,58	15,9366
0,6	17,1795
0,62	19,0769
0,64	20,9743
0,66	22,4182
0,68	23,6144
0,7	24,8107
0,72	25,7308
0,74	26,5355
0,76	27,3403
0,78	27,0839
0,8	26,4997
0,82	25,9155
0,84	29,8561

0,86	34,7759
0,88	39,6956
0,9	45,7275
0,92	51,9102
0,94	58,093
0,96	61,1397
0,98	63,9862
1	66,8327

B.3 Load of 8000 N

B.3.1 Adhesive 0% peeled

Normalised length from L = 101,6 mm	Stress (MPa)
0	115,082
0,02	110,436
0,04	105,791
0,06	101,708
0,08	98,1726
0,1	94,6459
0,12	93,78
0,14	92,9141
0,16	88,1268
0,18	79,4844
0,2	70,8456
0,22	63,1418
0,24	55,4379
0,26	48,2775
0,28	41,6542
0,3	35,0402
0,32	31,7856
0,34	28,531
0,36	27,6246
0,38	29,0459
0,4	30,4577
0,42	26,548
0,44	22,6382
0,46	19,1906
0,48	16,2024
0,5	13,2203
0,52	16,2024
0,54	19,1845
0,56	22,6336
0,58	26,5485
0,6	30,4623
0,62	29,0612
0,64	27,6601
0,66	28,5842
0,68	31,8356
0,7	35,087
0,72	41,6849
0,74	48,2846
0,76	55,4419
0,78	63,1595

0,8	70,8771
0,82	79,5379
0,84	88,2007
0,86	92,9716
0,88	93,829
0,9	94,6864
0,92	98,2092
0,94	101,739
0,96	105,82
0,98	110,458
1	115,095

B.3.2 Adhesive 10% peeled

Normalised length from L = 91,44 mm	Stress (MPa)
0	98,5014
0,02	99,0382
0,04	99,575
0,06	99,4711
0,08	97,1653
0,1	94,8594
0,12	89,423
0,14	80,0998
0,16	70,7766
0,18	59,779
0,2	47,9498
0,22	36,1207
0,24	30,889
0,28	22,8484
0,3	25,5565
0,32	28,2646
0,34	30,2551
0,36	30,8171
0,38	31,3791
0,4	29,3386
0,42	25,2233
0,44	21,1081
0,46	17,9428
0,48	15,0482
0,5	12,1555
0,52	15,0531
0,54	17,9507
0,56	21,1189
0,58	25,2339
0,6	29,349
0,62	31,3838
0,64	30,8165
0,66	30,2493
0,68	28,2563
0,7	25,5493
0,72	22,8424
0,74	26,4749
0,76	30,9051
0,78	36,1518
0,8	47,9813
0,82	59,8108
0,84	70,8053
0,86	80,1234

0,88	89,4414
0,9	94,873
0,92	97,1776
0,94	99,4822
0,96	99,5824
0,98	99,0461
1	98,5097

B.3.3 Adhesive 20% peeled

Normalised length from L = 81,28 mm	Stress (MPa)
0	118,196
0,02	105,861
0,04	93,526
0,06	77,8399
0,08	58,8091
0,1	39,7897
0,12	37,7906
0,14	35,7916
0,16	33,6672
0,18	31,4177
0,2	29,1674
0,22	24,3113
0,24	19,4551
0,26	18,1477
0,28	20,3841
0,3	22,6189
0,32	19,0578
0,34	15,4966
0,36	13,4113
0,38	12,8008
0,4	12,1905
0,42	13,268
0,44	14,3456
0,46	13,8805
0,48	11,873
0,5	9,86559
0,52	11,8777
0,54	13,8898
0,56	14,3437
0,58	13,2389
0,6	12,1341
0,62	12,7627
0,64	13,3916
0,66	15,4937
0,68	19,0703
0,7	22,6469
0,72	20,4228
0,74	18,1973
0,76	19,5188
0,78	24,3916
0,8	29,2643
0,82	31,4839
0,84	33,7026

0,86	35,8199
0,88	37,8356
0,9	39,8513
0,92	58,9005
0,94	77,9582
0,96	93,6523
0,98	105,975
1	118,299

B.3.4 Adhesive 30% peeled

Normalised length from L = 71,12 mm	Stress (MPa)
0	135,607
0,02	131,945
0,04	128,283
0,06	124,621
0,08	118,45
0,1	109,043
0,12	99,6369
0,14	90,2305
0,16	82,728
0,18	75,5347
0,2	68,3414
0,22	62,0073
0,24	57,7736
0,26	53,5399
0,28	49,3062
0,3	46,3545
0,32	43,9074
0,34	41,4604
0,36	39,1959
0,38	38,0074
0,4	36,8188
0,42	35,6302
0,44	34,233
0,46	32,6805
0,48	31,1279
0,5	29,5784
0,52	31,1291
0,54	32,6798
0,56	34,2305
0,58	35,6272
0,6	36,819
0,62	38,0107
0,64	39,2025
0,66	41,4747
0,68	43,9272
0,7	46,3797
0,72	49,3395
0,74	53,5774
0,76	57,8152
0,78	62,053
0,8	68,3933
0,82	75,5807
0,84	82,7681

0,86	90,2675
0,88	99,6818
0,9	109,096
0,92	118,51
0,94	124,658
0,96	128,314
0,98	131,971
1	135,628

B.3.4 Adhesive 40% peeled

Normalised length from L = 60,96 mm	Stress (MPa)
0	134,857
0,02	129,058
0,04	123,259
0,06	117,017
0,08	104,113
0,1	91,2085
0,12	78,6818
0,14	68,9113
0,16	59,1407
0,18	51,3458
0,2	52,622
0,22	53,8981
0,24	54,4671
0,26	52,7641
0,28	51,0611
0,3	49,1959
0,32	46,9446
0,34	44,6933
0,36	41,9047
0,38	38,1369
0,4	34,3691
0,42	31,9411
0,44	31,4189
0,46	30,8968
0,48	30,5722
0,5	30,4691
0,52	30,366
0,54	30,6434
0,56	31,2583
0,58	31,8731
0,6	34,3591
0,62	38,1539
0,64	41,9487
0,66	44,8364
0,68	47,2289
0,7	49,6214
0,72	51,4616
0,74	53,0711
0,76	54,6806
0,78	54,1679
0,8	52,9994
0,82	51,8309
0,84	59,7123

0,86	69,5519
0,88	79,3914
0,9	91,455
0,92	103,821
0,94	116,186
0,96	122,28
0,98	127,972
1	133,665

B.4 Stress over plate

B.4.1 Adhesive 0% peeled

Normalised length from L = 226 mm	Stress (MPa)
0	72,783
0,02	76,3433
0,04	79,9036
0,06	80,7338
0,08	81,1402
0,1	86,2137
0,12	93,0302
0,14	101,709
0,16	111,671
0,18	58,1519
0,2	71,0822
0,22	79,7288
0,26	76,3131
0,3	113,009
0,32	113,009
0,34	113,009
0,36	47,8347
0,38	47,8347
0,4	114,639
0,44	51,5199
0,46	57,8877
0,48	60,0724
0,5	58,0339
0,52	55,9906
0,54	53,9389
0,56	55,2557
0,58	68,1873
0,6	80,6865
0,62	88,6087
0,64	96,531
0,66	100,059
0,68	103,422
0,7	104,277
0,72	104,924
0,74	105,047
0,76	105,154
0,78	105,203
0,8	105,138
0,82	104,981
0,84	105,094

0,86	105,039
0,88	104,965
0,9	105,11
0,92	104,903
0,94	105,092
0,96	104,994
0,98	104,92
1	104,885

B.4.2 Adhesive 10% peeled

Normalised length from L = 226 mm	Stress (MPa)
0	17,2708
0,02	28,1798
0,04	39,0887
0,06	47,9953
0,08	56,4989
0,1	57,4448
0,12	54,493
0,14	55,0672
0,16	59,3594
0,18	61,6782
0,2	59,6849
0,22	58,2702
0,24	60,3778
0,26	62,4855
0,28	61,4036
0,3	60,217
0,32	60,8654
0,34	61,9863
0,36	62,2393
0,38	61,966
0,4	61,9824
0,42	62,3537
0,44	63,3686
0,46	66,0661
0,48	68,2454
0,5	65,9463
0,52	63,6473
0,54	72,2621
0,56	81,6851
0,58	86,5362
0,62	94,7879
0,64	100,687
0,66	104,142
0,68	104,983
0,7	105,307
0,72	105,112
0,74	105,291
0,76	105,685
0,78	105,267
0,8	104,996
0,82	105,404
0,84	105,108
0,86	104,968

0,88	105,332
0,9	104,78
0,92	105,295
0,94	104,789
0,96	105,083
0,98	105,197
1	105,213

B.4.3 Adhesive 20% peeled

Normalised length from L = 226 mm	Stress (MPa)
0	0,995196
0,02	7,31789
0,04	13,6406
0,06	25,5248
0,08	38,9552
0,1	47,2968
0,12	51,7127
0,14	53,8917
0,16	51,8434
0,18	50,4599
0,2	53,6254
0,22	56,7908
0,24	55,4405
0,26	53,6383
0,28	54,067
0,3	55,4954
0,32	55,7657
0,34	54,7404
0,36	54,1933
0,38	55,0541
0,4	55,9341
0,42	57,3475
0,44	58,7608
0,46	58,7529
0,48	58,4257
0,5	61,8726
0,52	67,8557
0,54	73,4949
0,56	78,5716
0,58	84,3595
0,6	93,8437
0,62	103,298
0,64	104,09
0,66	104,881
0,68	104,863
0,7	104,831
0,72	105,269
0,74	105,504
0,76	105,056
0,78	105,044
0,8	105,41
0,82	105,007
0,84	104,992

0,86	105,264
0,88	104,822
0,9	105,195
0,92	104,885
0,94	105,201
0,96	104,926
0,98	104,838
1	104,841

B.4.4 Adhesive 30% peeled

Normalised length from L = 226 mm	Stress (MPa)
0	2,60157
0,02	3,85792
0,04	5,11426
0,06	19,3791
0,08	37,6682
0,1	57,8918
0,12	79,8505
0,14	93,2024
0,16	85,367
0,18	77,8627
0,2	76,9635
0,22	76,0643
0,24	75,432
0,26	74,8633
0,28	75,6007
0,3	77,3347
0,32	78,5916
0,34	78,8663
0,36	79,2774
0,38	81,1288
0,4	82,9801
0,42	87,7067
0,44	92,9556
0,46	86,5079
0,48	72,4522
0,5	66,2986
0,52	73,857
0,54	81,5618
0,56	90,2982
0,58	99,0346
0,6	101,522
0,62	103,371
0,64	104,467
0,66	105,345
0,68	105,423
0,7	105,247
0,72	105,427
0,74	105,62
0,76	105,198
0,78	105,067
0,8	105,378
0,82	105,082
0,84	104,987

0,86	105,308
0,88	104,864
0,9	105,179
0,92	104,905
0,94	105,196
0,96	104,906
0,98	104,815
1	104,824

B.4.5 Adhesive 40% peeled

Normalised length from L = 226 mm	Stress (MPa)
0	0,768721
0,02	1,02011
0,04	1,27149
0,06	2,5972
0,0799999	4,3099
0,1	11,2338
0,12	24,0269
0,14	37,4228
0,16	53,1954
0,18	68,968
0,2	66,3907
0,22	62,4393
0,24	61,7894
0,26	62,8597
0,28	63,18
0,3	62,3012
0,32	61,7938
0,34	64,2265
0,36	66,6591
0,38	69,6096
0,4	72,659
0,42	73,0546
0,44	71,4221
0,46	73,8003
0,48	85,8022
0,5	97,5496
0,52	97,6213
0,54	97,693
0,56	99,9696
0,58	102,976
0,6	104,852
0,62	105,78
0,64	106,078
0,66	105,602
0,68	105,558
0,7	106,007
0,72	105,783
0,74	105,105
0,76	105,408
0,78	105,673
0,8	105,041
0,82	105,194
0,84	105,438

0,86	104,808
0,88	105,332
0,9	104,969
0,92	105,211
0,94	104,851
0,96	105,293
0,98	105,465
1	106,646

B.5 Elongation over specimen

B.5.1 Elongation over specimen with adhesive 0% peeled

Step increment (adim.)	Elongation (mm)
0	0,00000E+00
0,1	1,45728E-04
0,2	2,91457E-04
0,35	5,10049E-04
0,575	8,37938E-04
0,9125	1,32977E-03
1	1,45728E-03

B.5.2 Elongation over specimen with adhesive 10% peeled

Step increment (adim.)	Elongation (mm)
0	0,00000E+00
0,1	1,46029E-04
0,2	2,92057E-04
0,35	5,11100E-04
0,575	8,39664E-04
0,9125	1,33251E-03
1	1,46029E-03

B.5.3 Elongation over specimen with adhesive 20% peeled

Step increment (adim.)	Elongation (mm)
0	0,00000E+00
0,1	1,45687E-04
0,2	2,91375E-04
0,35	5,09906E-04
0,575	8,37703E-04
0,9125	1,32940E-03
1	1,45687E-03

B.5.4 Elongation over specimen with adhesive 30% peeled

Step increment (adim.)	Elongation (mm)
0	0,00000E+00
0,1	1,45658E-04
0,2	2,91317E-04
0,35	5,09805E-04
0,575	8,37536E-04
0,9125	1,32913E-03
1	1,45658E-03

B.5.5 Elongation over specimen with adhesive 40% peeled

Step increment (adim.)	Elongation (mm)
0	0,00000E+00
0,1	1,46054E-04
0,2	2,92109E-04
0,35	5,11191E-04
0,575	8,39813E-04
0,9125	1,33275E-03
1	1,46054E-03

B.6 Stress over specimen

B.6.1 Stress over specimen with adhesive 0% peeled

Step increment (adim.)	Stress (MPa)
0	0
0,1	10,4885
0,2	20,9771
0,35	36,7099
0,575	60,3091
0,9125	95,7079
1	104,885

B.6.2 Stress over specimen with adhesive 10% peeled

Step increment (adim.)	Stress (MPa)
0	0
0,1	10,5213
0,2	21,0427
0,35	36,8247
0,575	60,4977
0,9125	96,0072
1	105,213

B.6.3 Stress over specimen with adhesive 20% peeled

Step increment (adim.)	Stress (MPa)
0	0
0,1	10,4841
0,2	20,9682
0,35	36,6944
0,575	60,2836
0,9125	95,6675
1	104,841

B.6.4 Stress over specimen with adhesive 30% peeled

Step increment (adim.)	Stress (MPa)
0	0
0,1	10,481
0,2	20,9619
0,35	36,6833
0,575	60,2655
0,9125	95,6387
1	104,81

B.6.5 Stress over specimen with adhesive 40% peeled

Step increment (adim.)	Stress (MPa)
0	0
0,1	10,5242
0,2	21,0483
0,35	36,8346
0,575	60,514
0,9125	96,033
1	105,242

APPENDIX C. RESULTS FOR REALISTIC PATCH

C.1 First model

C.1.1 Main plate stresses

Normalised length from L = 300 mm	Stress (MPa)
0	104,993
0,04	105,005
0,06	104,995
0,08	104,997
0,14	104,977
0,16	104,911
0,18	104,843
0,22	104,762
0,24	104,787
0,26	104,78
0,28	104,775
0,3	104,788
0,32	104,789
0,38	104,8
0,4	104,781
0,42	104,773
0,46	104,791
0,52	104,805
0,54	104,778
0,56	104,771
0,58	104,798
0,6	104,792
0,62	104,768
0,64	104,784
0,66	104,796
0,68	104,784
0,7	104,781
0,72	104,787
0,74	104,769
0,76	104,745
0,78	104,751
0,8	104,745
0,82	104,71
0,84	104,917
0,86	105,283
0,88	104,865
0,9	104,575
0,92	105,48
0,94	106,96
0,96	109,168
0,98	98,2003
1	98,2003

C.1.2 Adhesive#1 stresses

Normalised length from L = 200 mm	Stress (MPa)
0	0,834669
0,02	0,825801
0,04	0,816933
0,06	0,808109
0,08	0,799949
0,1	0,791791
0,12	0,784749
0,14	0,785505
0,16	0,786261
0,18	0,785961
0,2	0,781086
0,22	0,776211
0,24	0,772746
0,26	0,77351
0,28	0,774275
0,3	0,77419
0,32	0,772229
0,36	0,769109
0,38	0,76929
0,4	0,769471
0,42	0,769496
0,44	0,769318
0,48	0,768979
0,5	0,768831
0,54	0,768842
0,56	0,769247
0,58	0,769651
0,6	0,769587
0,62	0,769229
0,64	0,76887
0,66	0,769936
0,68	0,771696
0,72	0,773523
0,74	0,772962
0,76	0,772401
0,78	0,775028
0,8	0,778524
0,84	0,781687
0,86	0,780632
0,88	0,779578
0,9	0,783675
0,92	0,788373
0,96	0,797575
0,98	0,802067
1	0,806559

C.1.2 Stress over doubler 1

Normalised length from L = 200 mm	Stress (MPa)
0	0,268978
0,02	0,289761
0,04	0,310549
0,06	0,331326
0,1	0,140568
0,12	0,150546
0,14	0,160524
0,16	0,167233
0,2	0,174274
0,22	0,170592
0,26	0,164642
0,28	0,163702
0,3	0,162816
0,32	0,164859
0,34	0,166903
0,36	0,166632
0,38	0,16423
0,4	0,161893
0,42	0,162375
0,44	0,162857
0,46	0,163303
0,48	0,163715
0,5	0,164073
0,52	0,162285
0,54	0,160497
0,56	0,160678
0,6	0,164491
0,62	0,162221
0,66	0,15961
0,68	0,161015
0,7	0,162357
0,72	0,161066
0,74	0,159775
0,76	0,159684
0,8	0,161691
0,82	0,161928
0,84	0,162165
0,86	0,163967
0,9	0,170596
0,92	0,181336
0,96	0,200498
0,98	0,206652
1	0,212806

C.1.3 Overall elongation

Step increment (adim.)	Elongation (mm)
0	0
1	0,00145824

C.1.4 Overall stress

Step increment (adim.)	Stress (MPa)
0	0
1	104,989

C.2 Second model

C.2.1 Main plate stresses

Normalised length from L = 300 mm	Stress (MPa)
0	104,992
0,04	105,006
0,06	104,993
0,0800001	104,996
0,12	104,996
0,14	104,965
0,16	104,863
0,18	104,724
0,2	104,525
0,22	103,63
0,24	102,354
0,26	98,8018
0,28	95,0692
0,3	91,4207
0,32	88,9637
0,34	87,8554
0,36	87,5336
0,38	87,481
0,42	87,3846
0,44	87,4026
0,46	87,3949
0,48	87,368
0,52	87,4069
0,56	87,3787
0,58	87,4095
0,6	87,431
0,62	87,4481
0,66	87,8476
0,68	88,9291
0,7	91,3294
0,72	95,0034
0,74	98,713
0,76	102,284
0,78	103,592
0,8	104,491
0,82	104,587
0,84	104,871
0,86	105,274
0,88	104,859
0,9	104,583
0,92	105,484
0,94	105,47
0,96	104,314
0,98	101,564
1	98,2042

C.2.2 Adhesive #1 stresses

Normalised length from L = 200 mm	Stress (MPa)
0	1,41489
0,02	1,26663
0,06	1,30816
0,08	1,84207
0,1	2,37597
0,12	3,48084
0,14	4,58803
0,16	5,36015
0,18	5,78679
0,2	6,21344
0,22	1,13963
0,24	1,09685
0,26	1,06597
0,28	1,04742
0,3	1,02887
0,32	1,01464
0,34	1,00044
0,36	0,984566
0,38	0,966943
0,4	0,94932
0,42	0,958546
0,44	0,968012
0,46	0,967592
0,48	0,956915
0,5	0,946239
0,52	0,95684
0,54	0,967631
0,56	0,968438
0,58	0,958918
0,62	0,96671
0,64	0,984246
0,66	0,99984
0,68	1,01344
0,72	1,04534
0,76	1,09365
0,78	1,13549
0,8	1,17734
0,82	5,79173
0,84	5,36446
0,86	4,59863
0,88	3,49114
0,9	2,38365
0,92	1,8451
0,94	1,3084
0,96	1,11293
0,98	1,25817
1	1,40342

C.2.3 Adhesive #2 stresses

Normalised length from L = 150 mm	Stress (MPa)
0	7,27618
0,02	6,50736
0,04	5,73854
0,06	4,96971
0,08	4,05032
0,1	3,05508
0,12	2,05984
0,14	1,32275
0,16	1,11013
0,18	0,8975
0,2	0,684874
0,22	0,67765
0,24	0,671381
0,26	0,665113
0,28	0,6254
0,3	0,568582
0,34	0,464957
0,36	0,438748
0,38	0,412538
0,4	0,386328
0,42	0,366133
0,44	0,345972
0,46	0,325811
0,48	0,319007
0,5	0,319082
0,52	0,319158
0,54	0,325903
0,56	0,346325
0,58	0,366746
0,6	0,387167
0,62	0,413774
0,64	0,440417
0,68	0,514103
0,7	0,571558
0,74	0,669825
0,76	0,676675
0,78	0,683526
0,82	0,901547
0,84	1,11336
0,86	1,32518
0,88	2,05801
0,9	3,0539
0,92	4,04981
0,94	4,97089
0,96	5,74144
0,98	6,51199
1	7,28254

C.2.4 Stress over doubler 1

Normalised length from L = 200 mm	Stress (MPa)
0	0,499622
0,02	0,558895
0,04	0,618168
0,06	1,18969
0,08	2,27378
0,1	3,37009
0,12	7,91624
0,14	12,4624
0,16	17,4661
0,2	28,3615
0,22	30,6283
0,24	32,8949
0,26	34,1483
0,28	34,41
0,3	34,6705
0,32	34,7613
0,34	34,852
0,36	34,9205
0,4	35,0136
0,42	34,9659
0,44	34,9182
0,46	34,9283
0,48	34,9943
0,5	35,0591
0,52	34,9921
0,54	34,9251
0,56	34,9179
0,6	35,0178
0,62	34,9667
0,64	34,9155
0,66	34,8462
0,7	34,6712
0,72	34,4038
0,76	32,8511
0,8	28,2927
0,82	22,8419
0,84	17,391
0,86	12,3873
0,9	3,26053
0,92	2,16387
0,94	1,06721
0,96	0,506161
0,98	0,471732
1	0,437296

C.2.5 Stress over doubler 2

Normalised length from L = 150 mm	Stress (MPa)
0	8,02951
0,02	8,02951
0,04	8,02951
0,06	8,02951
0,08	16,1666
0,1	16,2281
0,14	16,4048
0,16	16,6294
0,18	16,8541
0,2	17,0787
0,22	17,1834
0,24	17,2874
0,28	17,4219
0,3	17,4144
0,32	17,4069
0,34	17,4074
0,36	17,4243
0,38	17,4412
0,4	17,4581
0,42	17,4523
0,44	17,4463
0,46	17,4404
0,48	17,4384
0,5	17,4384
0,52	17,4385
0,54	17,4404
0,56	17,4462
0,58	17,452
0,6	17,4578
0,62	17,4412
0,64	17,4245
0,68	17,407
0,7	17,4143
0,72	17,4216
0,74	17,3923
0,76	17,2884
0,78	17,1846
0,8	17,0807
0,82	16,8579
0,84	16,6347
0,86	16,4115
0,88	16,2963
0,9	16,2355
0,94	8,04584
0,96	8,04584
0,98	8,04584
1	8,04584

C.2.6 Overall elongation

Step increment (adim.)	Elongation (mm)
0	0
1	0,00145823

C.2.7 Overall stress

Step increment (adim.)	Stress (MPa)
0	0
1	104,989

C.3 Third model

C.3.1 Main plate stresses

Normalised length from L = 300 mm	Stress (MPa)
0	104,992
0,0345242	105,009
0,0690481	104,988
0,103572	105,015
0,138096	104,974
0,172621	104,799
0,207121	104,445
0,241606	102,214
0,276088	95,693
0,310571	88,2851
0,345052	82,2679
0,379524	76,7506
0,414005	73,9352
0,448473	73,67
0,482947	73,5665
0,517415	73,6128
0,551887	73,6261
0,586349	73,9749
0,620825	76,7182
0,655287	82,2947
0,689755	88,2631
0,724221	95,7088
0,75868	102,166
0,793138	104,451
0,82759	104,624
0,862086	105,318
0,896544	104,431
0,931055	105,984
0,965507	103,994
1	98,2025

C.3.2 Adhesive #1 stresses

Normalised length from L = 200 mm	Stress (MPa)
0	1,35121
0,02	1,20669
0,06	1,21864
0,08	1,68058
0,1	2,14252
0,12	3,15555
0,14	4,17004
0,16	4,88576
0,18	5,29544
0,2	5,70511
0,22	2,20851
0,24	2,82955
0,26	3,17441
0,28	3,236
0,3	3,29759
0,32	2,54629
0,34	1,79039
0,36	1,31817
0,38	1,1368
0,4	0,955422
0,42	1,01092
0,44	1,06779
0,46	1,11903
0,48	1,16451
0,5	1,20998
0,52	1,16265
0,54	1,11478
0,56	1,06302
0,58	1,00728
0,6	0,951541
0,62	1,14342
0,64	1,33665
0,66	1,80333
0,68	2,54855
0,72	3,23153
0,74	3,16556
0,76	2,8277
0,78	2,21449
0,8	1,60128
0,82	5,28269
0,84	4,87734
0,86	4,18422
0,88	3,20201

0,9	2,2198
0,92	1,74763
0,94	1,27686
0,96	1,09575
0,98	1,20357
1	1,31139

C.3.3 Adhesive #2 stresses

Normalised length from L = 150 mm	Stress (MPa)
0	7,29127
0,02	6,57047
0,04	5,84966
0,08	4,41566
0,1	3,70631
0,14	2,53349
0,16	2,56302
0,18	2,59255
0,2	2,62207
0,22	2,3787
0,24	2,1339
0,26	1,8891
0,28	1,56468
0,3	1,20032
0,32	0,835953
0,34	0,577806
0,36	0,536999
0,38	0,496192
0,4	0,455385
0,42	0,46939
0,44	0,483483
0,46	0,497577
0,48	0,502337
0,5	0,502321
0,52	0,502305
0,54	0,497596
0,56	0,483425
0,58	0,469255
0,6	0,455084
0,62	0,495386
0,64	0,53597
0,68	0,832197
0,7	1,19598
0,72	1,55977
0,74	1,88484
0,76	2,13075
0,78	2,37667
0,8	2,62246
0,82	2,59409
0,84	2,56572
0,88	2,99869
0,9	3,70825
0,92	4,4178
0,94	5,13136
0,96	5,85282
0,98	6,57428
1	7,29574

C.3.4 Adhesive #3 stresses

Normalised length from L = 100 mm	Stress (MPa)
0	0,0509748
0,02	0,0482535
0,04	0,0455322
0,06	0,042811
0,08	0,0400897
0,1	0,0373684
0,12	0,0346472
0,14	0,0319259
0,16	0,0292047
0,18	0,0264834
0,2	0,0237621
0,22	0,105118
0,24	0,0994543
0,26	0,0937904
0,28	0,0881265
0,3	0,0824626
0,32	0,079742
0,34	0,077027
0,36	0,0743119
0,38	0,0715969
0,4	0,0688819
0,42	0,0718262
0,44	0,0747822
0,46	0,0777384
0,48	0,0806944
0,52	0,0807082
0,54	0,0777535
0,56	0,0747987
0,58	0,071844
0,6	0,0688893
0,62	0,0715891
0,64	0,0742999
0,66	0,0770107
0,68	0,0797215
0,72	0,0881003
0,74	0,0937731
0,76	0,099446
0,78	0,105119
0,8	0,110792
0,82	0,0264857
0,84	0,0291991
0,86	0,0319125
0,88	0,0346259

0,9	0,0373393
0,92	0,0400529
0,94	0,0427665
0,96	0,0454802
0,98	0,0481938
1	0,0509074

C.3.5 Stress over doubler 1

Normalised length from L = 200 mm	Stress (MPa)
0	0,499243
0,02	0,559242
0,04	0,619242
0,06	1,20068
0,08	2,30496
0,1	3,41867
0,12	7,97432
0,14	12,5314
0,16	17,6506
0,18	23,3336
0,2	29,0051
0,22	31,978
0,24	34,9512
0,26	36,9499
0,3	39,0238
0,32	39,7933
0,34	40,5629
0,36	41,1402
0,4	41,9152
0,42	41,9007
0,44	41,8862
0,46	41,9459
0,5	42,2094
0,52	42,0759
0,54	41,9424
0,56	41,8851
0,6	41,9169
0,62	41,5237
0,64	41,1305
0,66	40,5492
0,7	39,0183
0,72	37,9757
0,76	34,9112
0,78	31,9348
0,8	28,9465
0,82	23,268
0,86	12,4666
0,9	3,31493
0,92	2,19814
0,94	1,08136
0,96	0,509337
0,98	0,474113
1	0,43889

C.3.6 Stress over doubler 2

Normalised length from L = 150 mm	Stress (MPa)
0	8,08438
0,02	9,3404
0,04	10,5964
0,0600001	11,8524
0,08	12,6259
0,1	13,1615
0,14	13,4705
0,16	11,7131
0,18	9,95572
0,2	8,20327
0,22	7,97574
0,24	7,74821
0,26	7,52068
0,28	8,08594
0,3	9,05058
0,34	10,6409
0,36	10,5909
0,38	10,5409
0,4	10,491
0,42	10,5483
0,44	10,6061
0,48	10,6832
0,5	10,683
0,52	10,6829
0,54	10,6639
0,56	10,6064
0,58	10,5488
0,6	10,4913
0,62	10,5408
0,64	10,5906
0,68	10,0206
0,7	9,05515
0,72	8,08971
0,74	7,51764
0,76	7,74657
0,78	7,9755
0,82	9,95177
0,84	11,7114
0,88	13,7074
0,9	13,1729
0,94	11,8673
0,96	10,6117
0,98	9,35613
1	8,10053

C.3.7 Stress over doubler 3

Normalised length from L = 100 mm	Stress (MPa)
0	10,2937
0,02	10,2937
0,0399999	10,2937
0,06	10,2937
0,08	10,2937
0,0999999	10,2937
0,12	19,2282
0,14	19,1854
0,16	19,1425
0,18	19,0996
0,22	19,1169
0,24	19,1772
0,26	19,2375
0,28	19,2978
0,32	19,4409
0,34	19,5236
0,36	19,6064
0,38	19,6892
0,42	19,7519
0,44	19,7317
0,46	19,7115
0,48	19,6912
0,5	19,671
0,52	19,6911
0,54	19,7113
0,56	19,7315
0,58	19,7517
0,6	19,7719
0,62	19,6893
0,64	19,6065
0,66	19,5237
0,68	19,441
0,72	19,2979
0,74	19,2377
0,76	19,1775
0,78	19,1173
0,82	19,0995
0,84	19,142
0,86	19,1846
0,88	19,2271
0,9	19,2697
0,92	10,2882
0,94	10,2882
0,96	10,2882
0,98	10,2882
1	10,2882

C.3.8 Overall elongation

Step increment (adim.)	Elongation (mm)
0	0
1	0,00145823

C.3.9 Overall stress

Step increment (adim.)	Stress (MPa)
0	0
1	104,989

C.4 Aditional Bending Stresses

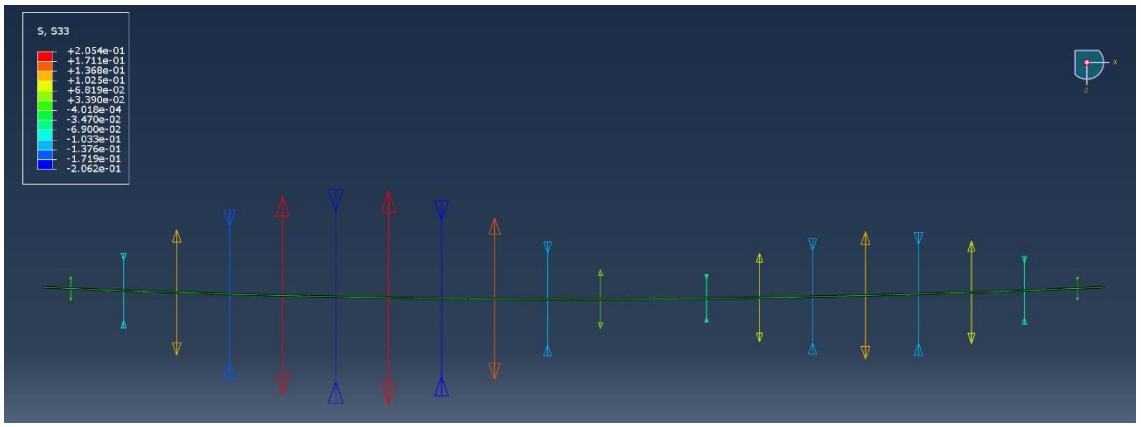

Fig C.1. Adhesive #1 for model #1.

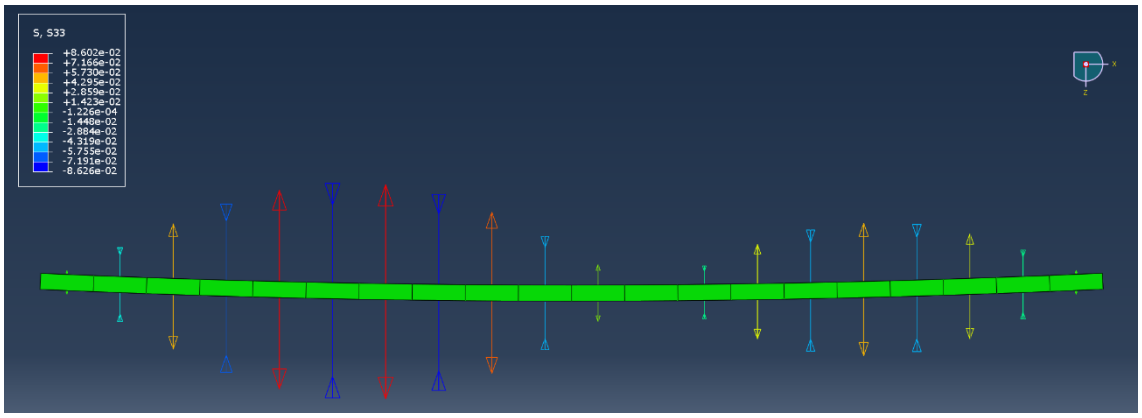

Fig C.2. Doubler #1 for model #1.

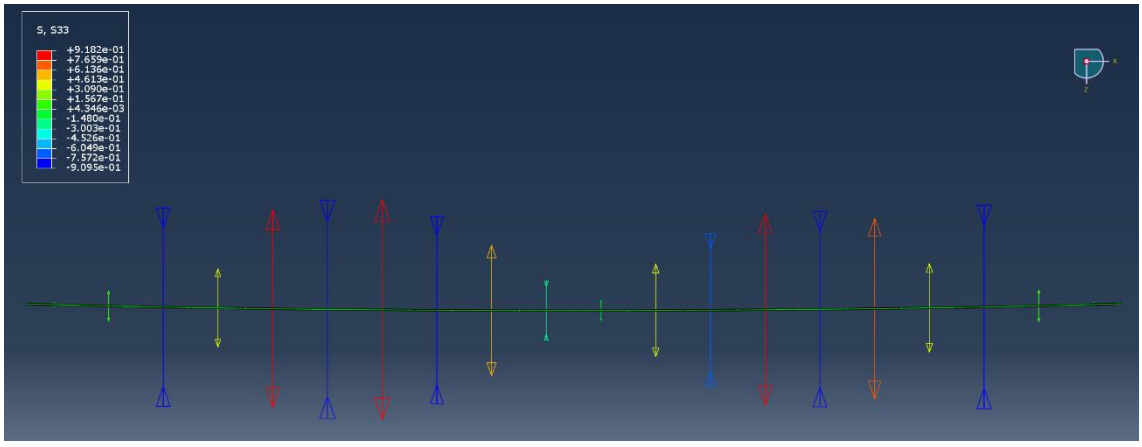

Fig C.3. Adhesive #1 for model #2.

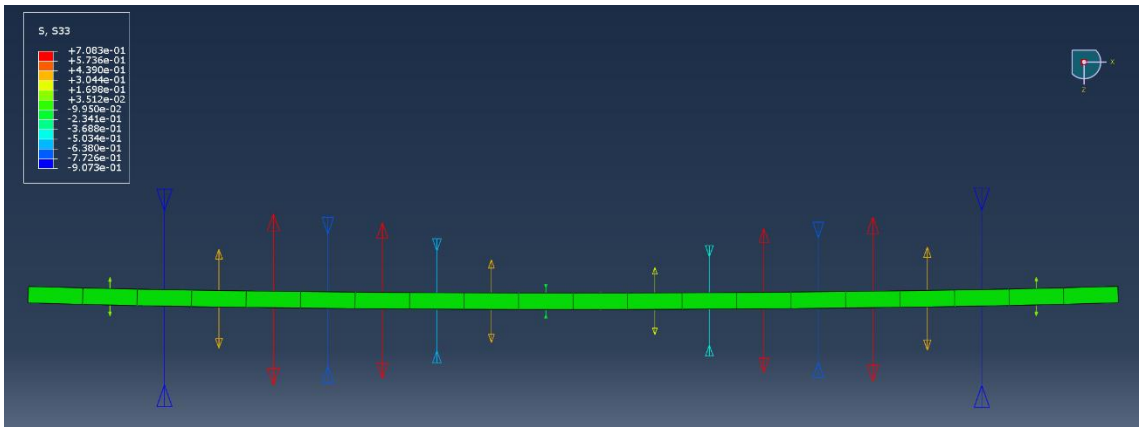

Fig C.4. Doubler #1 for model #2.

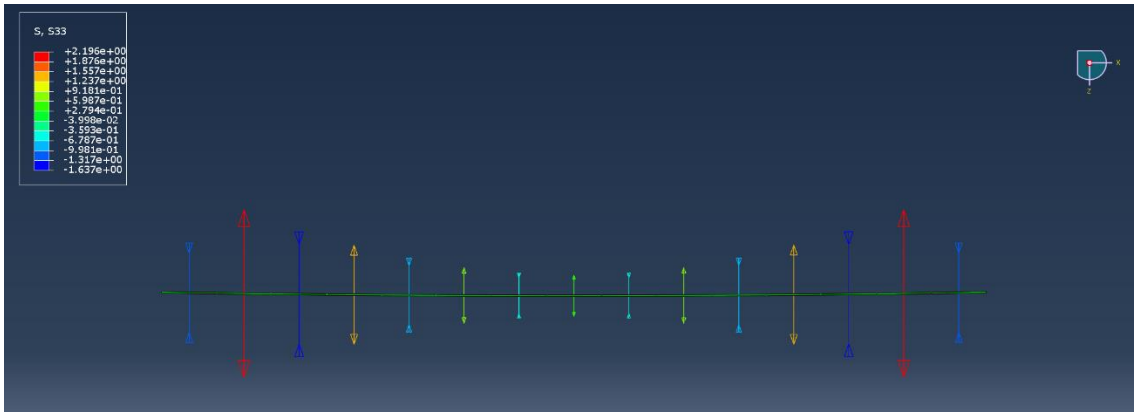

Fig C.5. Adhesive #2 for model #2.

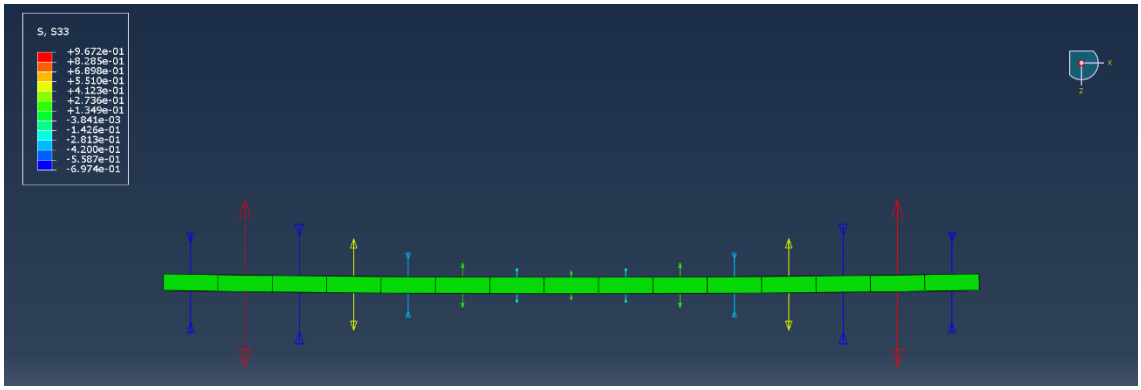

Fig C.6. Doubler #2 for model #2.

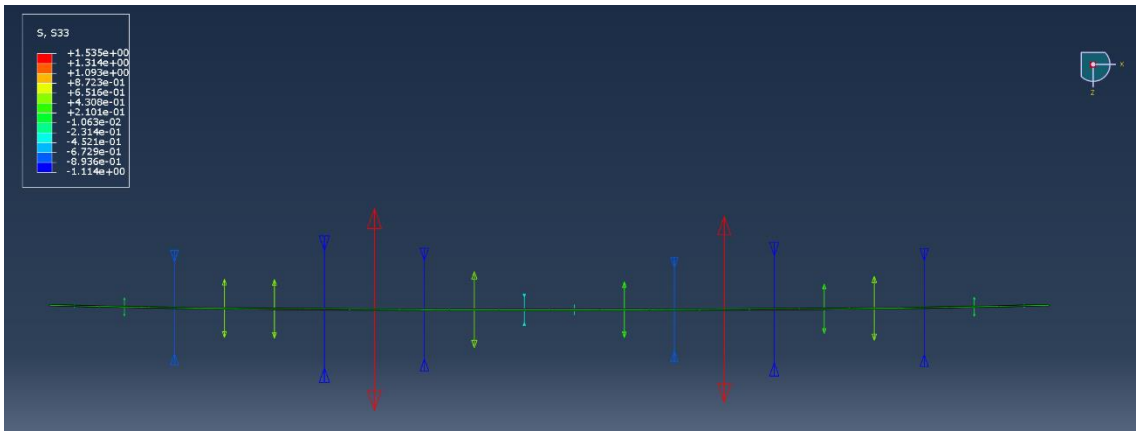

Fig C.3. Adhesive #1 for model #3.

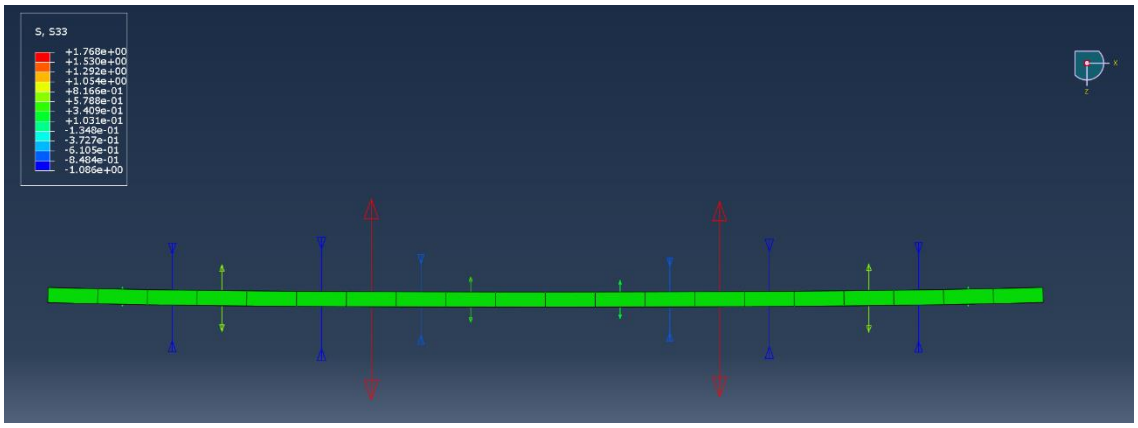

Fig C.6. Doubler #1 for model #3.

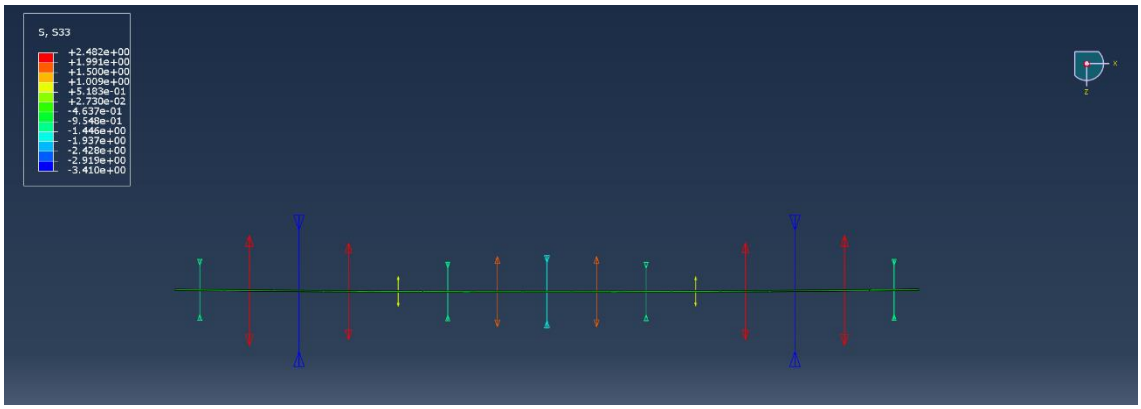

Fig C.3. Adhesive #2 for model #3.

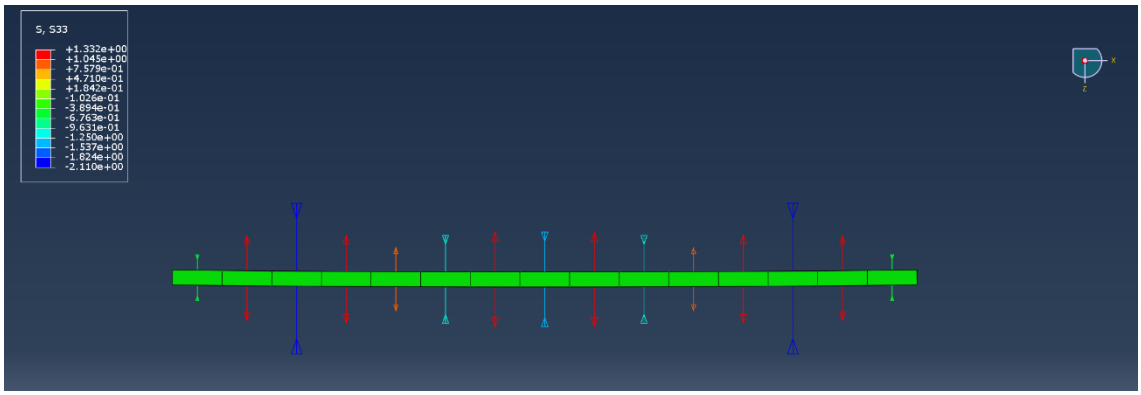

Fig C.6. Doubler #2 for model #3.

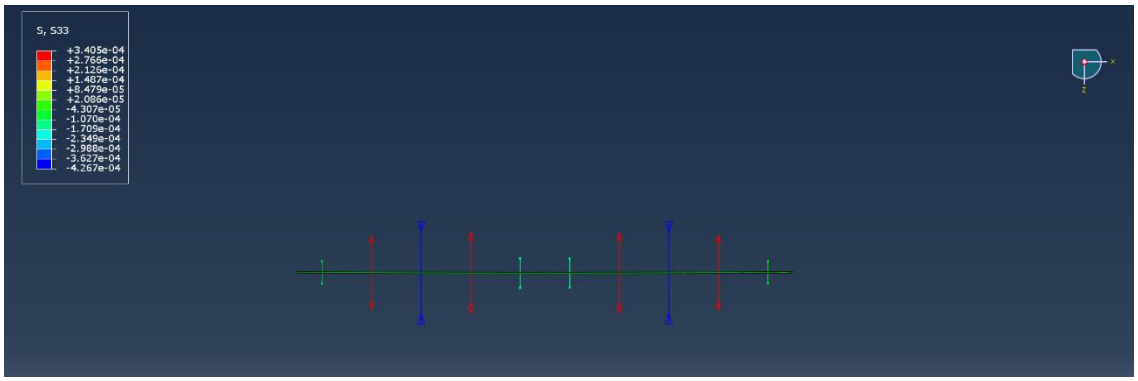

Fig C.3. Adhesive #3 for model #3.

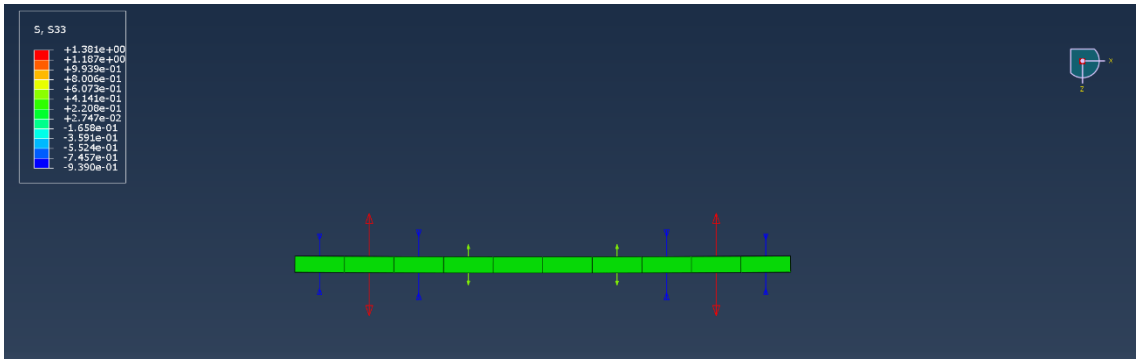

Fig C.6. Doubler #3 for model #3.